Nordic Society for Aerosol Research NOSA

NOSA Aerosol Symposium

with special focus on

Bioaerosols

Program
and
Conference Proceedings

www.dmu.dk/nosa2012

Nordic Society for Aerosol Research

NOSA (the Nordic Society for Aerosol Research)

NOSA has the ambition to arrange Nordic Aerosol conferences annually in one of the Nordic countries. The first steps towards the founding of NOSA were taken in 1978 in Stockholm and the first NOSA scientific meeting was arranged in Göteborg in 1982. Before the NOSA 2012 Aerosol Symposium, Sweden has hosted twelve meetings (including European Aerosol Conference 1988), Finland has arranged five meetings (including International Aerosol Conference 2010) and Denmark and Norway four. NOSA is an organization consisting of members primarily from the Nordic countries; however, members from other countries are very welcome as well. The aims of NOSA are:

- to strengthen the cooperation within the Nordic aerosol research community;
- to offer a network and a meeting place for Nordic aerosol scientists;
- to disseminate the results of Nordic aerosol research to other scientists;
- to widen the awareness regarding Nordic aerosol research among public and policymakers;
- to encourage a multi-disciplinary dialogue between aerosol scientists and scientists within other fields of science where aerosol expertise is needed.

The NOSA board

The board of NOSA has assisted the local organizing committee in arranging the NOSA 2012 conference, and currently the board consists of the following persons:

- Merete Bilde (NOSA President) Department of Chemistry, University of Copenhagen
- Michael Boy, Department of Physics, University of Helsinki
- Annica Ekman, Department of Meteorology, Stockholm University
- Jacob Klenø Nøjgaard, Aarhus University, Department of Environmental Science (former DMU)
- Joakim Pagels, Division of Ergonomics and Aerosol Technology, Faculty of Engineering, Lund University
- Ilona Riipinen, Department of Applied Environmental Science, Stockholm University
- Karl Espen Yttri Norwegian Institute for Air Research (NILU)

NOSA 2012 Local Organizing Committee

University of Copenhagen, Chemistry Department
Merete Bilde, Kirsten Inga Lieke, Thomas Bjerring Kristensen, Ole John Nielsen,

Aarhus University, Department of Environmental Science (former DMU)
Jacob Klenø Nøjgaard, Matthias Ketzel, Andreas Massling

Aarhus University, Chemistry Department
Marianne Glasius

Sponsors

We gratefully acknowledge sponsorship by

- TSI GmbH, Web: http://particle.tsi.com
- Danalytic ApS, E-mail: danalytic@post.tele.dk
- Oleico AB, Web: http://www.oleico.se/
- Digitel Elektronik GmbH, Web: http://www.digitel-ag.com/
- ZenZors A/S, Web: http://www.zenzors.com/
- Dekati Ltd., Web: http://www.dekati.com/
- Aarhus University
- University of Copenhagen

Symposium Venue

Konventum
LO-Skolens Conference Center
Gl. Hellebækvej 70
3000 Helsingør
Tel: +45 4928 0900

http://www.konventum.dk

The conference centre is beautifully situated at Helsingør (Elsinore) near the Sound and close to the (Hamlet) castle Kronborg. It offers superb view of the Øresund strait and Sweden. In addition to the natural setting the conference center offers fine food and recreational facilities, and displays a collection of paintings and sculptures.

Accomodation

Single and double rooms are provided at LO-Skolen.

Program 2012 NOSA Aerosol Symposium

Thursday, November 15

09:00-10:00	Registration and coffee
10:00-10:10	**Welcome and opening**
Session 1	**Bioaerosols – Chair: Merete Bilde**
10:10-11:00	**Invited talk by Ruprecht Jaenicke**: The atmospheric biological aerosol
11.00-11:10	Stretch of legs
Session 2	**Bioaerosols and air quality – Chair: Kirsten Inga Lieke**
11:10-11:25	**J. Jacobsen**,P. Wollmer, J. Löhndahl: Lung deposition of nano particles as a method for diagnosis of chronic obstructive pulmonary disease
11:25-11:40	**T. Šantl Temkiv**, K. Finster, T. Dittmar, B. M. Hansen, R. Thyrhaug, N. W. Nielsen, and U.G. Karlson: Can the diverse bacterial community grow on dissolved organic matter in a storm cloud?
11:40-11:55	**M. W. Gallagher**, N. H. Robinson, P. H. Kaye, and V. E. Foot: Hierarchical Agglomerative Cluster Analysis Applied to WIBS 5-Dimensional Bioaerosol Data Sets
11:55-12:10	**B. Mølgaard**, A. J. Koivisto, T. Hussein, and K. Hämeri: Air cleaner device performance tests
12:10-13:15	LUNCH
Session 3	**Physical/chemical characterization of anthropogenic aerosols – Chair: Matthias Ketzel**
13:15-13:30	**K. I. Lieke**, T. Rosenørn, A. C. Butcher, S. M. King, T. G. Frederiksen, K. Fuglsang, J. B. Pedersen, D. Larsson, and M. Bilde: Particles measured in a low speed ship engine: cloud condensation nuclei and microstructure
13:30-13:45	**J. Genberg**, P. Tornehed, Ö. Andersson, and K. Stenström: Do carbonaceous particles in diesel exhaust originate from the fuel or lubricant oil?
13:45-14:00	**A. C. Eriksson**, J. Pagels, J. Rissler, S. Sjögren, and E. Swietlicki: Physical and chemical characterization of urban aerosol particles through Soot Particle Aerosol Mass Spectrometry
14:00-14:15	**A. V. Samodurov**, S. V. Valiulin, V. V. Karasev, and S. V. Vosel: Determination of Nanoparticles Surface Tension in the Case of Ibuprofen and Elemental Sulfur
14:15-15:45	**Poster presentations, exhibitions and refreshments**
Session 4	**Nucleation – Chair: Miikka Dal Maso**
15:45-16:00	**D. Mogensen**: An essential formation mechanism to produce sulphuric acid in VOC rich environments
16:00-16:15	**N. Bork**, N. T. Tsona, and H. Vehkamäki: From free electrons to H2SO4 – new sources of ion catalysed SO2 oxidation
16:15-16:30	**T. Olenius**, O. Kupiainen, I. K. Ortega, and H. Vehkamäki: Clustering pathways of sulfuric acid, ammonia and dimethylamine molecules
16:30-16:45	**M. J. Ryding**, M. Patanen, G. Simões, A. Guiliani, O. Björneholm, G. B. S. Miller, T. Jokinen, C. Miron, and E. Uggerud: X-ray absorption photofragmentation of ammonium bisulphate cluster-ions
17:00-17:45	NOSA annual meeting, open for all symposium participants
19:00-	**Symposium Dinner**

Friday, November 16

Session 5	**Secondary organic aerosols – Chair: Birgitta Svenningsson**
9:00-9:15	**J. Elm**, S. Jørgensen, M. Bilde, and K. V. Mikkelsen: Computational methodology study of the oxidation of Atmospheric oxygenated organics by the OH radical.
9:15-9:30	**Å. K. Watne**, E. U. Emanuelsson, A. Lutz, and M. Hallquist: Characterization of secondary organic aerosol from ozonolysis of ß-pinene
9:30-9:45	**Q. T. Nguyen**, M. K. Christensen, F. Cozzi, A. M. K. Hansen, T. E. Tulinius, K. Kristensen, A. Massling, J. K. Nøjgaard, and M. Glasius: Organosulfates at urban curbside and semi-rural background of Denmark: Understanding anthropogenic influence on biogenic SOA
9:45-9:55	Stretch of legs
Session 6	**Biosphere and Climate – Chair: Erik Swietlicki**
9:55-10:45	**Invited talk by Caroline Leck**: Could the increase in Arctic summer sea-ice melt spur the activity of marine microbiota, increase cloudiness and counteract the melting?
10:45-11:00	**A. M. L. Ekman**, H. Struthers, A. Lewinschal, K. J. Noone, T. Iversen, A. Kirkevåg, and Ø. Seland: Can an influence of changing aerosol emissions be detected in the pattern of surface temperature change between 1970 and 2000?
11:00-11:20	Exhibitions and refreshments
Session 7	**Hygroscopic properties of organic aerosols – Chair: Andreas Massling**
11:20-11:35	**I. Crljenica**, T. Yli-Juuti, A. Zardini, J. Julin, M. Bilde, and I. Riipinen: Saturation vapour pressures of keto-dicarboxylic acids in aqueous solutions
11:35-11:50	**C. Wittbom**, B. Svenningsson, J. Rissler, A. Eriksson, E. Swietlicki, E. Z. Nordin, P. T. Nilsson, and J. Pagels: Changes in Hygroscopicity and Cloud-Activation of Diesel Soot upon Ageing
11:50-12:05	**T. B. Kristensen**, H. Wex, L. Du, Q. Nguyen, J. K. Nøjgaard, B. Nekat, D. Van Pinxteren, C. B. Koch, K. Dieckman, D. H. Lowenthal, L. Mazzoleni, T. F. Mentel, M. Glasius, H. Herrmann, H.G. Kjaergaard, A.G. Hallar, F. Stratmann, and M. Bilde: A detailed characterisation of HULIS from different environments
12:05-13:10	LUNCH
Session 8	**New particle formation – Chair: Ilona Riipinen**
13:10-13:25	**M. Dal Maso**, H. Korhonen, K. Lehtinen, and H. Vehkamäki: The effect of gas-phase kinetics and nanoparticle dynamics on observed particle formation
13:25-13:40	**M. Boy**, L. Zhou, D. Mogensen, T. Nieminen, S. Smolander, and M. Kulmala: Long term modelling of new particle formation and growth in a boreal forest
13:40-13:55	**R. Gierens**, L. Laakso, V. Vakkari, D. Mogensen, P. Beukes, P. Van Zyl, and M. Boy: Modelling studies of new particle formation and growth in Southern African savannah environment
13:55-14:05	Stretch of legs
Session 9	**Aerosols and climate – Chair: Adam Kristensson**
14:05-14:20	**N. Rastak**, S. Silvergren, P. Zieger, U. Wideqvist, J. Ström, B. Svenningsson, A. Ekman, P. Tunved, and I. Riipinen: Modeling aerosol water uptake in the Arctic and its direct effect on climate
14:20-14:35	**N. Babkovskaia**, M. Boy, S. Smolander, S. Romakkaniemi, and M. Kulmala: A study of aerosol production at the cloud edge with direct numerical simulations
14:35-14:50	**Closing remarks and awards for best student presentations**

Posters

Nr.	Author	TitleAbstract
1	E. Ahlberg, M. Frosch, W. H. Brune, B. Svenningsson	Characterization and first field deployment of the Lund University PAM chamber
2	M.K. Christensen, Q.T. Nguyen, A.M.K. Hansen, F. Cozzi, K. Kristensen, T.E. Tulinius, A. Tolloi, P. Barbieri, S. Licen, A. Massling, J.K. Nøjgaard and M. Glasius	Biogenic oxidation products and organic acids in aerosols from Denmark and Italy
3	F. Cozzi, I.J. Kwame Aboh, D. Henriksson, J. Laursen, M. Lundin, M. Glasius and N. Pind	Elemental characterization by EDXRF and source identification of $PM_{2.5}$ aerosols originating from an urban site
4	M. Dalirian, H. Keskinen, P. Miettinen, A. Virtanen, A. Laaksonen and I. Riipinen	CCN activation of insoluble silica aerosols coated with soluble pollutants
5	M. Fard, M. Johnson, M. Bilde	Hygroscopic Growth of Selected Amino Acids in Organic Aerosols, Using Water Activity Measurements
6	M. Frosch, E. Ahlberg, A. Eriksson, S. Sjögren, J. Pagels, J. Rissler, E. Swietlicki, W. H. Brune and B. Svenningsson	Effects of intense ageing on volatility and chemical composition of urban aerosol particles
7	F. Grantén, P.-A. Larsson, M. Ramstorp, M. Bohgard and J. Löndahl	Airborne Bacteria in Operating Theaters
8	E. Hermansson, P. Roldin, E. Swietlicki, D. Mogensen, A. Rusanen and M. Boy	Modeling of secondary aerosol formation from β-pinene oxidation
9	M. Johansson, A. Kristensson, E. Swietlicki, M. Dal Maso, N. Kivekäs, T. Hussein, T. Nieminen, H. Junninen, H. Lihavainen, P. Tunved, and M. Kulmala	Development of the NanoMap method for geographical mapping of new particle formation events
10	J. Julin, M. Shiraiwa, R. E. H. Miles, J. P. Reid, U. Pöschl and I. Riipinen	The effect of droplet size on the evaporation and mass accommodation processes of water: a molecular dynamics study
11	N. Kelbus, A. Massling, M. Fiebig, B. Henzing, M. Glasius, M. Bilde, M. Moerman, G. de Leeuw, M. Dal Maso, and A. Kristensson	NanoShip project: Is new particle formation taking place over the North Sea?
12	H. C. Knap, J. D. Crounse, K. B. Ørnsø, S. Jørgensen, F. Paulot, P. O. Wennberg and H. G. Kjaergaard	Atmospheric Fate of Methacrolein
13	W.-Y. H. Leung, A. M. L. Ekman, M. Komppula, A. Kristensson, K. Noone, H. Portin, S. Romakkaniemi, J. Savre	Large-eddy simulations and observations of a stratiform cloud event at the Puijo hill in Kuopio, Finland
14	J. Löndahl, O. Nerbrink, N. Burman, T. Tjärnhage, C. von Wachenfeldt and U. Gosewinkel Karlson	Methods for generation of bioaerosol
15	L. Ludvigsson, C. Isaxon, P. T. Nilsson, M. Hedmer, H. Tinnerberg, M. E. Messing, J. Rissler, V. Skaug, M. Bohgard, J. Pagels	Emission measurements of multi-walled carbon nanotube release during production
16	A. Lutz, E. U. Emanuelsson, Å. K. Watne and M. Hallquist	An evaluation method to describe differences in thermal properties of organic aerosols

17	S. Marini, P. T. Nilsson, A. Wierzbicka,K. Kuklane,J. Nielsen and A. Gudmundsson	Emissions of particles during hair bleaching
18	E. M. Mårtensson and E. D. Nilsson	In situ measurements of size resolved sea spray aerosol emissions with the eddy covariance method at Svalbard (78.9°N)
19	A. Massling, A.G. Grube, H. Skov, J.H. Christensen, B. Jensen, Q.T. Nguyen, M. Glasius, J.K. Nøjgaard, L.L. Sørensen	Implications for black carbon and sulphate aerosol at a high Arctic site
20	C. Meusinger, U. Dusek, S.M. King, R. Holzinger, M. Bilde, T. Röckmann and M.S. Johnson	Chemical and 13-Carbon Isotopic Composition of Secondary Organic Aerosol from Alpha-Pinene Ozonolysis
21	L. B. Nielsen, H. C. Knap, K. B. Ørnsøe, S. Jørgensen, H. G. Kjærgaard.	Atmospheric Fate of an Oxidanyl Radical Formed in The Degradation of Isoprene.
22	E. D. Nilsson, C. Fahlgren, U. L. Zweifel (presented by E.M. Mårtenson)	One year seasonal cycle of airborne bacteria and fungus in southern Sweden: implications on sinks, sources and turn over time
23	J.K. Nøjgaard, R. Bossi, A. Massling and T. Ellermann	Sources to Benzo[a]pyrene in Wintertime Urban Aerosols
24	E. Z. Nordin, A. C. Eriksson, R. Nyström, E. Pettersson, J. Rissler, E. Swietlicki, M. Bohgard, C. Boman and J. Pagels	Physical and Chemical Characterization of Biomass Burning Aerosol
25	R.K. Pathak, M. Hallquist, A. Watne, N. M. Donahue, S. N. Pandis, T. F. Mentel, B. Svenningsson, E. Swietlicki, W. Brune,	The complexity of aerosols as short-lived climate forcers: Interactions between soot and secondary organic aerosol (SOA) in a changing climate
26	A.-M. Pessi, Satu Saaranen, and Auli Rantio-Lehtimäki	Pollen forecast – from pollen counts to model-assisted allergen information service
27	P. Roldin, E.Z. Nordin, A.C. Eriksson, D. Mogensen, A. Rusanen, E. Swietlicki, M. Boy and J. Pagels	ADCHAM - A multilayer aerosol dynamics, gas and particle chemistry chamber model
28	C. A. Skjøth, J. Sommer and U. Gosewinkel Karlson	Are agricultural areas the main source of Alternaria fungal spores in the atmosphere?
29	C.R. Svensson, M. E. Messing, M. Lundqvist, A. Schollin, K. Deppert, S. Snogerup Linse, J. Pagels, J. Rissler and T. Cedervall	The fate of aerosol AuNP upon deposition into physiological fluids – Protein corona and aggregation in solution
30	N.Tsona, N. Bork, H. Vehkamäki.	Gase-phase oxidation of SO_2 by $O_2^-(H_2O)n$ molecular clusters - a density functional theory study
31	F. Wang, M. Ketzel, A. Massling and A. Kristensson	New particle formation events at the Lille Valby semi-rural background site in Denmark
32	J. Werner, N. Ottosson, G. Öhrwall, J. Söderström, N. L. Prisle, M. Dal Maso, J. Julin, I. Riipinen, O. Björneholm and I. Persson	Direct probing of liquid and aerosol surfaces by XPS

Abstracts in alphabetical order

Characterization and first field deployment of the Lund University PAM chamber

E. Ahlberg[1,2], M. Frosch[1], W. H. Brune[3], B. Svenningsson[1]

[1]Division of Nuclear Physics, Lund University, Box 118, SE-22100, Lund, Sweden
[2]Centre for Environmental and Climate Research, Lund University, Box 118, SE-22100, Lund, Sweden
[3]Department of Meteorology, Pennsylvania State University, University Park, PA 16802, USA

Keywords: PAM, SOA, VOC, oxidation

Introduction

Atmospheric oxidation of trace gases can form low volatility products which produce secondary aerosol particles and, by condensing on existing particles, alter the properties of the ambient aerosol. Secondary organic aerosols (SOA) are formed from the oxidation of volatile organic compounds (VOCs) and constitute a significant fraction of the global aerosol load. The study of atmospheric oxidation processes and products have traditionally been performed using large chambers with volumes of several m^3 and residence times of at least a few hours. By using a continuous flow chamber with extreme amounts of ozone and hydroxyl radicals, the processes are accelerated, leading to reduced wall interactions, and online field measurements can be performed. Here we report on the first characterizations and field measurements of a potential aerosol mass (PAM) chamber at Lund University.

Methods

The concept of PAM was introduced by Kang et al. (2007), and defined as the maximum aerosol mass that oxidation of precursor gases produces. The PAM chamber we use is built at the Pennsylvania State University, and is a modification of the original design, similar to the chamber characterized by Lambe et al. (2011). The chamber is a 42 cm long and 20 cm ID metal tube. Flow through the chamber is theoretically laminar (Re << 2300). With a low surface area to volume ratio and the possibility of dumping the air flowing closest to the walls, wall interactions are low. Oxidants are produced by two mercury lamps (peaks at 185 and 254 nm) mounted inside the chamber. The concentration of oxidants is controlled by adjusting the lamp voltages and the relative humidity (RH). This method of production gives oxidant ratios similar to atmospheric conditions.

The first field measurements were performed during January-February 2012, at a busy street side in Copenhagen. A denuder with activated carbon was used to remove ozone after the PAM chamber.

Results and conclusions

A flow of 5 lpm, yielding an average residence time of 164 s, was used. Applying a lamp voltage of 150-200 V yielded ozone concentrations of 10-30 ppm. With these settings particle losses of up to 10 %, for the high and low ends of the particle size spectrum, is expected from diffusion and settling theory. With lamps turned off and a low flow of 1 lpm, losses of around 50 % (compared to a theoretical value of 30 %) for small particles (~10 nm in diameter) were observed. It is possible that the lamps induce convection inside the chamber. This can be tested by measuring the penetration of inert particles.

Water vapour has a significant effect on photochemistry (figure 1). OH exposure was calculated from the measured loss of SO_2. The levels of OH are linear with RH and correspond to an atmospheric lifetime of 10-20 days (ambient OH levels ~ 1.5 x 10^6 molecules cm^{-3}). Ozone decreases with RH due to the UV absorption of water vapour and reactions with the formed radicals.

During the field campaign large amounts of small SOA particles were created in the PAM chamber. Particle mass did not change much due to losses of larger particles. With a particle filter before PAM, virtually no particles above a mobility diameter of 100 nm were seen.

After a change in lamp voltage, stabilization in both ozone and number concentration data take several minutes. This and other problems, such as the impact of UV light on particles and reducing ozone after the chamber without affecting particle measurements, calls for further work.

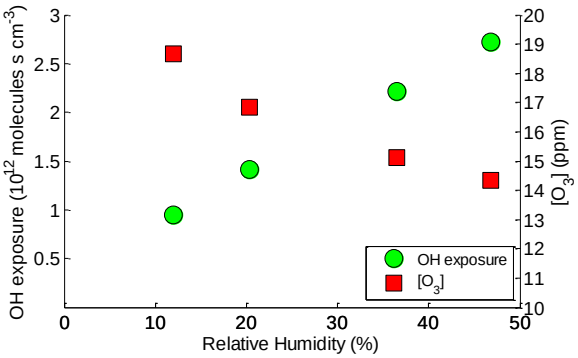

Figure 1. Ozone concentration and OH exposure as a function of relative humidity at 22.5°C.

This work was financed by Formas and VR

Kang, E. et al., (2007). *Atmos. Chem. Phys.* **7**,5727-5744.

Lambe, A. T. et al., (2011). *Atmos. Meas. Tech*. **4**, 445-461.

A study of aerosol production at the cloud edge with direct numerical simulations

N. Babkovskaia[1], M. Boy[2], S. Smolander[1], S. Romakkaniemi[2] and M. Kulmala[1]

[1]Department of Physics, University of Helsinki, PO Box 48, Erik Palmenin aukio, 1, 00014, Finland
[2]Department of Applied Physics, University of Eastern Finland, P.O. Box 1627, 70211 Kuopio, Finland

Keywords: DNS, aerosol, clouds

Introduction

Aerosol clouds are dynamic systems with spatially and temporally varying properties. More cloud droplets may form due to in-cloud activation or due to entrainment of air from cloud edges that might lead to formation of fresh cloud droplets. On the other hand, cloud droplets may be evaporated because of mixing at cloud boundaries or in-cloud dynamics causing part of droplets to evaporate. The latter of these can be important in stratus type clouds with long in-cloud residence time of air parcel. The mixing at cloud boundaries takes place in all clouds, and the type of mixing is dependent on the conditions and mixing time scales.

Methods

To study the structure of the cloud edge area we use the direct numerical simulation (DNS) high-order public domain finite-difference PENCIL Code for compressible hydrodynamic flows. The PENCIL Code is a powerful tool for studying the aerosol dynamics in a turbulent medium with complicated chemical composition (PENCIL Code, 2001; Babkovskaia *et al.*, 2011). The scientific goals for the construction of the new model are to investigate the spatial distribution of aerosol particles, turbulent mixing of clouds with the environment and the influence of turbulence on aerosol dynamics (and vice versa).

Conclusions

We study the activation process at the cloud edge. We consider the flux of aerosol particles, which goes through the boundary between the dry and wet air. For a test purpose we start from a zero-dimensional problem. Following by Andrejczuk *et al.* (2004), we take into account the condensation and evaporation of the aerosol particles covered by liquid water. Next, we consider a one dimensional problem to study a motion and evolution of the front between the dry and wet air. This approach allows us to analyze the effect of the fluid mechanics on the aerosol dynamics (and vice versa) in a laminar regime. Finally, we make 3D simulation with a more complicated velocity field at the cloud edge. We assume that the dry air flux is coming into the computational domain in its middle part and coming out near its boundaries. Wet air is moving in horizontal direction with velocity U_x=50 cm/s. The third velocity component initially equals to zero, U_z=0 cm/s.

We study the effect of air mixing, comparing the results of simulation with zero, U_{in}=0 cm/s, and non-zero, U_{in}=20 cm/s, inlet velocity. We find that for U_{in}=0 cm/s (no mixing) the most efficient growing of particles due to condensation occurs inside the front. In a case of U_{in}=20 cm/s the intensive mixing of air results to evaporation and increasing of the supersaturation in the front area. Additionally, comparing the results of simulation for such two cases (with U_{in} =0 cm/s and U_{in}=20 cm/s) we conclude that the air mixing leads to increase of the number of activated particles (with the size larger than 5 μm). It happens because of extending of the front area where the most efficient growing of particles occurs. Also, we study the effect of the aerosol dynamics on the air motion. We conclude that its influence is very small and does not significantly change velocity field.

We thank the Helsinki University Centre for Environment (HENVI), the Academy of Finland (251427, 139656) and computational resources from CSC – IT Center for Science Ltd are all gratefully acknowledged. This work was supported by the Magnus Ehrnrooth Foundation.

Andrejczuk, M., Grabowski, W., Malinowski, S., Smolarkiewicz, P. (2004). *Numerical simulations of Cloud-clear air interfacial mixing.* J. of Atmospheric Sciences, 61, 1726-1739.

Babkovskaia, N., Haugen, N., Brandenburg, (2011). *A high-order public domain code for direct numerical simulations of turbulent combustion,* J. of Computational Physics, 230, 1-12.

The PENCIL Code, http://pencilcode.googlecode.com, (2001).

From free electrons to H_2SO_4 – new sources of ion catalysed SO_2 oxidation

N. Bork[1,2], N.T. Tsona[1] and H. Vehkamäki[1]

[1]Department of Physics, University of Helsinki, Helsinki, 00014, Finland
[2]Department of Chemistry, University of Copenhagen, Copenhagen, 2100, Denmark

Keywords: Ion-induced nucleation, catalysis, ions, SO_2 oxidation

Introduction

The possibility of cosmic rays effecting cloud properties has sparked a growing interest in ion induced nucleation. However, the mechanism behind ion induced nucleation remains elusive. It is most commonly explained by the increased binding energies within an ionic cluster of molecules. However, due to self dampening the resulting effect on cloud condensation nuclei concentrations is probably small.

A fundamentally different explanation is via ion induced atmospheric chemistry. It is well known that nucleation rates are closely related to H_2SO_4 concentrations. Recently, a number of studies have found evidence of a new synthesis mechanism, complimentary to the known UV induced mechanism (Kirkby *et al*, 2011, Svensmark *et al*, 2007).

We have investigated the possibility of ions catalysing SO_2 oxidation and hence both increasing nucleation rates and equally important increasing the growth rates of the freshly formed particles (Bork *et al*, 2012). It is well known that both O_2^-, O_3^- and CO_3^- are capable of oxidising SO_2, see also Fig. 1 (Bork et al, 2011).

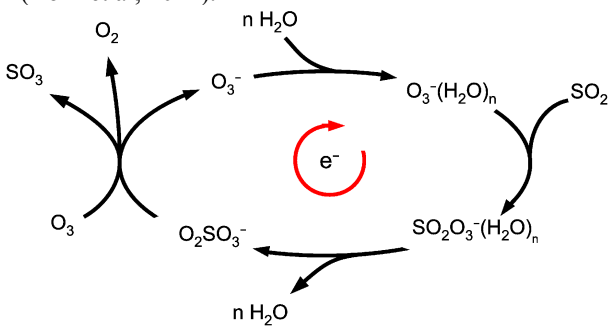

Fig. 1: The reactions involved in a simple catalytic cycle converting SO_2 to SO_3. The catalyst is the electron.

We have continued these studies by considering the chemistry of SO_4^- and NO_3^- with SO_2. Both of these ions are much more abundant than O_2^-, O_3^- and CO_3^- and are frequently seen in field studies and experiments (Ehn *et al*, 2010).

Methods

We have calculated the thermodynamic properties of all relevant species and complexes using density functional theory. Reaction rates were determined using transition state theory.

Results

Despite favourable thermodynamics we find that both reactions are effectively hindered by high energy barriers. However, since the binding energies between the ions and SO_2 are high, the molecular complexes are long lived and may react with other oxidants.

We are then lead to investigate the reactions

$$[NO_3SO_2]^- + HO_2 \Rightarrow HNO_3 + SO_4^-, \text{ and}$$
$$[SO_4SO_2]^- + O_2 \Rightarrow SO_3 + SO_5^-.$$

Both reactions involve several intermediates and energy barriers, see Fig. 2. However, we find that both of these reactions are fast and probably the dominant sinks.

Although several effects remain unknown, we estimate the effects of ion induced SO_2 oxidation and we find that it may be a significant contributor locally and possibly globally.

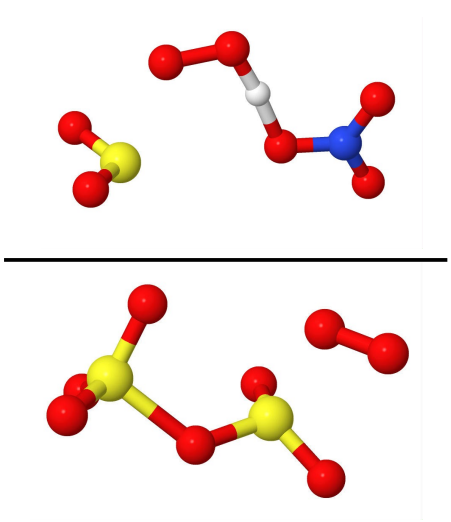

Fig. 2: Transition states of the two investigated reactions. Top: As the incoming HO_2 radical transfers a proton to NO_3^- the resulting $[SO_2O_2]^-$ cluster may evaporate. Bottom: The incoming O_2 molecule stabilizes SO_3^- as $[SO_3O_2]^-$ and enables the neutral SO_3 to evaporate.

Bork, *et al.* (2012), *Atmos. Chem. Phys.* 12, 3639.
Ehn, *et al.* (2010) *Atmos. Chem. Phys.*, 10, 8513.
Kirkby et al (2011) *Nature*, 476.
Svensmark *et al.* (2007), *Proc, Royal Soc.*, 463.

LONG TERM MODELLING OF NEW PARTICLE FORMATION AND GROWTH IN A BOREAL FOREST SITE

M. Boy[1], L. Zhou[1], D. Mogensen[1], T. Nieminen[1], S. Smolander[1] and M. Kulmala[1]

[1]Division of Atmoshperic Sciences, Department of Physics, University of Helsinki, Finland

Keywords: Nucleation, particle growth, VOC, PBL, Atmospheric Modelling

Introduction

Natural and anthropogenic aerosols may have a great impact on climate as they can directly interact with solar radiation and indirectly affect the Earth's radiation balance and precipitation by modifying clouds. In order to quantify the direct and indirect effect, it is essential to understand the complex processes that connect an aerosol particle to a cloud droplet. However, while modern measurement techniques are able to detect particle sizes down to nanometre all the way from ground up to the stratosphere, the data does not serve for all of our needs for understanding the processes. Hence we will demonstrate a modelling approach to investigate the complex processes of aerosols in the atmospheric boundary layer (ABL).

Methods

SOSAA (model to Simulate the concentration of Organic vapours, Sulphuric Acid, and Aerosols) is a 1D chemical-transport model with detailed aerosol dynamics. It was constructed to study the emissions, transport, chemistry, as well as aerosol dynamic processes in the PBL in and above a canopy (Boy et al., 2011). As a first application of the model after the aerosol dynamics module was implemented, we tested different nucleation theories by simulating the new particle formation events in the year 2010 at SMEAR II station, Finland. Since there had been numerous evidences that condensable organic vapours are the dominant contributors to the aerosol particle growth particularly in regions where biogenic volatile organic compound emissions are high, we simulated the concentrations of a set of organic compounds and used their first reaction products from oxidation by O_3, OH and NO_3 in the condensation of the nucleated clusters.

Conclusions

Different nucleation coefficients including ones suggested by Paasonen et al. 2010 has been tested in our simulations. The modelled nucleation rates are comparable with the measurements, out of which organic nucleation theory gives the best match. Our model generally gives closer estimation to the measurements in the spring and summer than in autumn and winter. One reason could be that the emission of organics in autumn and winter is underestimated. There could also be not identified other compounds like e.g. amines governs the nucleation.

The modelled growth rates between 3 and 25 showed good agreement with measurements in the spring. With the same consideration that the emission of organics is underestimated in the model in autumn and winter, it gives the expected slower growth rates in comparison with the measurements.

With the best nucleation coefficient selected, SOSAA catches most of the event days in 2010 and is able to predict the start and evolution of the events precisely (Figure 1). There are some days when we only see a burst particles appeared directly without trace of nucleation, the model predicts a complete formation event instead. These days should be looked in more detail in future.

SOSAA has showed the ability to reconstruct the general behaviour of atmospheric trace gases and new particle formation in a boreal forest environment with reasonable uncertainties.

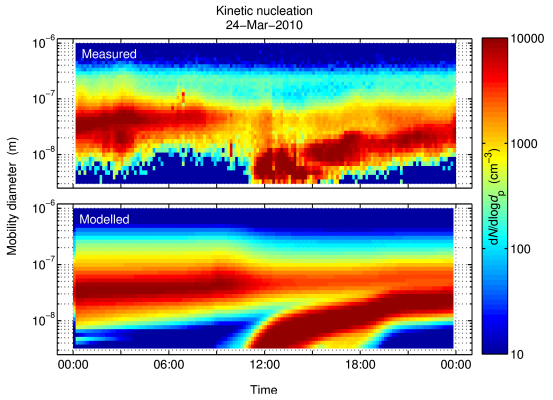

Figure 1: Modelled and measured particle size distribution at SMEAR II, Hyytiälä Finland

We thank Helsinki University Centre for Environment (HENVI) and the Academy of Finland Centre of Excellence program (project no. 1118615), for their financial support. We thank CSC – IT Centre for Science for providing computing facilities.

Boy, M. et al., *Atmos. Chem. Phys.* 11, 43-51, 2011

P. Paasonen et al., Atmos. Chem. Phys. 10, 11223-11242, 2010

Biogenic oxidation products and organic acids in aerosols from Denmark and Italy

M.K. Christensen[1], Q.T. Nguyen[1,2], A.M.K. Hansen[1], F. Cozzi[1], K. Kristensen[1], T.E. Tulinius[1], A. Tolloi[3], P. Barbieri[3], S. Licen[3], A. Massling[2], J.K. Nøjgaard[2] and M. Glasius[1]

[1]Department of Chemistry, Aarhus University, Langelandsgade 140, DK-8000 Aarhus C, Denmark
[2]Department of Environmental Science, Aarhus University, Frederiksborgvej 399, DK-4000 Roskilde, Denmark
[3]Department of Chemical and Pharmaceutical Science, University of Trieste, Via L. Giorgieri 1, I-34127 Trieste, Italy
Keyword: Secondary organic aerosols, Organic acids

Introduction

Specific carboxylic acids, such as pinic acid and adipic acid, are important molecular tracers of secondary organic aerosols (SOA) formed by photochemically oxidised volatile organic compounds of either biogenic or anthropogenic origin. Carboxylic acids may undergo further reactions to form higher molecular weight compounds, such as dimer esters (Kristensen et al., 2012). In this study we use molecular tracers to investigate the atmospheric processes leading to formation of SOA in differing environments, including an urban and a semirural background environment (Denmark) and a background area (Northern Italy).

Method

Two field campaigns were conducted at the curbside site H.C. Andersens Boulevard in Copenhagen and a semirural background site in Risø (Denmark) during May-June 2011 and the background area site near Trieste (Italy) during June 2012. Particles were collected on quartz fibre filters using high-volume samplers. Extracted particle samples were analysed by HPLC coupled through an electrospray inlet to a quadrupole time-of-flight mass spectrometer following the method of Kristensen and Glasius (2011).

Conclusion

Pinonic acid and its oxidation product 3-methyl-1,2,3-butanetricarboxylic acid (3-MBTCA) were major contributors to the total carboxylic acid concentration. The total concentration of organic acids seemed to follow the degree of aging, calculated as the amount of 3-MBTCA (Figure 1). Generally the aerosols were more aged in the beginning of the sampling period.

The concentration levels of total organic acids in the samples from Trieste (average 100 ng/m^3) were higher than the Danish samples (average 31 ng/m^3).

Future work will include more in-depth analysis of other possible influencing factors, such as regional ozone levels in addition to air mass back trajectories and meteorological data at the local sites.

We thank the VILLUM Foundation for funding this work.

K.Kristensen *et al*. (2012). *Atmos. Chem. Phys. Discuss* 12, 22103

K.Kristensen and M.Glasius (2011). *Atmos. Environ* 45, 4546.

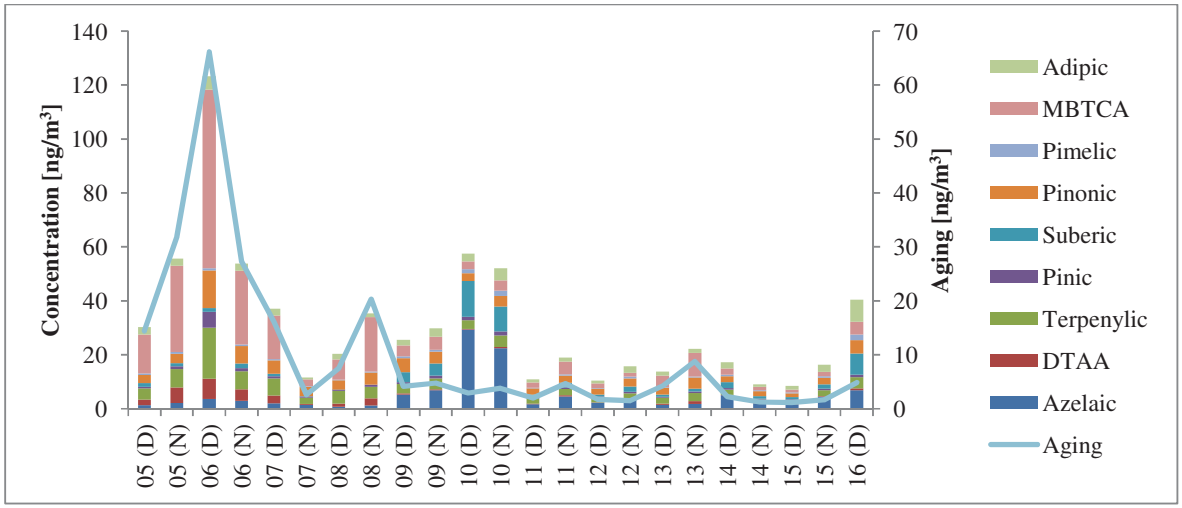

Figure 1 - Concentrations of organic acids and degree of aging in day (D) and night (N) samples from the period June 5th to June 16th 2011 on H.C. Andersens Boulevard in Copenhagen

Elemental characterization by EDXRF and source identification of $PM_{2.5}$ aerosols originating from an urban site

F. Cozzi[1], I.J. Kwame Aboh[2], D. Henriksson[2], J. Laursen[3], M. Lundin[2], M. Glasius[1] and N. Pind[1]

[1] Department of Chemistry, University of Aarhus, 8000 Århus C, Denmark
[2]School of Engineering, University of Borås, 50190, Borås, Sweden
[3] Department of Basic Sciences and Environment, Faculty of Life Sciences, University of Copenhagen, 1871 Frederiksberg C, Denmark

Keywords: EDXRF, PM2.5, PCA, source apportionment

Introduction

Among the different air pollutants airborne particulate matter (PM) is known to have both short and long term adverse effects on human health. In cities air pollution levels tend to be higher and thus urban air quality assessment is a top priority in scientific and political agenda. The $PM_{2.5}$ fraction is particularly dangerous since it is able to penetrate deeply into the respiratory system and carry there hazardous substances like e.g. metals (Pope III & Dockery, 2006).

Methods

$PM_{2.5}$ samples were collected in the city centre of Borås (SW of Sweden) in the period March-August 2006; the sampling site was located approximately 25 m above street level and can be classified as an urban background one. The sampling time was 24h and the samples were analysed for their elemental composition (As, Br, Ca, Cl, Co, Cr, Cu, K, Mn, Ni, Pb, Rb, S, Se, Si, Sr, Ti, V and Zn) by Energy Dispersive X-ray Fluorescence (EDXRF) at the Royal Veterinary and Agricultural University of Denmark.

Enrichment factors (EF) relative to earth's crustal composition were calculated in order to assess the anthropogenic impact on the element concentrations (Lopez *et al*., 2005).

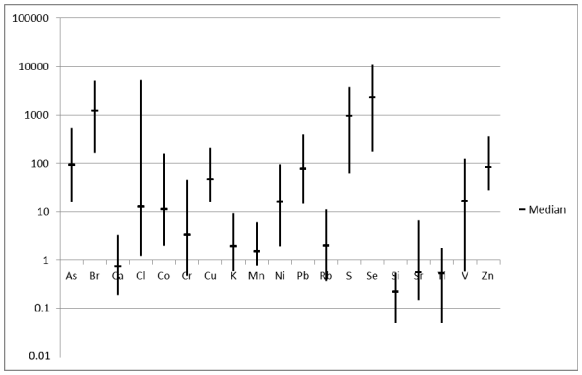

Figure 1. EF (range and median) for the analysed elements

Elements with 1< EF <10 are predominantly of crustal origin (Ca, Cr, K, Mn, Rb, Si, Sr and Ti), elements with 10< EF <100 are enriched by non-crustal sources to some extent (As, Cl, Co, Cu, Ni, Pb, V and Zn) and for elements with EF>100 non-crustal sources predominate (Br, S and Se).

Varimax-rotated Principal Component Analysis (PCA) rotation is widely used in the analysis of atmospheric aerosol (Contini *et al*., 2010) and thus it was performed to qualitatively determine the sources of the elements in the $PM_{2.5}$.

Four factors were obtained representing more than 80% of the total variability for the site: the first factor accounting for more than 50% of the total variance was dominated by Ca, Co, Cr, Fe, Mn, Rb, Si and Ti suggesting a predominant crustal source.

Factor 2 explaining around 15% of the total variance was dominated by Ni, S, Se and V; these elements are related to heavy fuel combustion.

The last two factors account each for less than 10% of the total variance: factor 3 was dominated by As, Pb and Zn that could be released from solid waste incineration activities (which are located 1 km far from the sampling site) and factor 4 was dominated by Cl; which points to a source connected to road de-icing materials: this is confirmed by time series analysis.

Additional work, based on a modification of a model by Keiding *et al*., will be applied to the sources to assess the absolute source contributions.

Conclusions

The results of this study have permitted the qualitative identification of four sources for the elements in $PM_{2.5}$: three of them are related to anthropogenic activities and two of these are connected to hazardous elements like As, Ni and Pb.

Contini, D., Genga, A., Cesari, D., Siciliano, M., Donateo, A., Bove, M.C., Guascito, M.R. (2010). *Atmos. Res.,* 95,40–54.

Keiding K., Sørensen M.S. and Pind N. (1987). *Analytica Chimica Acta*, 193, 295-307.

Lopez, J. M., Callen, M. S., Murillo, R., Garcia, T., Navarro, M. V., & de la Cruz, M. T., et al. (2005). *Environmental Research*, 99,58–67.

Pope C.A., Dockery D.W. (2006). *J Air and Waste Management Association*, 54,709-742.

Saturation vapour pressures of keto-dicarboxylic acids in aqueous solutions

I. Crljenica [1], T. Yli-Juuti [2], A. Zardini [3], J. Julin [1], M. Bilde [3], I. Riipinen [1,4]
[1]Department of Applied Environmental Science (ITM), Stockholm University, 10691 Stockholm, Sweden
[2]Department of Physics, University of Helsinki, P.O. Box 64, 00014 Helsinki, Finland
[3]Department of Chemistry, University of Copenhagen, Universitetsparken 5, 2100 Copenhagen, Denmark
[4]Center for Atmospheric Particle Studies, Carnegie Mellon University, Doherty Hall 1106, Pittsburgh, PA 15213, USA

Keywords: saturation vapour pressure, organic acids, group contribution methods, evaporation

Introduction

Organic aerosols constitute a significant mass fraction of aerosols in the atmosphere, and contain a large number of compounds with varying and poorly known physical properties. But these properties are needed to incorporate organic aerosols into large scale models. One way to estimate these physical properties is by using the various readily available group contribution methods (UNIFAC Dortmund, GCVOL-OL-60, GC-MG, Fuller et al.), and modelling. We modelled the saturation vapour pressure using experimental data for low volatility compounds of similar structure. That way the contribution of a single group can be analyzed.

Methods

The experimental data (particle diameter vs time) were obtained from a controlled-humidity laminar flow reactor and measured with an SMPS, as described in Bilde *et al.* 2003.

The evaporation is modelled with a binary mass transport model with fixed relative humidity and temperature, and dynamic activity coefficients, based on the model in Riipinen *et al.* 2006.

The physical properties of organic acids used in the model have been estimated through group contribution methods, using Poling *et al.* 2007. Activity coefficients have been calculated using the UNIFAC Dortmund method. Density has been predicted by the GCVOL-OL-60 method (Ihmels *et al.* 2003). Surface tension has been estimated with the GC-MG method (Conte *et al.* 2008). Diffusion coefficients have been calculated using the Fuller et al. method (Poling *et al.* 2007, 11.10).

The physical properties of the binary mixture have been calculated as a mass weighted average for density, and as mole weighted average for surface tension.

The comparison between the experimental data and the model results gives us the value for the saturation vapour pressure of the organic acid.

Results and Conclusions

In Figure 1 we have a typical measurement dataset for keto-dicarboxylic acids with the modelled evaporation curve, and a comparison with the modelled curve for the relevant dicarboxylic acid.

The calculated saturation vapour pressures are summarized in Table 1, alongside values from other available studies. After completing these calculations, we will investigate the performance of group contribution methods in capturing the effect of the keto-group on the saturation vapour pressures of dicarboxylic acids.

Acid name	Saturation vapour pressure		
	Keto-*acid*$_l$	Keto-*acid*$_s$†	*Acid*$_l$
	(10^{-5} Pa)	(10^{-5} Pa)	(10^{-3} Pa)
Succinic	7.7	1.0	0.89 - 1.59
Glutaric	*	1.6 - 3.2	0.75 - 1.03
Pimelic	*	0.3	/

Table 1. Values for saturation vapour pressure of liquid keto-dicarboxylic acids from this study and solid state from Frosch *et al.* 2010(†) compared to subcooled liquid dicarboxylic acids (Koponen *et al.* 2007). Values in preparation are marked *.

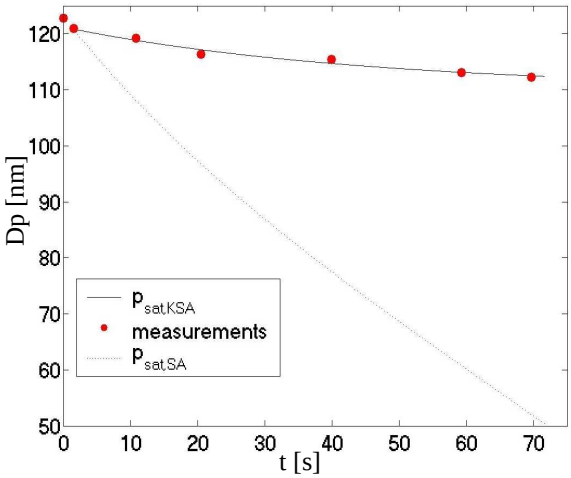

Figure 1. Modelled evaporation curve and the measurements (short residence time) for keto-succinic acid in comparison with the modelled evaporation curve for succinic acid.

This work was supported by the ERC Grant 278277 ATMOGAIN (Atmospheric Gas-Aerosol Interface: From Fundamental Theory to Global Effects).

Bilde *et al.* (2003). *En. Sci. Tech.*, 37, 1371-1378.
Riipinen *et al.* (2006). *Atmos. Research*, 82, 579-590.
Poling *et al.* (2007). *The Properties of Gases and Liquids (Fifth Edition)*. Singapore, Singapore: McGraw-Hill Education (Asia).
Ihmels *et al.* (2003). *Ind. Eng. Chem. Res.*, 42, 408-412
Conte *et al.* (2008). *Ind. Eng. Chem. Res.*, 47, 7940-7954
Frosch *et al.* (2010). *Atmos. Chem. Phys.*, 10, 5873-5890.
Koponen *et al.* (2007). *En. Sci. Tech.*, 41, 3926-3933.

CCN activation of insoluble silica aerosols coated with soluble pollutants

M. Dalirian[1], H. Keskinen[2], P. Miettinen[2], A. Virtanen[2], A. Laaksonen[2] and I. Riipinen[1]

[1] Department of Applied Environmental Science (ITM) and Bert Bolin Centre for Climate research, Stockholm University, Stockholm, Sweden
[2] Department of Applied Physics, University of Eastern Finland, Kuopio, Finland

Keywords: silica, coating, CCN activation

Introduction

Insoluble particles, e.g. mineral dust, silica and soot, can act as CCN if they acquire some deliquescent material. Extensive data and theories on CCN activation of completely soluble and insoluble particles exist but the CCN activation of coated particles has been less investigated. In this study laboratory measurements were conducted on CCN activation of insoluble silica particles coated with soluble species. The experimental results were compared to the theoretical calculations using the framework introduced by Kumar *et al*. (2011b).

Measurements

Particles with insoluble core and soluble coating were generated and analyzed in this study. Fumed silica was used as the insoluble particle. Three different kinds of species were used as soluble coatings: ammonium sulphate, sucrose and a protein (bovine serum albumin known as BSA). The fractions of soluble species were 5%, 10% and 25% of total particulate mass. Particle number distribution measurements were conducted using a scanning mobility particle sizer (SMPS). Size-resolved CCN activity is carried out using the Scanning Mobility CCN Analysis (SMCA) and the structure of atomized particles from aqueous suspension was defined by transmission electron microscopy (TEM).

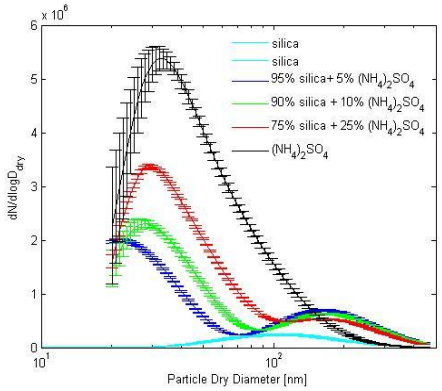

Figure 1: SMPS data for number size distributions of silica particles coated with $(NH_4)_2SO_4$.

Theory

κ-Köhler theory (Petters & Kreidenweis, 2007) was used to estimate the critical supersaturation of soluble particles. Critical supersaturation of pure silica particles, on the other hand, were calculated using the FHH adsorption theory (Sorjamaa and Laaksonen, 2007; Kumar *et al*., 2009 & 2011a). For mixed soluble and insoluble particles a shell-and-core model (introduced by Kumar *et al*., 2011b) was used in calculations.

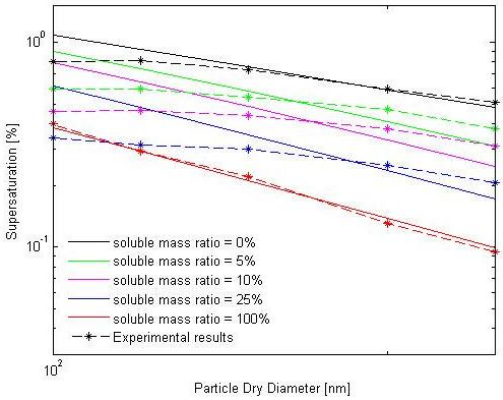

Figure 2: Calculated and experimental critical suparsaturations for silica + sucrose particles

Conclusions

Pure and mixed particles of silica and soluble compounds (AS, sucrose and BSA) were generated. Morphology of silica and BSA agglomerates changed with particle size, while $(NH_4)_2SO_4$ and sucrose were spherical. The coated particles resembled pure silica agglomerates. For pure soluble components the results were in good agreement with k-Köhler theory and for pure silica reasonable agreement was observed with adsorption theory, but deviation from the size-dependence was observed. The reason of these deviations could be: first, the adsorption parameters which were still uncertain and semi-empirical and second, the effect of changing particle morphology with size. So, our next step is quantification of the morphology effect. Mixed particles had Reasonable agreement if we knew the exact properties of the pure compounds, also morphology could be an important effect.

Financial support from CRAICC and Vetenskapsrådet is gratefully acknowledged.

Kumar, P., Sokolik, I. N., and Nenes, A., (2011a), *Atmos. Chem. Phys.*, 11, 3527.
Kumar, P., Sokolik, I. N., and Nenes, A., (2011b), *Atmos. Chem. Phys.*, 11, 8661.
Petters, M. D. and Kreidenweis, S. M. (2007), *Atmos. Chem. Phys.*, 7, 1961.
Sorjamaa, R. and Laaksonen, A. (2007). *Atmos. Chem. Phys.*, 7, 6175.

The effect of gas-phase kinetics and nanoparticle dynamics on observed particle formation

M. Dal Maso[1], H. Korhonen[2], K. Lehtinen[2], H. Vehkamäki[1]

[1]Tampere University of Technology, PO Box 962, 33010 Tampere, Finland
[2]Finnish Meteorological Institute, Kuopio Unit, P.O.Box 1627, 70211 Kuopio

Keywords: nanoparticle formation, BVOCs, sulphuric acid, laboratory experiments

Introduction

A major problem in quantitatively explain atmospheric particle formation (e.g. Kulmala et al. 2004) is the current inability to identify and quantitatively measure the actual vapors participating in particle formation. The logarithm of the nanoparticle formation rate as a function of the logarithm of vapour concentration is often used to gain insight into the formation mechanism. However, there are suggestions that such analysis is inaccurate and the effect of this on the power- law fits is unknown (Vuollekoski et al., 2010).

We investigate the most frequently used conceptual models for particle formation, such as oxidation of plant volatiles and the subsequent participation of the oxidation products in nanoparticle formation, or formation of stable clusters from sulphuric acid and oxidised plant emissions. We investigate the predictions of for the dependence of the particile formation rate on commonly measurable parameters, such as sulphuric acid concentration, probable volatile organic aerosol precursors, hydroxyl radical concentration, and the sink of nanoparticles and non-volatile vapours caused by pre-existing aerosol.

Methods

In addition to theoretical predictions derived from gas- phase kinetics analysis, we use a model that simulates the early stages of growing atmospheric nanoparticles on a resolution of a single molecule, similarly to the model described in Lehtinen and Kulmala, (2003). In practise, the model is given a formation rate and size of a stable condensation nuclei (CN); these nuclei then grow by colliding with either vapour monomers or other CN. This results in a size distribution of small CN. The coagulation coefficient for CN collisions and CN-monomer -collisions are calculated using the Fuchs coagulation kernel for the wet aerosol sizes assuming spherical particles (Lehtinen et al., 2007).

Discussion

There are several phenomena affecting the detection of atmospheric particle formation rates. One of them is the loss of fresh particles due to coagulation to background, and also apparent losses due to change in the size distribution shape. This has been extensively studied theoretically (Lehtinen et al., 2007, Anttila et al., 2010). Another process affecting the determination of the apparent particle formation rate is the intermodal coagulation affecting the shape of the just-formed particle mode. Our model simulations show that the new particle population shape quickly changes shape, starting to resemble a log-normal size distribution due to collisions between young clusters. This, in turn, affects the time derivative of CN measured at larger sizes than the nucleation size, as the edge of the fresh mode passes the detection threshold of the measuring instrument. We discuss the effect of these processes as well as the effect of different temporal behaviour of the temporal profile of the condensing vapour production rate.

Conclusions

The magnitude of the reaction pathways leading to aerosol formation in comparison to non-aerosol forming pathways is a key factor determining the functional dependence of the observed formation rate on measurable parameters. In addition, nano-size aerosol dynamics add another layer of complexity to the analysis.

References

Anttila, T., et al (2010): Paramererizing the formation rate of new particles: The effect of nuclei self-coagulation, J. Aerosol Sci., 41, 621–636, doi: 10.1016/j.jaerosci.2010.04.008, 2010. 18783, 18785

Kulmala, M.,et al (2004) Formation and growth rates of ultrafine atmospheric particles: A review of observations Aerosol Science 35, 143-176.

Lehtinen, K E J. and Kulmala, M. (2003): A model for particle formation and growth in the atmosphere with molecular resolution in size, Atmos. Chem. Phys., 3, 251-258

Lehtinen, K.E.J. et al: (2007) Estimating nucleation rates from apparent particle formation rates and vice versa: Revised formulation of the Kerminen–Kulmala equation J. Aerosol. Sci 38 (9), 988-994.

Vuollekoski, H., et al (2010) A numerical comparison of different methods for determining the particle formation rate Atmos Chem Phys Discuss, 10, 18781–18805

Can an influence of changing aerosol emissions be detected in the pattern of surface temperature change between 1970 and 2000?

Annica M. L. Ekman[1,2], H. Struthers[1,2,3], A. Lewinschal[1,2], K. J. Noone[2,3], T. Iversen[4,5], A. Kirkevåg[4] and Ø. Seland[4]

[1)] Department of Meteorology, Stockholm University, Sweden
[2)] Bert Bolin Center for Climate Research, Stockholm University, Sweden
[3)] Department of Applied Environmental Science, Stockholm University, Sweden
[4)] Norwegian Meteorological Institute, Oslo, Norway
[5)] Department of Geosciences, University of Oslo, Norway

Keywords: aerosol, temperature, large-scale circulation, precipitation

Introduction

Since the 1970's, there has been a rapid change in the magnitude and spatial distribution of anthropogenic aerosol particle and precursor emissions in the world with a significant decrease over e.g. Europe and North America and a substantial increase over large parts of Asia. During the same time period, there has been a significant increase in global greenhouse gas concentrations. In the present study, the global climate model CAM-Oslo (Seland *et al*., 2008; Struthers *et al.*, 2011) is used to examine if the shift in aerosol emissions between 1970 and present day results in a clear fingerprint in the modeled atmospheric circulation, precipitation and temperature change patterns. CAM-Oslo includes a comprehensive module of the atmospheric aerosol cycle as well as descriptions of the direct and indirect effects of aerosol particles on radiation, cloud reflectivity and precipitation. We also examine if the temperature response pattern differs when aerosol effects are considered separately or simultaneously with a change in greenhouse gas concentration.

Methods

70 years of equilibrium simulations for the year 1970 and 2000 were performed using the global climate model CAM-Oslo coupled to a slab ocean. Aerosol direct effects on radiation (and subsequent semi-direct effects), indirect effects on cloud albedo (first indirect effect) and precipitation formation (second indirect effect) were simulated online within CAM-Oslo, i.e. the aerosols affect temperature, cloud and precipitation formation and vice versa. The last 40 years of the simulations were utilized in the analysis. In order to obtain instantaneous anthropogenic aerosol radiative forcing (RF) estimates (as defined by Forster *et al*., 2007), five year-long simulations with diagnostic calculations of the direct and first indirect effect were also conducted. Note that in these RF calculations, there are no feedbacks between the aerosols and the modeled meteorology. To evaluate the model, we compared the simulations to station-based observational data of temperature (CRUTS3.1), and re-analysis data of 300 hPa geopotential height from NCEP/NCAR.

Conclusions

The simulated aerosol RF (comparing the year 2000 and 1970) is in general poorly correlated with the surface temperature response (Figure 1). The global average RF is negative (-0.18 Wm^{-2}), resulting in an overall cooling of the northern hemisphere (-0.24 K). Simulations including both changes in greenhouse gases and aerosols display that it is mainly over South Asia that a clear local response due to anthropogenic aerosols is visible. The results are in line with e.g. Palmer (1999), Boer and Yu. (2003) and Lewinschal *et al*. (2012) and illustrate that the forcing signal (e.g. spatial pattern of temperature change) to a large extent is governed by local feedback processes and by changes to the residence frequency of quasi-stationary circulation regimes.

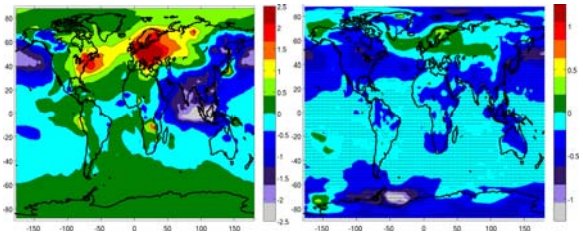

Figure 1. Simulated instantaneous RF (left figure, Wm^{-2}) and surface temperature change (right figure, K) comparing the years 2000 and 1970. Only changes in aerosol emissions are considered. Dotted areas in the right hand figure denote statistical significance at the 90% confidence level.

Boer, G. J., Yu, B. *Climate Dynamics*, 20, 415-429, 2003.

Forster, P., V. et al. In: Climate Change 2007: The Physical Science Basis. Contribution of Working Group I to the 4th AR of the IPCC. 2007.

Lewinschal, A. Ekman, A. M. L., Körnich, H. *Submitted to Climate Dynamics*, 2012.

Palmer, T. *J. Clim.*, 12, 575-591, 1999.

Seland, Ø., et al., *Tellus A*, 60, 459-491. 2008.

Struthers, H. et al., *Atmos. Chem. Phys.*,11, 3459-3477, 2011.

Computational methodology study of the oxidation of atmospheric oxygenated organics by the OH radical.

Jonas Elm, Solvejg Jørgensen, Merete Bilde and Kurt V. Mikkelsen

Department of Chemistry, University of Copenhagen, H. C. Ørsted Institute, 2100 Copenhagen Ø, Denmark

Keywords: Oxidation of organics, quantum mechanics, reaction mechanism, tunnelling,

Introduction

In the recent decade significant scientific progress have been made in the characterization of the initial formation of pre-nucleation clusters and their successive growth to critical clusters, but the exact mechanism still remain elusive. The mechanism is known to be multi-component with H_2SO_4-H_2O-X, where X has been suggested to be either ammonia, amines, ions or organics. Enhanced nucleation by organic oxidation products has under laboratory conditions been shown to be significant. Oxidation of organic compounds by the OH radical can lead to more volatile oxidation and degradation products. Identifying reaction mechanisms and thereby quantifying which oxidation products are formed can be a laborious task experimentally and by utilizing quantum mechanical methods it is possible to get insight into oxidation pathways at the molecular level and thereby study the reaction mechanisms in detail.

We have computationally studied the gas phase hydrogen abstraction reaction kinetics of short chained oxygenated organics by the OH radical in order to identify an applicable methodology which is able to reproduce experimentally determined rate constants and branching ratios.

Theory

The rate constant of the *i*'th hydrogen abstraction pathway is modelled using conventional transition state theory using a complex two-step mechanism which initially involves the barrier-less formation of a reactant complex. The total rate constant is then calculated as the sum over the individual reaction paths by taking the reaction path degeneracy and quantum mechanical tunnelling contribution into account. From the individual and total rate constants the branching ratios and hence the reaction mechanisms of the compounds can be estimated.

Methodology

A test set of 9 atmospheric relevant oxygenated compounds (CH_3OH, CH_3CH_2OH, H_2CO, CH_3CHO, CH_3COCH_3, CH_3OCH_3, HCOOH, CH_3COOH, $HCOOCH_3$) and a total of 18 hydrogen abstraction reactions is chosen as a representative benchmark for the study. The rate constants and branching ratios are investigated with density functional theory (BH&HLYP, BMK, M06-2X, mPW1K) with the large aug-cc-pVTZ basis set, complete basis set extrapolation procedures (CBS-QB3, G3), Møller Plesset second order perturbation theory (MP2/aug-cc-pVTZ) and compared to Coupled-Cluster Singles Doubles (CCSD/6-311+G(d,p)) and experimental data. The performance of DFT in predicting the imaginary vibrational frequency of the nuclear motion at the transition state is evaluated in order to assess tunnelling effects using Wigner, Bell and Eckart tunnelling corrections. Several different hybrid methodologies utilizing DFT/MP2 structures and vibrational frequencies with high level single point energy corrections using explicitly correlated Coupled Cluster Singles Doubles with perturbative triples (CCSD(T)-F12a/VTZ-F12) are studied in order to identify an approach for obtaining reliable reaction kinetics for atmospheric relevant organics.

Conclusions

From the investigated benchmark we find several effects important in order to compute accurate rate constants consistent with experimental values. Due to the exponential dependence of the rate constant high level single point energy corrections are needed. We find big discrepancies in the performance of the different methods in predicting the imaginary vibrational frequency of the nuclear motion at the transition state which is of high importance to evaluate the tunnelling corrections. Furthermore we find the quantum mechanical tunnelling factor to be non negligible and extremely important in order to explain the correct reaction mechanism. We find that the BH&HLYP functional is able to reproduce the correct nuclear motion of the transition state and yield reaction rates with a mean absolute error as low as a factor of ~2 compared to experiments as well as describing the correct reaction mechanism.

The identified methodology can be utilized to investigate the reaction mechanism of complex organic molecules of natural, anthropogenic and biological origin to identify which oxidation products are most likely to be formed.

Physical and chemical characterization of urban aerosol particles through Soot Particle Aerosol Mass Spectrometry

A.C. Eriksson[1], J. Pagels[2], J. Rissler[2], S. Sjögren[1] and E. Swietlicki[1]

[1]Division of Nuclear Physics, Lund University, Box 118, 22100, Lund, Sweden
[2]Division of Ergonomics and Aerosol Technology, Lund University, Box 118, 22100, Lund, Sweden

Keywords: Ambient aerosols, black carbon, SPAMS

Introduction

Urban aerosol particles consist of complex mixtures, including organic compounds, salts and black carbon. The physical and chemical properties of the particles determine their effects on human health and climate, and gives clues to their origins and atmospheric fates. We report a preliminary characterisation of the submicrometer street side Copenhagen aerosol during the winter of 2011-12.

Method

Aerosol mass spectrometry (AMS) is a powerful tool for on-line chemical measurements of PM1. The High Resolution Time of Flight (HR-ToF)-AMS probes non-refractory PM (NR-PM) with high sensitivity and time resolution, and with a mass resolution sufficient for elemental analysis. Size-resolved measurements are possible through use of Particle Time of Flight (PToF). NR-PM is defined as the fraction of PM that vaporizes when impacted on a heated (600 °C) tungsten (W) surface under vacuum.

Refractory black carbon (rBC) is an important component of PM. This has prompted the development of the Soot Particle-AMS (SP-AMS), in which an intracavity laser (1064 nm) is used to vaporize particles which contain rBC (Onasch et al 2012). In this campaign the SP-AMS was used in dual vaporizer mode, where the W vaporizer is used alternated with combined laser and W vaporization. The data produced is comparable with standard HR-ToF AMS data, but contains additional information about the rBC content of particles. Furthermore, comparing the two alternating measurements yields information on the internal mixing of rBC with other species.

Results and Conclusions

It was found that on average the particles sampled consisted of 44% organic compounds, 20% rBC, 14% nitrate, 13 % sulphate and 6 % ammonium by mass. About half of the rBC occurred in small particles, with a high degree of internal mixing with organic PM. Virtually no nitrate or sulfate was found in these smaller particles, which likely originated from freshly emitted vehicular exhaust. The remaining rBC was found in larger size particles, to some degree internally mixed with organic and inorganic compounds. This fraction of rBC is attributed to long range transport.

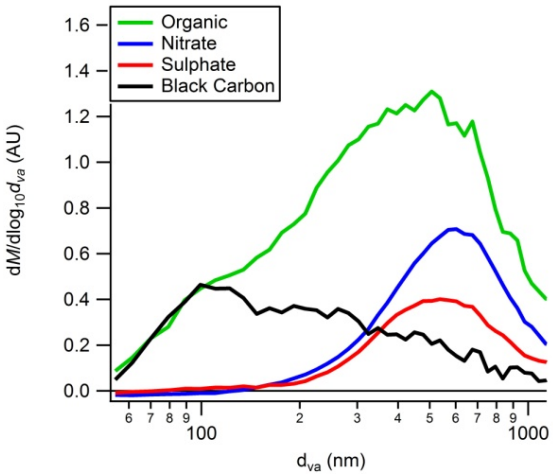

Figure 1: Chemically resolved size distributions, campaign average.

The mass loadings of rBC and organic aerosol were highly variable, brief (<1 min) spikes with elevated loadings were frequent. These likely originate from exhaust emitted close to the measurement site.

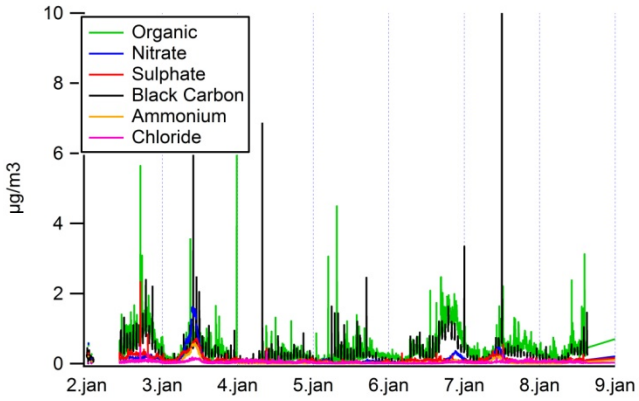

Figure 2: Timeseries from the first week of january 2012.

Onasch, T.B., Trimborn, A., Fortner, E.C., Jayne, J.T., Kok, G.L., Williams, L.R., Davidovits, P. and Worsnop, D.R. *Aerosol Science and Technology*, 46, 804-817, 2012.

Hygroscopic Growth of Selected Amino Acids in Organic Aerosols, Using Water Activity Measurements

Mehrnoush M. Fard[1], Matthew S. Johnson[1], Merete Bilde[1]

[1]Department of Chemistry, University of Copenhagen, Copenhagen, Denmark

Keywords: Hygroscopicity, water activity, WSOC, Hydrophobicity

Introduction

The chemical composition of a particle determines its hygroscopic behavior. Over the years, studies have shown that up to 50% of tropospheric aerosols are composed of organic compounds. These organic species contribute to the water uptake properties of aerosols and impact climate, health, and visibility on Earth. Our knowledge about the hygroscopic behavior of organic carbon (OC) in particles is limited and uncertain. Most published studies on hygroscopic growth of OC in particles have focused on water-soluble organic carbon (WSOC) and the water uptake behavior of hydrophobic species is largely unknown. For this reason we have built a new set up to measure the partial pressure of water over saturated aqueous solutions at controlled temperature. From these measurements we plan to infer the hygroscopic growth factor (G_f) of some selected amino acids ranging from highly soluble to sparingly soluble, and their mixtures with NaCl (Sodium Chloride) and $(NH_4)_2SO_4$ (Ammonium Sulfate).

Methods

A vapor pressure apparatus adopted from the design of Zamora et.al (2011) was built as shown in Figure.1. Solutions are prepared by adding the solid component to the filtered water and stirring to ensure a homogeneous composition. The sample vessel containing the solution is connected to the apparatus and goes through several freezing/purging/thawing cycles to purify the sample and evacuate the gas headspace above the solution. Next, the sample vessel is submerged in a constant temperature bath at the target temperature and its water vapor pressure is measured. The equilibrium water vapor pressure over the solution obtained from this method is used to calculate the water activity (a_w) of each solution, which is defined as:

$$a_w = \frac{p_v(T)}{p_{v,s}(T)}$$

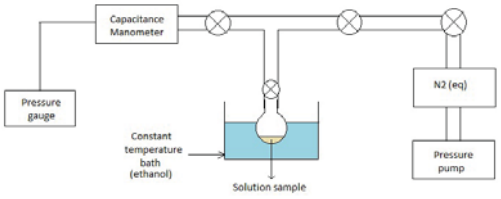

Figure.1 Experimental Setup

The hygroscopic growth factor (G_f) of aerosols is defined as D_{wet}/D_{dry} where D_{dry} refers to the dry particle diameter and D_{wet} is the wet particle diameter at a specific RH. The water activity data obtained from vapor pressure experiment will be used to calculate G_f for each solution.

The vapour pressure apparatus was calibrated against values for pure water obtained from Seinfeld & Pandis (2006) for temperatures ranged from 273.15K to 298.15 K (Figure.2).

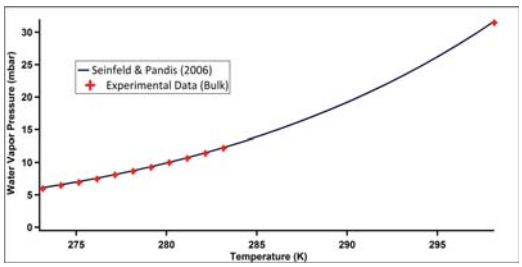

Figure.2

Outlook

The setup will be presented in detail, along with the first results obtained from amino acid solutions and their mixture with inorganic salts and possible implications of the findings.

Zamora, I., et al. (2011) *J. Geophys. Res*, 116, D23207.

Seinfeld, J. H., and S. N. Pandis (2006), *Atmospheric Chemistry and Physics: From Air Pollution to Climate Change*, (John Wiley, New York), 12-14.

Effects of intense ageing on volatility and chemical composition of urban aerosol particles

M. Frosch[1], E. Ahlberg[1], A. Eriksson[1], S. Sjögren[1], J. Pagels[2], J. Rissler[2], E. Swietlicki[1], W. H. Brune[3] and B. Svenningsson[1]

[1] Division of Nuclear Physics, Lund University, Box 118, 22100, Lund, Sweden
[2] Division of Ergonomics and Aerosol Technology, Lund University, Box 118, 22100, Lund, Sweden
[3] Department of Meteorology, Pennsylvania State University, University Park, PA 16802, USA

Keywords: Ambient aerosol, oxidative ageing, Potential Aerosol Mass, AMS

Introduction

Aerosol particles form a ubiquitous component of the Earth's atmosphere, which has profound effect on for example visibility, human health and climate change.

A significant source of organic aerosol (OA) is oxidation of volatile organic compounds (VOC) in the gas phase, leading to formation of less volatile compounds. These can nucleate to form secondary organic aerosol (SOA) particles or condense on existing particles. The lifetimes and fates of atmospheric species depend strongly on physical properties, e.g. phase, and chemical properties.

We here characterize particles at street level in central Copenhagen in terms of mass and number, chemical composition and volatility. Particles were in some cases exposed to additional ageing.

Methods

Particles were sampled in central Copenhagen during Jan-Feb 2012 and characterized using a scanning mobility particle sizer (SMPS), an aerosol mass spectrometer (AMS) and a thermodenuder (TD). Effects of ageing were investigated with a potential aerosol mass (PAM) chamber.

PAM is defined as the maximum aerosol mass produced through oxidation of precursor gasses. In the PAM chamber, SOA production occurs in a highly oxidizing environment ensuring rapid reaction of precursor gasses. Thus, all processes instigated by photo-oxidation of gas phase components occur in minutes in PAM as they would over hours or days in the atmosphere (Kang et al., 2007).

In the present study, particles were exposed to high levels of ozone (up to 16 ppm) and OH radical (exposure up to $1\text{-}2\cdot10^{12}$ molecules·s·cm^{-3}, corresponding to 1-2 weeks of OH exposure under ambient conditions).

Results

Large numbers of fresh particles were generated by nucleation in the PAM chamber, but these were too small to significantly alter the particle mass detected with AMS. However, alterations of the organic fraction were detectable with AMS, possibly a consequence of condensation or heterogeneous reactions. The main change was an increase of O:C ratio and decrease in H:C ratio (Figure 1).

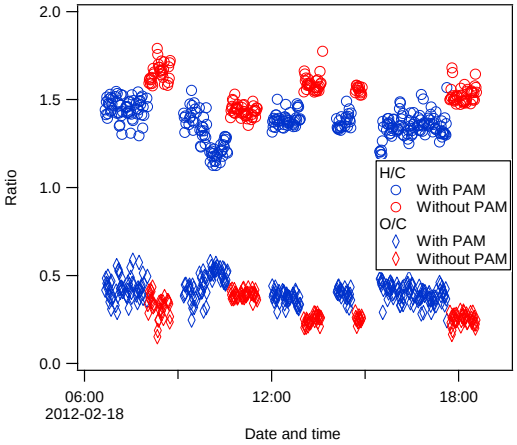

Figure 1: O:C and H:C ratios sampled with/without PAM chamber.

Also, volatilities of the OA components were influenced by the reaction in the PAM chamber (see Figure 2): The fractions of m/z 43 and 44 to total OA mass (f_{43} and f_{44}) were used as markers for hydro-carbon like and oxidized OA, respectively. Absolute values of f_{43} and f_{44} of particles exposed to elevated temperatures in the TD varied, depending on whether particles were sampled through the PAM chamber.

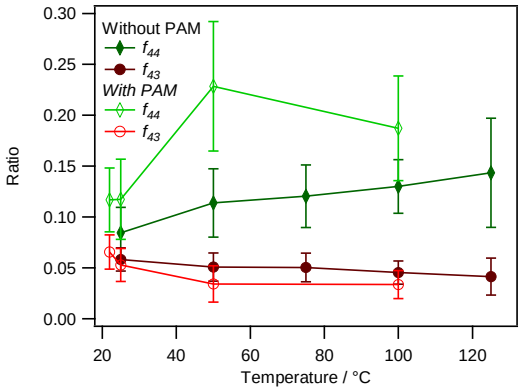

Figure 2: f_{43} and f_{44} of particles sampled with/without PAM exposed to different temperatures

We acknowledge support from VR and FORMAS.

Kang, E. Root, M. J., Toohey, D. W. & Brune, W. H. *Atmos. Chem. Phys.*, 7, 5727-5744, 2007.

Hierarchical Agglomerative Cluster Analysis Applied to WIBS 5-Dimensional Bioaerosol Data Sets

M.W. Gallagher[1], N.H.Robinson[1,4] , P. H. Kaye[2], and V.E. Foot [3]

[1]Centre for Atmospheric Science, University of Manchester, Simon Bldg, Oxford Rd, Manchester, M13 9PL, UK

[2] Centre for Atmospheric & Instrumentation Research, STRI, University of Hertfordshire, Hatfield, AL10 9AB, UK

[3] DSTL, Porton Down, Salisbury, Wiltshire, SP4 0JQ, UK

[4] Now with UK Meteorological, Office, Fitzroy Road, Exeter, Devon, EX1 3PB, UK

Keywords: Hierarchical Cluster Analysis, Bioaerosol, UV-fluorescence, WIBS, Rainfall

Introduction

Primary biological aerosol particle (PBAP) classification requires discrimination of particles various diverse sources which may have wide reaching effects in the atmosphere. In order to predict these effects under future emissions scenarios it is useful to be able to identify ambient PBAP concentration. To date, this has largely been achieved by the use of off-line techniques, which, whilst allowing accurate identification of different aerosols, are labour intensive and have poor time resolution.

To improve on this we have investigated the use of hierarchical agglomerative (HA) cluster analysis applied to single-particle multi-spatial (5-D) datasets comprising optical diameter, particle asymmetry and three induced fluorescence waveband measurements, from two commonly used dual Waveband Integrated Bioaerosol Spectrometers (WIBS), (Kaye et al., 2005). We show that HA cluster analysis, without the need for any *a-priori* assumptions concerning the expected aerosol types, can reduce the level of subjectivity compared to the more standard analysis approaches for multi-parameter aerosol measurements.

Methods

We use two WIBS– a model 3 and a model 4 (Gabey *et al*., 2011). In both models the single particle elastic scattering intensity (at 633 nm) is used to infer particle optical-equivalent diameter, D_O. A quadrant PMT measures the variation in azimuthal scattering and hence provides a particle asymmetry factor, A_F. This measurement triggers pulses from filtered xenon flash-lamps at 280 nm and 370 nm, designed to excite tryptophan and NAD(P)H molecules within the particle. Fluorescence is measured in two wavelength regimes, FL1 & FL2 providing three fluorescence channels; FL1 & FL2 following the 280 nm excitation and FL2 following the 370 nm excitation. The FL1 and FL2 fluorescence detection regimes overlap spectrally in the WIBS3, but have been separated in the WIBS4.

A software tool (WIBS Analysis Program, WASP) was developed that applies the average-linkage HA-cluster analysis algorithm (Everitt, 1993, Robinson et al. 2012) to WIBS data. Average-linkage defines the two most similar clusters as those with the smallest distance across an n-dimensional space, where n is the number of particle diagnostics. The distance between two clusters is defined as the average squared Euclidian distance between all possible pairs of particles, or

$$L_{A,B} = \frac{1}{pq}\sum_{i=1}^{p}\sum_{j=1}^{q}\left\|A_i - B_j\right\|^2$$

where $L_{A,B}$ is the cluster distance, $\boldsymbol{A}$ the coordinate vector of cluster $\boldsymbol{A}$ containing p members, and $\boldsymbol{B}$ the vector for cluster B with q members. Physically realistic cluster solutions and particle apportionment is achieved with *d*-metrics and z-score analysis. This was applied to laboratory test data using NIST non-fluorescent and fluorescence particles. It was then applied to ambient measurements collected during the BEACHON-RoMBAS experiment at an elevated pine forest (Manitou National Forest, Colorado USA).

Conclusions

We successfully demonstrate application of the HA-cluster analysis approach to real-time induced fluorescence bioaerosol data sets. Different diehl cycles for the various bioaerosol classes, associated with fungal spores, bacteria, dust etc., are presented from a forest ecosystem. The different influences of rainfall on different bioaerosol classes is highlighted as an example of the power of the technique. Finally micrometeorological fluxes of different bio-aerosol classes are inferred from multi-height measurements.

This work was supported by the UK NERC

Everitt, B. S. (1993). Cluster Analysis (3rd ed.). *New York: John Wiley & Sons*.

Gabey, A. M., Gallagher, M. W., *et al.* (2010). *Atmospheric Chemistry and Physics*, 10(10), 4453-4466.

Kaye, P. H., *et al.* (2005). *Opt. Express*, 13, 3583. 6389.

Robinson, N.H., *et al.*. (2012). *Atmos. Meas. Tech. Discuss*., 5, 6387–6422.

Do carbonaceous particles in diesel exhaust originate from the fuel or lubricant oil?

J. Genberg[1], P. Tornehed[2], Ö. Andersson[3] and K. Stenström[1]

[1]Division of nuclear physics, Lund University, Lund, Sweden
[2] XXS – Business Statistics, Scania, Södertälje, Sweden
[3]Dept of Energy Sciences, Lund University, Lund, Sweden

Keywords: Traffic related aerosols, carbonaceous aerosol, bio diesel, ^{14}C

Introduction

Sources of atmospheric particles have been studied extensively for many years. One source commonly mentioned when looking at carbonaceous particles is diesel powered transportation since their exhaust contain both organic and elemental carbon. But from what carbon source in the engine do the particles form? We investigated diesel exhaust to determine if the particulate originated from the diesel fuel or the lubricant oil.

Methods

Filter samples were collected while the engine run the World Harmonized Transient Cycle (WHTC) or was kept at a static load point. The engine was powered by biodiesel with a $F^{14}C$ value of 0.946 while the oil was fossil mineral oil. Filters were analysed for organic carbon (OC) and elemental carbon (EC) content and ^{14}C content of total carbon (TC). Also the chain length of the hydrocarbons (HC) were analysed using GC which is used to determine between fuel-HC and oil-HC. This gives us two separate measures of the source of the particles.

Results

HC and OC analyses showed that most of the OC found on the filter could be attributed to unburnt fuel or oil (Figure 1). The GC analysis results of the HC could therefore be translated into a $F^{14}C$ of the OC fraction. Together with the $F^{14}C$ of the total carbon the source of the EC could be calculated. This shows that almost all EC originate from the diesel fuel for the last two runs (Table 1).

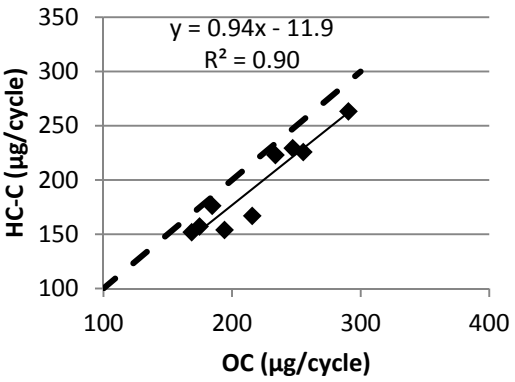

Figure 1. HC-C (carbon mass in HC) and OC measured on the same filters.

During the first two runs, the exhaust contained more HC and EC of oil origin. This led to a total particulate emission which was much higher for these runs compare to the engines normal performance.

Table 1. EC/TC quotients and percent fuel origin of EC for 4 WHTC runs.

Sample	EC/TC	% fuel EC
WHTC 1.1	0.46	79
WHTC 1.2	0.51	79
WHTC 2.1	0.24	95
WHTC 2.2	0.20	95

Besides WHTCs, static load points were also investigated. With increasing motor load and speed, oil contributed to HC to a higher degree (Figure 2).

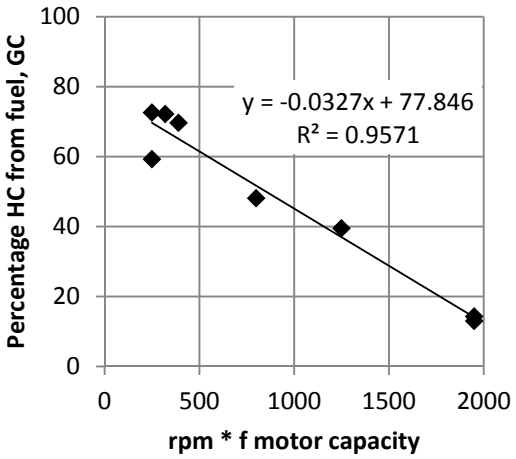

Figure 2. Percentage of HC originating from fuel with varying engine settings. On the x-axis, engine speed (rpm) times fraction of maximum engine capacity is plotted.

Modelling studies of new particle formation and growth in Southern African savannah environment

R. Gierens[1], L. Laakso[2,3], V. Vakkari[1], D. Mogensen[1], P. Beukes[3], P. Van Zyl[3] and M. Boy[1]

[1]Department of Physics, Division of Atmospheric Sciences, University of Helsinki, Helsinki, 00014, Finland.
[2]Finnish Meteorological Institute, Research and Development, FI-00101, Finland.
[3]School of Physical and Chemical Sciences, North-West University, Potchefstroom, South Africa.

Keywords: aerosol modelling, particle formation and growth, boundary layer, South African Savannah

Africa is one of the least studied continents in respect to atmospheric aerosols. In this study measurements from a relatively clean savannah environment in South Africa were used to model new particle formation and growth. There are already some combined long-term measurements of trace gas concentrations together with aerosol and meteorological variables available (Laakso et al., 2008), but to our knowledge this is the first time detailed simulations, that include all the main processes relevant to particle formation, were done.

MALTE (Model to predict new Aerosol formation in the Lower TropospherE) is a onedimensional model, which includes modules for boundary layer meteorology, emissions from the canopy as well as aerosol dynamical and chemical processes (Lauros et al. , 2011). Previous studies indicate that this model is able to predict new particle formation events at the surface and in the boundary layer with good agreement compared with measurements.

The measurements utilized in this study were done at a relatively clean background savannah site in central southern Africa. The location is characterized with relatively low pollutant concentrations with occasional polluted air masses from the industrial areas 100-300 km to the east. New particle formation at the site has been found to take place during most of the sunny days, 69 % of the days showing clear nucleation with additional 14 % of the days with nongrowing nucleation mode (Vakkari et al., 2011).

The observational data was used for input and comparisons with the simulations. We selected a couple of days of continuous data and varying conditions of clean and polluted background air. Figure 1 shows the measured and modelled particle size distributions for one day (the 10th of October 2007), during which a relatively polluted air mass was advected on the site. The model was able to reproduce the nucleation event and the growth of the particles, but the particles grow to the detected size, which is shown in the figure with a white line, later than observed.

The frequent new particle formation events and particle growth for the simulated days was evaluated in detail. We were able to simulate the aerosol number concentrations of newly formed particles with a reasonable good agreement with the measurements. This work will present new model results to give a better understanding on the new particle formation process in South Africa and discuss the reasons for high frequency of nucleation episodes observed.

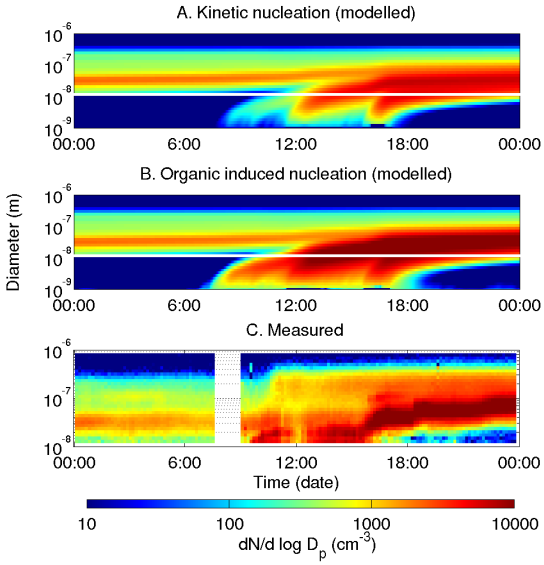

Figure 1. Particle number size distribution on the 10th of Oct assuming a) kinetic nucleation and b) organic induced nucleation in the simulation, and c) from the measurements. The white line in a and b show the detection limit of the instrument at 10nm.

This work was supported by the Finnish Academy, Finnish Center of Excellence and Helsinki University Center for Environment.

Lauros, J., Sogachev, A., Smolander, S., Vuollekoski, H., Sihto, S.-L., Laakso, L., Mammarella, I., Rannik, Ü., and Boy, M. (2011). *Atmos. Chem. Phys.*, 11 , 5591-5601.

Vakkari, V., Laakso, H., Kulmala, M., Laaksonen, A., Mabaso, D., Molefe, M., Kgabi, N. and Laakso, L. (2010). *Atmos. Chem. Phys.*, 11 , 3333-3346.

Airborne Bacteria in Operating Theaters

F. Grantén[1], P.-A. Larsson[2], M. Ramstorp[1], M. Bohgard[1] and J. Löndahl[1]

[1]Department of Design Sciences, Lund University, SE-221 00, Lund, Sweden
[2] Research department, Region Skåne - Helsingborgs lasarett, SE-251 87, Helsingborg, Sweden

Keywords: Bioaerosol, Operating Theater, Live Surgery, Health

Introduction

Postoperative infections are the third most common nosocomial infection in Sweden and occur at about 7% of all surgeries (SIS, 2011). The infection is usually caused by contamination during the operation itself. A contributive part of the infections are bioaerosols, or more specific airborne bacteria, and given the increasing antibiotic resistance, a larger understanding of bioaerosols is paramount. Previous studies have suggested that operating theatres (OTs) with laminar air flow (LAF) ceiling ventilation is considerably cleaner and more aseptic than standard OTs, but all studies do not agree (Lindblom, 2007). A number of parameters affect the generation and movement of bioaerosols. The purpose of this study was to measure these parameters during live surgery to improve understanding of airborne bacteria in OTs.

Methods

A ventilated measuring trolley was constructed to contain the equipment, and guarantee hygiene, electrical safety, low noise and experimental control. The instrumentation consisted of an aerodynamic particle sizer (APS, TSI model 3321) for detailed size sampling, a DustTrak (TSI, model 8520), and a bacteria sampler. Also CO_2, absolute pressure, temperature and relative humidity was monitored. During the surgery, notes were taken with door openings, people in the OT, level and type of activity. The measurements were conducted in two different OT:s with either normal ventilation or LAF ceiling, both during orthopedic surgery. Bacteria were sampled from the air on gelatin filters (Sartorius, MD8) and incubated on blood agar plates for two days at 37ºC.

Results

Measurement location	*CFU/m³(**Mean** ± SD)*
Mixed ventilation OT	**20,91** ± 22,81
-Low activity	**8,12** ± 6,80
-High activity	**55** ± 11,40
Laminar ventilation OT	**1** ± 2,41
-Under LAF	**0** ± 0
-Outside of LAF	**2** ± 3,26
Preparation room	**5** ± 3,53
Clean corridor	**8,75** ± 5,30
Patient corridor	**65** ± 14,14

Table 1: average Colony Forming Units(CFU) per m³ with standard deviation for different Operating Theatres and adjacent corridors.

It was found that in the regular ventilated OT, the CFU/m3 is largely dependent on the surgical procedure, and in the LAF OT not a single CFU was detected in the clean zone. Further results indicate that particle concentration increase with number of attending people, activity around operating table and door openings. (see fig.1)

Figure 1: Particle size distribution (red=high conc.) with

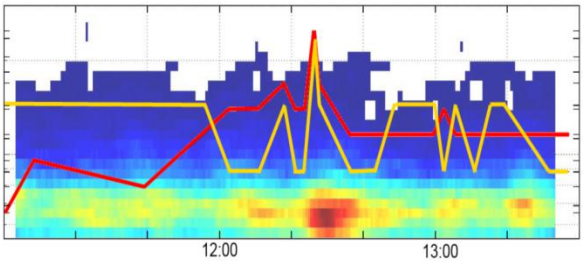

overlying number of people (red line and relative activity level (yellow line).

Conclusions

The position of the sample point appears to be crucial. It was in general crowded around the patient and therefore difficult to sample near the incision. Hygiene and noise are also parameters to keep in mind when choosing equipment.

Future measurements should contain multiple simultaneous measurement points as well as CFU measurements with higher throughput and resolution. Either an easier setup, a person dedicated for taking notes or video surveillance for more detailed notes. Classification of bacteria may provide important source information and a longer measurement campaign for statistically verifiable results.

Measurements with a number of instruments during live surgery are possible, but special precautions are necessary to avoid influencing safety of the patient.

References

SIS, (2011) "*renhet i operationssalar" Remiss 9252*

Lindblom, A. (2008) "*Ventilation med ultraren luft jämfört med konventionell ventilation på operationssalar"*. Smittskyddsinstitutet

Modeling of secondary aerosol formation from α-pinene oxidation

E. Hermansson[1,2], P. Roldin[1,2], E. Swietlicki[1,2], D. Mogensen[3], A. Rusanen[3] and M. Boy[3]

[1]Division of Nuclear Physics, Department of Physics, Lund university, P.O. Box 118 SE-221 00, Lund, Sweden
[2]Centre for Environmental and Climate Research, Lund university, P.O. Box 118 SE-221 00, Lund, Sweden
[3]Atmospheric Sciences Division, Department of Physics, University of Helsinki, P.O. Box 64 FI-000 14, Finland

Keywords: Secondary organic aerosol, α-pinene, ADCHAM, MCMv3.2

Introduction

Biogenic volatile organic carbon compounds, such as α-pinene, are emitted by the vegetation and oxidized in the atmosphere to form less volatile compounds. These compounds can take part in the formation of secondary organic aerosols (SOA) and thus increase the aerosol load and also the concentration of cloud condensation nuclei which will affect climate. The aim of this study is to investigate how well we can model SOA formation due to oxidation of α-pinene and compare the modeled SOA formation using two different methods to estimate liquid saturation vapor pressures.

Method

The formation of SOA is modeled with ADCHAM which is the aerosol dynamic and particle phase chemistry module from the ADCHEM model (Roldin *et al.*, 2011) with the Master Chemical Mechanism version 3.2 (Jenkin *et al.*, 1997; Saunders *et al.*, 2003). For the α-pinene simulations the model considers the gas-to-particle partitioning of 154 oxidation products. The equilibrium vapor pressures of each oxidation product are decided by first estimating the liquid saturation vapor pressures using either the group contribution method SIMPOL (Pankow & Asher, 2008) or the method proposed by Nannoolal *et al.* (2008). The equilibrium vapor pressures are then derived with the Kelvin effect and Raoult's law with corrections for non-ideal solutions using the AIOMFAC model (Zuend *et al.*, 2011).

Results and conclusions

The modeled SOA-yield is compared with predicted SOA-yield by the 7-product parameterization done by Pathak *et al.* (2007) (Figure 1). The model seems to be able to handle SOA formation in what are considered to be typical background organic aerosol concentrations (1 to 20 μgm^{-3}) (Figure 1a). The model gives higher SOA-yield, and also, less α-pinene is needed to start the SOA formation compared with Pathak *et al.* (2007) (Figure 1b). The two group contribution methods give similar results. These are preliminary results and we are in the process of modeling SOA formation also from other chamber experiments with α-pinene used as the precursor gas.

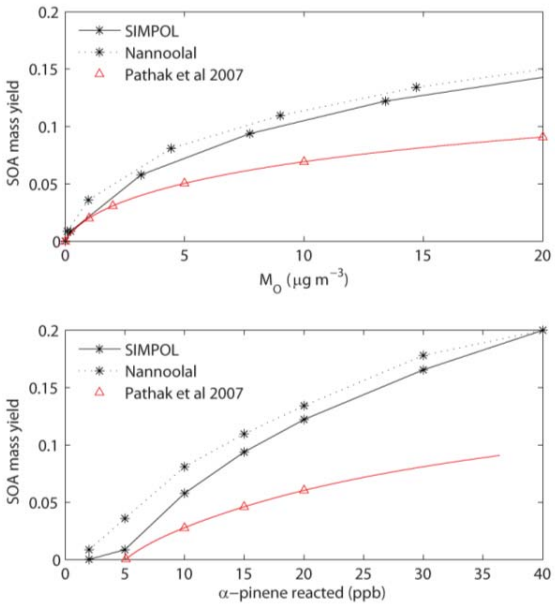

Figure 1. Modeled SOA-yield for low NO_x conditions with chamber UV light turned on as a function of (a) organic particle concentration and (b) reacted α-pinene compared with predicted SOA yield by Pathak *et al*. (2007) (triangles).

Jenkin, M. E., Saunders, S. M., & Pilling, M. J. (1997). *Atmos. Environ.*, 31, 81-104.

Nannoolal,Y., Rarey, J., & Ramjugernath, D. (2008). *Fluid Phase Equilibria*, 269, 117-133.

Pankow, J. F., & Asher, W. E. (2008). *Atmos. Chem. Phys.*, 8, 2773-2796.

Pathak, R. K., Presto, A. A., Lane, T. E., Stanier, C. O., Donahue, N. M., & Pandis, S. N. (2007). *Atmos. Chem. Phys.*, 7, 3811-3821.

Roldin, P., Swietlicki, E., Schurgers, G., Arneth, A., Lehtinen, K. E. J., Boy, M & Kulmala, M. (2011). *Atmos. Chem. Phys.*, 11, 5867-5896.

Saunders, S. M., Jenkin, M. E., Derwent, R. G., & Pilling, M. J. (2003). *Atmos. Chem. Phys.*, 3, 161-180.

Zuend, A., Marcolli, C., Booth, A. M., Lienhard, D. M., Soosin, V., Krieger, U. K., Topping, D. O., McFiggans, G., Peter, T., & Seinfeld, J.H. (2011). *Atmos. Chem. Phys.*, 11, 9155-9206.

LUNG DEPOSITION OF NANO PARTICLES AS A METHOD FOR DIAGNOSIS OF CHRONIC OBSTRUCTIVE PULMONARY DISEASE

Jonas Jacobson[1], Per Wollmer[2], Jakob Löndahl[1]

[1]Division of Aerosol Technology (EAT), Lund Institute of Technology, 221 00, Lund, Sweden
[2]Dept. of Clinical Sciences Malmö, Lund University, 205 02, Malmö, Sweden

Keywords: Nano particles, deposition, COPD, Emphysema

Introduction

Chronic Obstructive Pulmonary Disease (COPD) is one of the most common causes of death worldwide and is projected to increase to the third leading cause of death by 2030, depending on smoking habits, air pollution and demographic changes in many countries (Halbert et al., 2006).
An early diagnosis is crucial to the outcome for the patient but current methods lack in precision.

It has been theoretically and experimentally shown that lung deposition of nano particles differ between healthy humans and COPD patients. (Löndahl et al., 2012)
The objective of this study is to investigate if lung deposition of nano particles can be used as a tool for detecting physiological changes in human lungs and diagnosing emphysema and COPD.

Methods

A unique instrument has been constructed at LU to perform measurements of lung deposition of nano particles in human subjects.
A well controlled aerosol of polystyrene nanosphere particles with a narrow size distribution is generated. The aerosol is diluted with clean air to a concentration around 2000 particles/cm^3.
The subject inhales the aerosol with a vital capacity manoeuvre and holds his breath for some seconds. The particle concentration of the inhaled and exhaled aerosol is measured by a CPC.

The exhaled aerosol is compared to the inhaled aerosol and the fraction of deposited particles is calculated. The lung deposition fraction is compared to the results of a normal lung evaluation in pursuit of correlations.

Results

Figure 1 shows the result of measurements on 18 individuals with a clinical suspicion of airflow obstruction. The subjects are categorized from the results of lung function tests. The standard deviation for three measurements on the same volunteer is around 0.35%, while the variability between the subjects is 3.3%.

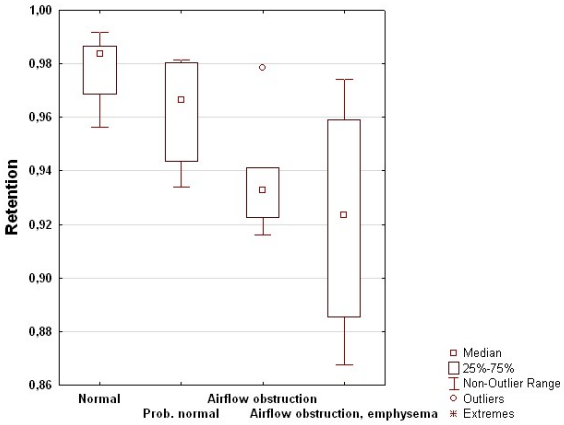

Figure 1: The result of measurements on 18 individuals.

Conclusions

The preliminary results are promising. The constructed instrument shows both sensitivity between different individuals and consistency when measuring on the same individual at different occasions.

The measurements performed by this instrument yields information similar to that of a MRI examination of the lungs, using hyperpolarized He^3, but at a significant lower cost and with minimal discomfort for the subject.

Hopefully this technology can provide a valuable contribution to the diagnosis of COPD and emphysema in a near future.

Acknowledgements

We gratefully acknowledge The Swedish Research Council (project 621-2011-3560), the Crafoord foundation and the Swedish heart and lung foundation for financial support.

References

Halbert RJ, Natoli JL, Gano A, et al. Global burden of COPD: systematic review and meta-analysis. Eur Respir J 2006;28:523-532.

Löndahl J, Swietlicki W, Rissler J, Bengtsson A, Boman C, Blomberg A, Sandström T. (2012), *Experimental Determination of Diesel Combustion Particles in Patients with Chronic Obstructive Pulmonary Disease.* Particle and Fibre Toxicology 2012, 9:30

Development of the NanoMap method for geographical mapping of new particle formation events

M. Johansson[1], A. Kristensson[1], E. Swietlicki[1], M. Dal Maso[2], N. Kivekäs[3], T. Hussein[2,4], T. Nieminen[2], H. Junninen[2], H. Lihavainen[3], P. Tunved[5], and M. Kulmala[2]

[1]Department of Physics, Lund University, Lund, SE-221 00, Sweden
[2]Department of Physics, University of Helsinki, Helsinki, FI-000 14, Finland
[3]Finnish Meteorological Institute FMI, P.O. Box 503, FI-00101 Helsinki, Finland
[4]Department of Physics, University of Jordan, 11942, Amman, Jordan
[5]Department of Applied Environmental Science, University of Stockholm, SE-106 91, Stockholm, Sweden

Keywords: SMPS, DMPS, nucleation

Introduction

The formation of new nanometer sized particles around 1.5 nm diameter during so called new particle formation events is frequent in the atmosphere. After condensational growth to cloud condensation nuclei sizes, the nanometer sized particles have a potential to influence the global radiation balance of the atmosphere. Potentially, up to 50 % of world's CCN come from formation events (Merikanto et al., 2009).

There are an increasing number of ground stations in Europe, where measurements of the particle size distribution are performed, and hence at these sites a full characterization of formation events can be performed. However, there is a lack of information where and when the formation events take place in between the stations. For example, in favourable regions we expect "hot-spots" with a higher frequency of events and conversely "cold-spots" where gaseous precursor concentrations necessary for the formation are low.

Fortunately, this information is possible to attain. In Kristensson et al. (2011) we explain briefly the methodology, which employs existing particle number size distribution data from field sites and meteorological back trajectories. With this methodology it is possible to calculate as an end product the probability of formation of 1.5 nm diameter particles during formation events in the boundary layer in grid cells with arbitrary horizontal resolution over a European geographical mesh.

Method development

We have chosen to develop this methodology in the NanoMap project for the EUSAAR site Hyytiälä in southern Finland, since there are over 15 years of size distribution data, which gives high geographical coverage and statistics.

In Figure 1 is shown an example of the applied methodology for Hyytiälä. 10 years of data is included, and it is obvious that the probability of formation of 1.5 nm diameter particles is highest north-west of Hyytiälä, even over the Baltic Sea the probability is high.

It should be remembered however, that it is not fair to compare the events for different cardinal sector directions, since the north-westerly points are mostly for north-westerly air masses, which are more favourable for formation than for example easterly air masses. Instead, comparing the results between different measurement field stations and equal cardinal wind directions is more suitable. With the dense network of field stations in Europe, it is possible to create these maps with a high geographical coverage for different cardinal wind directions.

The validation of the absolute value of the probability of formation events is the most difficult part of the method, and ongoing work is taking place to sort this matter out. Several different methods can be used for this purpose.

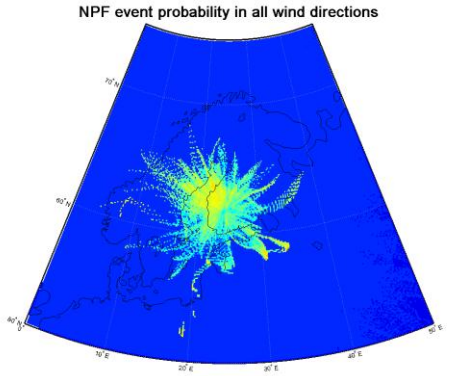

Figure 1. The probability (relative scale) of formation of 1.5 nm diameter particles during formation events around the Hyytiälä field site. Plot is based on data between Jan 1 1996 and Aug 31 2006 and the geographical grid box resolution is $0.2 \times 0.1^{\circ}$ in the latitudinal and longitudinal direction respectively.

This work was supported by the Swedish Research council FORMAS under grant 2010-850.

Kristensson, A., Swietlicki, E., et al. (2011). EAC proceedings, Manchester, September 2011.

Merikanto, J., Spracklen, D. V., Mann, G. W., Pickering, S. J., et al. (2009) *Atmos. Chem. Phys.* **9**, 8601-8616.

The effect of droplet size on the evaporation and mass accommodation processes of water: a molecular dynamics study

J. Julin[1], M. Shiraiwa[2], R. E. H. Miles[3], J. P. Reid[3], U. Pöschl[4] and I. Riipinen[1]

[1]Department of Applied Environmental Science (ITM), Stockholm University, SE-10691 Stockholm, Sweden
[2]Department of Chemical Engineering, California Institute of Technology, Pasadena, CA 91125, USA
[3]School of Chemistry, University of Bristol, Bristol, BS8 1TS, UK
[4]Max Planck Institute for Chemistry, Biogeochemistry Department, P.O. Box 3060, 55128 Mainz, Germany

Keywords: mass accommodation, evaporation, water, simulations

Introduction

Understanding the growth processes of ultrafine atmospheric aerosol particles has a central role in understanding the climate effects of aerosols. The condensational growth of ultrafine particles is quite sensitive to their ability to uptake various gaseous species, an ability which is quantified by the mass accommodation coefficient α_m. Unfortunately, even for the case of water-on-water the reported values for α_m range from 0.1 to 1 (see e.g. review by Kolb *et al.* and references therein). In part this can stem from the diverse selection of theoretical descriptions used in modelling the mass accommodation and evaporation processes. In this work we use molecular dynamics (MD) simulations, the kinetic multilayer model KM-GAP (Shiraiwa *et al.* 2012), and basic kinetic condensation equations to study these processes for water and shed light on the applicability of the more simplified descriptions.

Methods

The MD simulations are performed using the TIP4P-Ew water potential and the GROMACS software. To study the dependence of α_m on droplet size, mass accommodation simulations are done at T=273.15 K for two different droplet sizes, 1000 and 10000 molecules, and the planar surface. To study the temperature dependence of α_m the planar surface case is repeated for three additional temperatures. A set of evaporation simulations is also performed for all the same conditions except the larger droplet, to get an evaporation rate that is unperturbed by the incident molecules.

We use the MD simulations to identify the region corresponding to the KM-GAP outermost surface layer from which all the evaporation to the gas phase occurs, and from there determine the desorption lifetime needed as input by KM-GAP. This is used to perform KM-GAP runs corresponding to the conditions of water droplet growth in the experiments of Winkler *et al.* (2006).

Conclusions

We find that the simulated evaporation rates agree qualitatively well with the basic kinetic equations for evaporation rate, see Fig. 1. Furthermore, the desorption lifetime has little effect on the success that KM-GAP has in predicting the experimental results of water droplet growth, indicating that the process is controlled by gas phase diffusion. Thus, the simplified picture of the kinetic condensation equations can be considered sufficient when describing the condensation and evaporation of water. Figure 2 shows that the mass accommodation coefficient is close to unity regardless of droplet size.

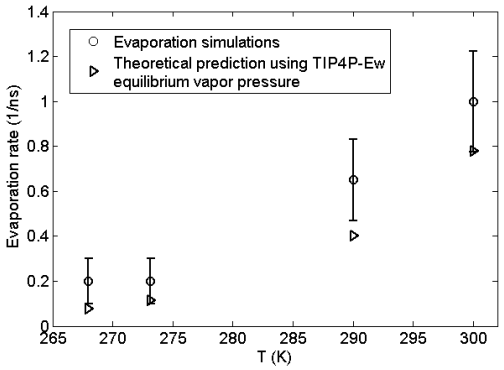

Figure 1. Simulated evaporation rates compared to theoretical prediction $J_{\mathrm{evap}}=(p_e/kT)\bar{v}A\alpha/4$.

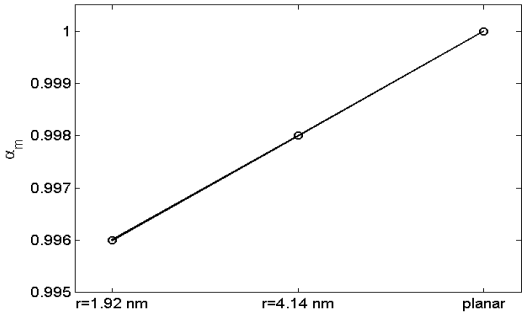

Figure 2. Mass accommodation coefficient as a function of droplet size.

This work was supported by the European Research Council ATMOGAIN (No. 278277).

Kolb, C. E. *et al.* (2010). *Atm. Chem. Phys.* 10, 10561-10605.

Shiraiwa, M., Pfrang, C., Koop, T. & Pöschl U. (2012). *Atm. Chem. Phys.* 12, 2777.

Winkler, P. M. *et al.* (2006). *J. Geophys. Res.* 111, D19202.

NanoShip project: Is new particle formation taking place over the North Sea?

N. Kelbus[1,2], A. Massling[3], M. Fiebig[4], B. Henzing[5], M. Glasius[6], M. Bilde[7], M. Moerman[5], G. de Leeuw[5,8,9], M. Dal Maso[8], and A. Kristensson[2]

[1]Dept. of Physical Geography and Ecosystem Sci., Lund University, P. O. Box 118, SE-221 00 Lund, Sweden
[2]Department of Physics, Lund University, P. O. Box 118, SE-221 00 Lund, Sweden
[3]Department of Environmental Science, Aarhus University, P. O. Box 358, DK-4000 Roskilde, Denmark
[4]Norwegian Institute for Air Research (NILU), NO-2007 Kjeller, Norway
[5]TNO, Princetonlaan 6, P.O.Box 80015, 3508TA Utrecht, the Netherlands
[6]Department of Chemistry, Aarhus University, Langelandsgade 140, DK-8000 Aarhus, Denmark
[7]Department of Chemistry, University of Copenhagen, DK-2100, Copenhagen, Denmark
[8]Department of Physics, University of Helsinki, P. O. Box 64, FI-00014, Helsinki, Finland
[9]Finnish Meteorological Institute FMI, P.O. Box 503, FI-00101 Helsinki, Finland

Keywords: SMPS, DMPS, nucleation, shipping emissions, sulphur dioxide

Introduction

The formation of atmospheric nanoparticles through gas-to-particle conversion occurs in many areas over the world. After subsequent condensational growth to sizes relevant for cloud formation, these particles become important for the global radiation balance. Potentially, the nanoparticle formation route might be responsible for up to 50% of world's cloud condensation nuclei (Merikanto et al., 2009), with a large uncertainty which stems from poor knowledge of formation routes. In this study, we seek to widen our knowledge in one of the formation routes. A basic question in this context is:

How frequent are ship-induced new particle formation events, and what conditions are favourable for their appearance?

Method

In our NanoShip project, particle number size distribution measurements are carried out at a site at the Danish peninsula Jutland during March-May 2012 to investigate if formation events are linked to winds from the North Sea. Also data from the Norwegian and Dutch EUSAAR sites Birkenes and Cabauw from 2008 until present are used to infer the appearance and frequency of formation events during conditions with winds from south-east and north-west respectively.

By following the growth of nanoparticles after the formation, and using back trajectories it is possible to infer where the formation of 1.5 nm diameter particles has taken place over the sea. This method is described by Kristensson et al. (2011).

Conclusions

Using the data from Jutland, it can be concluded that we have formation of 1.5 nm diameter particles over many places in the North Sea (Figure 1), hence it is taking place over heavily trafficked ship-lanes. Even if emissions of SO_2 are large from ship traffic, it is still not certain that ship emissions are main cause of the observed events. Also emissions from oil flaring in the North Sea, and from continental stationary sources are contributing to VOC emissions (Figure 2). Hence, these may be contributing emission sources provided VOC are necessary for formation.

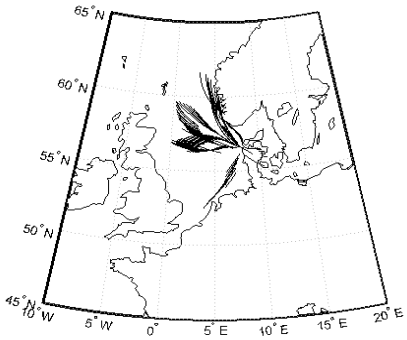

Figure 1. The geographical position of where new particle formation events take place of 1.5 nm diameter particles according to NanoMap.

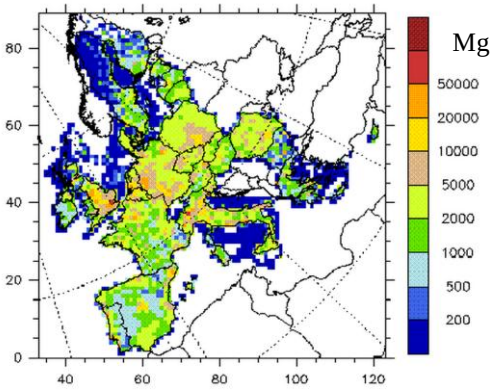

Figure 2. 2010 non methane volatile organic carbon (VOC) emissions according to EMEP (EMEP, 2012).

This work was supported by the Swedish Research council FORMAS under grant 2010-850.

Emep 2012. http://www.ceip.at/webdab-emission-database/emissions-as-used-in-emep-models/

Kristensson, A., Swietlicki, E., et al. (2011). EAC proceedings, Manchester, September 2011.

Merikanto, J., Spracklen, D. V., Mann, G. W., Pickering, S. J., et al. (2009) *Atmos. Chem. Phys.* **9**, 8601-8616.

Atmospheric Fate of Methacrolein

H. C. Knap[1], J. D. Crounse[2], K. B. Ørnsø[1], S. Jørgensen[1], F. Paulot[3], P. O. Wennberg[2] and H. G. Kjaergaard[1]

[1]Department of Chemistry, University of Copenhagen, DK-2100 Copenhagen Ø, Copenhagen, Denmark
[2]Department of Geological and Planetary Science, California Institute of Technology, Pasadena, California 91125, United States
[3] Division of Engineering and Applied Science, California Institute of Technology, Pasadena, California 91125, United states

Keywords: Methacrolein, hydroxyl radical, isoprene, addition and abstraction mechanism

Introduction

Isoprene (2-methyl-1,3-butadiene) is emitted by plants in large quantities (~600 Tg yr^{-1}).[1] The oxidation of isoprene by the hydroxyl radical (OH) is suggested to produce a large fraction of the secondary organic aerosol (SOA) present in the atmosphere. One of the well known products from isoprene degeneration is methacrolein (MACR). It has earlier been demonstrated that the atmospheric fate of MACR, is dominated by its reaction with OH.[2] This proceeds *via* two reaction channels with approximately equal rates:[3] addition to the double bond (primarily at the external carbon atom) leading to formation of a hydroxy peroxy radical that isomerizes and decomposes with significant OH recycling[4] (Figure 1) or abstraction of the aldehydic hydrogen atom leading to formation of an acetyl radical that isomerizes to an α-lactone[5] (Figure 2). We investigate the oxidation of MACR by the hydroxyl radical, theoretically.

Theoretical Methods

We have calculated the structures and energies along the reaction paths with B3LYP/6-31+G(d,p) and B3LYP/aug-cc-pVTZ (avtz). The transition state (TS) are shown to connect the reactant and product on either side *via* intrinsic reaction coordinate (IRC) calculations with the B3LYP/6-31+G(d,p) method. We improve the energy barriers by calculating single point energies with the explicitly correlated CCSD(T)-F12a/VDZ-F12 method (F12) at the B3LYP/aVTZ optimized structures. The F12 energies are zero point vibrational energy corrected (ZPVE) with the B3LYP/aVTZ harmonic frequencies.

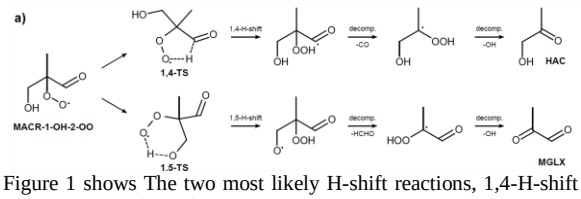

Figure 1 shows The two most likely H-shift reactions, 1,4-H-shift and 1,5-H-shift, of MACR-1-OH-2-OO and the ensuing decompositions.

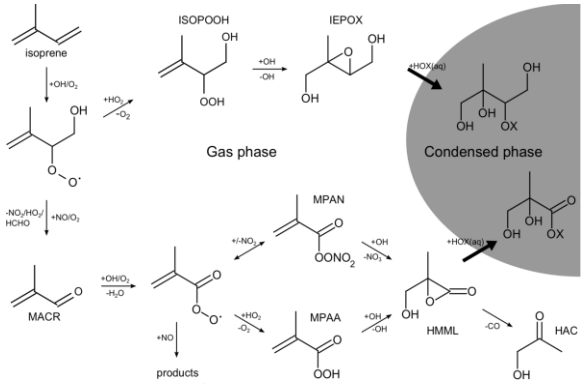

Figure 2 Mechanism for the isoprene oxidation under low NO_x condition to form di-hydroxy-epoxides (IEPOX)[6] and under high NO_x condition to form methacrolein (MACR). MACR further oxidizes (hydrogen abstraction) either *via* methyl-peroxyacetyl-nitrate (MPAN) or methyl-peracrylic acid (MPAA) to form hydroxymethyl-methyl-α-lactone (HMML).

Conclusions

In the abstraction channel, the NO_3 (or OH) radical can leave 'hot', whereby the HMML will have insufficient internal energy to overcome the barrier for decomposition (E-TS). The estimated (GEOS-CHEM) annual HMML production may be as high as 9 Tg yr^{-1} with a significant aerosol formation potential in high NO_x environment. The addition channel provides evidence for significant OH recycling and support a less oxidant consuming atmospheric breakdown of isoprene. In both reaction channels, we show that these newly proposed reactions are crucial importance.

References

1 Guenther, A.; Karl, T.; Harley, P.; Wiedinmyer, C.; Palmer, P. I.; Geron, C. Atmospheric Chemistry and Physics **2006**, 6, 3181-3210.
2 Gierczak, T.; Burkholder, J. B.; Talukdar, R. K.; Mellouki, A.; Barone, S. B.; Ravishankara, A. R. Journal of Photochemistry and Photobiology a-Chemistry **1997**, 110, 1-10.
3 Tuazon, E. C.; Atkinson, R. International Journal of Chemical Kinetics **1990**, 22, 1221-1236.
4 Crounse, J. D.; Knap, H. C.; Ørnsø, K. B.; Jørgensen, S.; Paulot, F.; Kjaergaard, H. G.; Wennberg, P. O. Journal of Physical Chemistry A, **2012**, 116, 5756-5762.
5 Kjaergaard, H. G.; Knap, H. C.; Ørnsø, K. B.; Jørgensen, S.; Crounse, J. D.; Paulot, F.; Wennberg, P. O. Journal of Physical Chemistry A, **2012**, 116, 5763-5768.
6 Paulot, F.; Crounse, J. D.; Kjaergaard, H. G.; Kurten, A.; St Clair, J. M.; Seinfeld, J. H.; Wennberg, P. O. *Science* **2009**, *325*, 730-733.

A detailed characterisation of HULIS from different environments

T.B. Kristensen[1], H. Wex[2], L. Du[1], Q. Nguyen[3,4], J.K. Nøjgaard[3], B. Nekat[2], D. Van Pinxteren[2], C. Bender Koch[1], K. Dieckman[2], D.H. Lowenthal[5], L. Mazzoleni[6], T.F. Mentel[7], M. Glasius[3], H. Herrmann[2], H.G. Kjaergaard[1], A.G. Hallar[5,8], F. Stratmann[2], and M. Bilde[1]

[1]Department of Chemistry, University of Copenhagen, Universitetsparken 5, DK-2100 Copenhagen, Denmark
[2]Leibniz Institute for Tropospheric Research, 04318, Leipzig, Germany
[3]Department of Environmental Science, Aarhus University, DK-4000, Roskilde, Denmark
[4]Department of Chemistry, Aarhus University, DK-8000, Aarhus, Denmark
[5]Desert Research Institute, Reno, NV-89512, USA
[6]Department of Chemistry, Michigan Technological University, Houghton, MI-49931, USA
[7]Institute for Energy and Climate Research: Troposphere, Research Center Jülich GmbH, 52425 Jülich, Germany
[8]Desert Research Institute, Storm Peak Laboratory, Steamboat Springs, CO-80488, USA

Keywords: HULIS, CCN activity, FTIR, LC-MS

Introduction

Humic-Like Substances (HULIS) are present in significant amounts in aerosol particles in various environments. HULIS absorb in the ultraviolet-visible (UV-Vis) range and may thus influence climate directly by absorption of incoming sunlight. HULIS can also influence climate indirectly via an impact on cloud condensation nuclei (CCN) activity and cloud optical properties. It is unclear from previous studies how the composition of HULIS may affect the optical properties or the hygroscopicity (CCN activity included). This study will focus on the chemical composition and the hygroscopic properties of different HULIS samples.

Methods

Particulate Matter (PM) was sampled in an urban (HC Andersens Blvd. (HCAB), Copenhagen, Denmark), a rural (Melpitz (Mel), Germany) and in a remote environment (Storm Peak Lab. (SPL), CO, USA). HULIS were extracted as described by Varga *et al.* (2001). Suwannee River Fulvic Acid Standard (SRFA) was included in the study for comparison.

UV-Vis spectra were measured with a Perkin Elmer Lambda 1050 UV/Vis/NIR spectrometer. A VERTEX 70 (Bruker) Fourier transform infrared (FTIR) spectrometer was used to measure the absorbance in the IR range. Raman spectra of the HULIS samples were measured with a Bruker RFS 100 FT-Raman spectrometer using an excitation wavelength of 1064 nm. Mass spectra were obtained with a HPLC-QTRAP-MS consisting of a liquid chromatograph (Agilent 1200) interfaced to an ion trap mass spectrometer that employed Turbo Ionspray ionization (AB Sciex QTrap 5500, AB Applied Biosystem - MDS Analytical Technologies). The hygroscopic growth and CCN activity of generated HULIS particles were measured with the mobile version of the Leipzig Aerosol Cloud Interaction Spectrometer (mobile-LACIS) and with a DMT CCN counter, respectively.

Results

The FTIR spectra showed that the relative abundance of different functional groups was similar for the Mel and HCAB HULIS samples. The SPL sample contained relatively more carboxylic acid groups. The observed range of molecular masses (M_w) of the SPL sample went up to 1000 Da, whereas the range of M_w for the Mel (up to 700 Da) and HCAB (up to 500 Da) are typical ranges for HULIS samples studied in the literature. The estimated average M_w correlated with the relative absorbance at higher wavelengths in the UV range.

The hygroscopic growth and CCN activity were similar for all three samples and relatively low compared to results reported in the literature (Kristensen *et al.*, 2012). The CCN activity of the SPL HULIS sample is shown in Figure 1 with pure $(NH_4)_2SO_4$ included for comparison. The measured hygroscopicities of the atmospheric HULIS samples were slightly higher than the hygroscopicity of SRFA. However, significant differences were observed in the chemical composition. The atmospheric HULIS samples were mainly aliphatic compounds, while the content of aromatics was significantly higher in the SRFA sample.

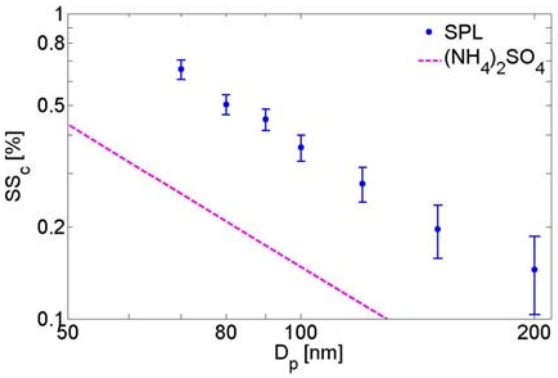

Figure 1. Critical supersaturation (SS_c) vs dry mobility particle diameter (D_p) for SPL with the theoretical values for $(NH_4)_2SO_4$ included. The error bars represent ± 2 standard deviations.

Kristensen et al. (2012) *J. Geophys. Res.* (Accepted)
Varga B., Kiss, G., Ganszky, I., Gelencsér, A., & Krivácsy, Z. (2001) *Talanta* **55**, 561-572.

Large-eddy simulations and observations of a stratiform cloud event at the Puijo hill in Kuopio, Finland

W.-Y. H. Leung[1], A. M. L. Ekman[1], M. Komppula[4], A. Kristensson[3], K. Noone[2], H. Portin[4, 5], S. Romakkaniemi[5], J. Savre[1]

[1] Department of Meteorology, Stockholm University, Stockholm, Sweden
[2] Department of Applied Environmental Science, Stockholm University, Stockholm, Sweden
[3] Division of Nuclear Physics, Department of Physics, Lund University, Lund, P.O. Box 118, 221 00 Lund, Sweden
[4] Finnish Meteorological Institute, Kuopio Unit, P.O. Box 1627, FI-70211, Kuopio, Finland
[5] University of Eastern Finland, Department of Applied Physics, P.O. Box 1627, FI-70211, Kuopio, Finland.

Keywords: black carbon, measurements, modelling

Introduction

Black carbon (BC) aerosols, which are generated by incomplete combustion of fossil fuels, biofuels, and biomass, have significant influence on global climate, directly and indirectly. The direct effect refers mainly to the absorption of solar radiation by the BC aerosols. This absorption changes the thermal structure of the atmosphere, which could change cloud formation processes and lead to evaporation of clouds. The first indirect effect refers to that an increasing amount of BC aerosols, can act as cloud condensation nuclei (CCN), increase the initial cloud droplet number concentration and thus enhance the cloud albedo. The decrease in cloud droplet size may also suppress precipitation formation and increase cloud lifetime, which is known as the second indirect effect. The hygroscopicity of BC aerosols is enhanced as they age, and this ageing process has large influence on their ability to serve as CCN, which in turn controls the residence time of BC aerosols (e.g. McMeeking et al., 2011). In order to better quantify the effects of BC aerosols on climate forcing, it is crucial to understand how they are activated, processed, and scavenged in clouds.

Model and selected case

A stratiform cloud event observed at the Puijo hill, Kuopio, Finland is chosen as a case study. The goal of the study is to investigate the climate impacts and scavenging pathways of BC aerosols. A new LES model (MIMICA) will be used to simulate the event. This model is based on a cloud resolving model (MIT-CRM) developed by Wang and Chang (1993). The model includes a multimodal aerosol module (Ekman et al., 2004), which can simulate the evolution of sulfate, organic carbon, black carbon, and other aerosol mixtures through time and space. We will first evaluate the performance of the LES model by simulating this stratiform cloud event and comparing the observed meteorological variables and cloud properties with the simulated data. Preliminary results of this model-observation data comparison will be presented here. Sensitivity simulations will also be performed to study how the cloud properties change under various assumptions on the initial number concentration and size distribution of different aerosol modes.

Finally, total BC and interstitial BC data collected at the Puijo tower measurement station near the town of Kuopio, Finland will be compared with the model-simulated data to evaluate the BC particle activation processes and the number and mass scavenging efficiencies throughout the cloud development. The evolution of the droplet spectra, effective radii and BC size distribution will be studied and various scavenging pathways of BC will be discussed.

This work is supported by FORMAS, the Swedish Research Council through Modeling Aerosol-Cloud-Climate Interactions and Impacts (MACCII) project.

Ekman, A. M. L., Wang, C., Wilson, J., and Ström, J. (2004). *Atmos. Chem. Phys*., 4, 773-791.

McMeeking, G. R., Good, N., Petters, M. D., McFiggans, G., and Coe, H. (2011). *Atmos. Chem. Phys. Discuss*., 11, 917-950.

Wang, C. and J. S. Chang. (1993). *J. Geo. Res*., 98, 14827-14844.

Particles measured in a low speed ship engine: cloud condensation nuclei and microstructure

K. I. Lieke[1], T. Rosenørn[1,2], A. C. Butcher[1], S. M. King[1], T. G. Frederiksen[2], K. Fuglsang[2], J. B. Pedersen[3], D. Larsson[3] and M. Bilde[1]

[1]Copenhagen Center for Atmospheric Research, Department of Chemistry, University of Copenhagen, 2100 Copenhagen, Denmark.
[2]Force Technology, Park Allé 345, 2605 Brøndby, Denmark.
[3]MAN Diesel & Turbo SE, Teglholmsgade 41, 2450 Copenhagen, Denmark

Keywords: ship emissions, CCN, mixing state, microstructure, soot

Introduction

Transport by ship plays an important role in global logistics. Current international policy initiatives by the International Maritime Organization (IMO) are taken to reduce emissions from ship propulsion systems (NO and SO, primarily). However, particulate emissions (e.g. soot) from ships are yet not regulated by legislations. To date, there is still a lack of knowledge regarding the global and local effects of the particulate matter emitted from ships at sea. Particles may influence the climate through their direct effects (scattering and absorption of long and shortwave radiation) and indirectly through formation of clouds.

Many studies have been carried out estimating the mass and particle number from ship emissions (e.g. Petzold et al. 2008), many of them in test rig studies (e.g. Kasper et al. 2007). It is shown that particulate emissions vary with engine load and chemical composition of fuels. Only a few studies have been carried out to characterize the chemical composition and cloud-nucleating ability of the particulate matter (e.g. Corbett et al. 1997). In most cases, the cloud-nucleating ability of emission particles is estimated from number size distribution.

Methods

We applied measurements to characterize particulate emissions from a MAN B&W Low Speed engine on test bed. A unique data set was obtained through the use of a scanning mobility particle sizing system (SMPS), combined with a cloud condensation nucleus (CCN) counter and a thermodenuder - all behind a dilution system. In addition, impactor samples were taken on nickel grids with carbon foil for use in an electron microscope (EM) to characterize the mineral phase and mixing state of the particles. The engine was operated at a series of different load conditions and an exhaust gas recirculation (EGR) system was applied. Measurements were carried out before and after the EGR system respectively.

Results

The measurements show changes in number size distribution and CCN activity with varying conditions. Micrstructural characteristics are changing form before to after scrubber. Results of transmission electron microscopy revealed salt condensates of nanometer size attached to soot particles. High resolution structural analysis of single particles shows that at least three different phases (graphitic soot, crystalline salt and amorphous condensed organic matter) may be present in the same particle volume. A closure between CCN activation curves, EM samples, and SMPS size distribution will be presented and used to identify climate active parts in single particles.

Acknowledgements

We thank the Danish Agency for Science, Technology and Innovation for support through the NaKIM project (www.nakim.dk).

References

Corbett, J. J. and Fischbeck, P. (1997): Emissions from Ships, Science 278, 823–824.

Kasper, A., Aufdenblatten, S., Forss, A., Mohr, M. and Burtscher, H. (2007): Particulate Emissions from a Low-Speed Marine Diesel Engine, Aerosol Science and Technology 41, 24–32.

Petzold, A., Hasselbach, J., Lauer, P., Baumann, R., Franke, K., Gurk, C., Schlager, H. and Weingartner, E. (2008): Experimental studies on particle emissions from cruising ship, Atmospheric Chemistry and Physics 8, 2387–2403.

Methods for generation of bioaerosol

J. Löndahl[1], O. Nerbrink[2], N. Burman[1], T. Tjärnhage[2], C. von Wachenfeldt[3] and U. Gosewinkel Karlson[4]

[1]Department of Design Sciences, Lund University, SE-221 00, Lund, Sweden
[2]FOI, Umeå, Swedish Defence Research Agency, SE-901 82 Umeå, Sweden
[3]Department of Biology, Lund University, SE-221 00, Lund, Sweden
[4]Department of Environmental Science, Aarhus University, Roskilde, DK-2000, Denmark

Keywords: bioaerosols, generation of aerosols, atmospheric aerosols, IN, CCN, bacterial activity

Introduction

Bioaerosols include viable bacteria, viruses, dead bacterial cells, pollen, fungi and cell fragments, as well as numerous organic compounds derived from biomolecules as, for example, sugars, amino acids and methyl-derivatives. It has been shown that airborne bacteria may be viable also in the harsh conditions at high altitudes in the atmosphere and act as cloud condensation nuclei (CCN) and ice nuclei (IN). In order to study for instance IN and CCN properties of bioaerosols in a laboratory setting it is necessary to use a generation methodology that preserves bacterial viability, minimize coating with redundant solvent impurities and have a low background of non-bacterial particles. The objective of this work is to compare various aerosol generators for bacteria, spores and vesicles.

Methods

Six aerosol generators are investigated: atomizer (TSI Inc., Model 3075), Collison nebulizer (BGI Inc., 3-jet), bubbling aerosol disperser, sparging liquid aerosol generator (SLAG, CH Technologies), vibrating orifice aerosol generator (VOAG, TSI model 3450) and electrospray (TSI Inc., model 3480).

At this point, exclusively the rod-shaped, Gram-positive model bacterium *Bacillus subtilis*, is studied. Particle number size distributions were measured with a scanning mobility particle sizer (SMPS, design: Lund University) and an aerodynamic particle sizer (APS, TSI Inc., Model 3321) in a stainless steel flow tube with controlled dilution (Figure 1). Bacteria are collected on tryptic soy agar plates with a rotating slit sampler.

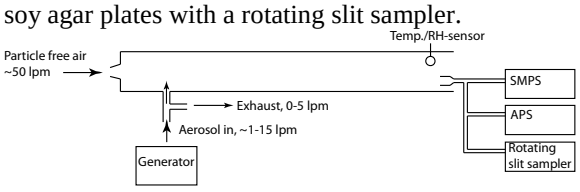

Figure 1. Experimental set-up

Bacterial viability is analysed by counting colony forming units (CFU). The initial droplet size from the generators is assessed by generating a solution with 1% mass ammonium sulphate and calculating the drop size from the mass of the dried particle.

Results

Preliminary results clearly show that many of the methods commonly used for generation of bioaerosols are unsuitable for examination of key properties of the particles such as CCN or IN ability. For instance the vibrating orifice aerosol generator (VOAG) produces uniform, but comparably large droplets (typically 20-40 µm). When dried, the background particles therefore may have a size of several µm and the bacteria will be covered with a thick layer of residues. Surface coating of bioaerosols may significantly alter their properties.

All generators (possibly with exception for the electrospray) produce a substantial background of non-bacterial particles from impurities in the used liquid. The background to bacteria ratios were on similar levels. The output of bacteria as colony forming units (CFU) was highest from the Collison nebulizer, closely followed by the TSI atomizer and the sparging liquid aerosol generator. The bubbling aerosol disperser had two orders of magnitude lower bacterial output.

Conclusions

It is often difficult to provide bioaerosols from distilled water of high purity since the organism typically need some surrounding additives (salts etc.) for survival. It seems that the electrospray method is optimal for particles up to 200 nm (virus, spores and vesicles). This instrument leaves a minor surface coating due to a small initial droplet size. For larger particles it may be crucial to use a differential mobility analyser or a virtual impactor to reduce the background of unwanted particles.

Future experiments will include Gram-positive bacteria that are not spore forming, Gram-negatives and isolated spores. In addition fluorescence will be used to get a ratio between bacterial particles, non-bacterial ones and CFU.

This work was supported by the Swedish research councils VR and FORMAS.

Emission measurements of multi-walled carbon nanotube release during production

L. Ludvigsson[1,2], C. Isaxon[2], P. T. Nilsson[2], M. Hedmer[3], H. Tinnerberg[3] M. E. Messing[1], J Rissler[2], V. Skaug[4], M. Bohgard[2], J. Pagels[2]

[1]Solid State Physics, University of Lund, SE-22100, Lund, Sweden
[2]Ergonomics and Aerosol Technology, University of Lund, SE-22100, Lund, Sweden
[3]Occupational and Environmental Medicine, University of Lund, SE-22100, Lund, Sweden
[4]National Institute of Occupational Health, PB 8149 Dep, 0033 Oslo, Norway

Keywords: Carbon nanotubes, emission measurement, SEM

Introduction

The fields in which carbon nanotubes (CNTs) are found useful are rapidly growing, causing an increased demand worldwide. The industry is looking for ways to improve their production and thus increase the amount of CNTs being handled. This, together with the fear that exposure to CNT particles may cause similar health effects as asbestos (Donaldsson, 2006), create a need for accurate methods of emission assessments. We present results from field measurement performed utilizing a range of measurement techniques to assess emissions at a small-scale CNT producer that utilize the arc-discharge method for production of multi-walled CNTs.

Methods

Different tasks in the production were measured as well as full-shift personal measurement. Air samples were collected both in the emission zone and in the respiratory zone of the workers. By using cyclones (BGI4L, BGI) respirable (<5 µm aerodynamic diameter) dust fractions, were collected on polycarbonate (37 mm, 0.4 µm pores) filters. Filters were analysed using scanning electron microscopy (SEM) and online instruments were used both in the emission zone (<10 cm from the source) and in the background (3 m from the closest source).

Table 1. SEM results from filter measurements.

Task	Total ± σ (0.01-5 µm) (cm^{-3})	CNT containing particles ± σ (cm^{-3})
Sieving, mechanical work-up and packaging	324±4	11±1
Cleaving of deposits	410±10	3.4±0.9
Opening of the reactor	1095±43	N.D.
Functionalization Part I	162±4	1±0.4
Personal Exposure Measurement	120±2	2.0±0.2

Conclusions

Emissions of CNTs were detected in 9 out of 16 samples (selected results in Table 1). CNT structures were found in all personal exposure measurements. The CNT structures found in the respirable fraction did seldom exceed a length of 5 µm and CNT structures classified as fibres (aspect ratio >3:1 (Figure 1)) were in most cases shorter than 3 µm. The fraction of CNT structures compared to other particles was small. Emissions during activities occurred as peaks (Figure 1).

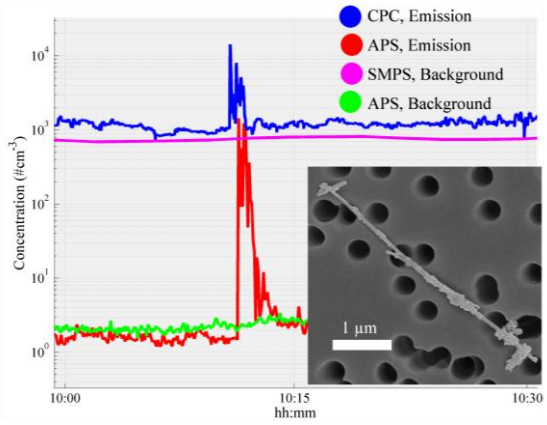

Figure 1 Example of peak emissions from measured time series, and an example of a long CNT fibre.

The CNT concentration was estimated to 11 CNT containing particles/cm^3 during the task performed in Figure 1 (Cleaving of deposits). CNT concentration in the personal exposure measurement was measured to 2 CNT containing particles/cm^3. The combination of online instrumentation and SEM analysis gave a deep understanding of when emissions occur and a detailed description of what kind of particles that were emitted. The results show that several tasks in the production could cause workplace exposure occur.

This work was performed within the FAS centre METALUND and supported by the Swedish Council for Working Life and Social Research (FAS) and nmC@Lund

(REF) K. Donaldsson *et. al.* (2006) *Toxicological Sciences* 92(1), 5–22 (2006)

An evaluation method to describe differences in thermal properties of organic aerosols

A. Lutz, E. U. Emanuelsson, Å. K. Watne and M. Hallquist

Department of Chemistry and Molecular Biology, University of Gothenburg, 412 96 Gothenburg, Sweden

Keywords: Volatility, VTDMA, Volume Fraction Remaining

Introduction

Secondary Organic Aerosols (SOA) contributes significantly to the total organic aerosol budget but the formation mechanisms of SOA are poorly understood. When organic compounds are oxidised, depending on their structure, products of lower volatility than the precursor may form. The products can in turn contribute to gas-particle conversion, i.e. formation of particles (Hallquist *et al*., 2009). Volatility of complex mixture is not easily described in terms of vapour pressures or heat of vaporisation. Consequently several different measures are used based on specific instruments.

In addition to the comparison issues between different measures of volatility, it is a challenge to clearly present volatility data. In this study we developed a method that makes it easier to compare volatilities derived from a VTDMA system.

Methods

The thermal properties, i.e volatility, can be measured with a Volatility Tandem Differential Mobility Analyzer (VTDMA). The VTDMA measures the difference in particle diameter before and after heating.

The volatility of the particles can be presented in several different ways. Volume Fraction Remaining (VFR_T) is derived from the measured particle modal diameter (D_p) at a certain temperature T and compared to a fixed reference diameter (D_{pRef}).

$$VFR_T=(D_{pT}/D_{pRef})^3$$

Alternatively to present VFR at a specific temperature one may use VFRs measured at several temperatures, this type of plot is named a thermogram. The thermogram has often a sigmoidal shape and can be fitted to a Hill function. The following Hill function was used to describe the VFR versus evaporative temperature:

$$f(x) = base + \frac{(max - base)}{1 + \left(\frac{X_{1/2}}{x}\right)^{rate}}$$

Where *base* is the *f(x)*-value at large *x*, *max* is the *f(x)* at small *x*, *rate* is the slope and $x_{1/2}$ is the x-value where *f(x)=(base+max)/2*. From this fit, $T_{VFR0.5}$, the temperature where half of the particles volume is evaporated, and S_{VRF}, the maximum slope of the curve, is derived.

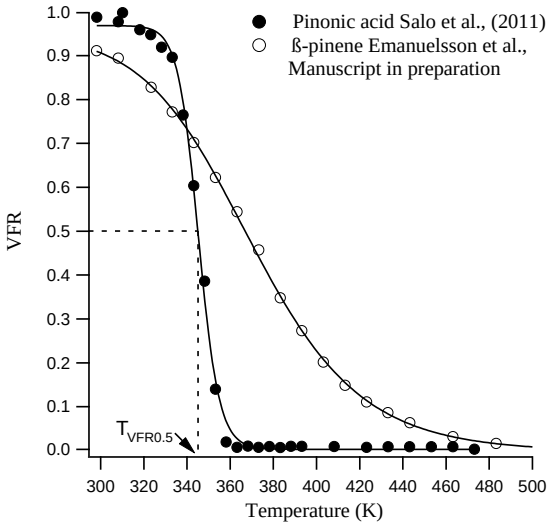

Figure 1. Thermogram of pinonic acid and β-pinene.

In Figure 1, thermograms of pure pinonic acid and SOA formed from ozonolysis of β-pinene are compared. A less steep slope indicates a wider distribution of volatility e. g. a more complex chemical composition. The thermogram of pure pinonic acid (S_{VFR} = -72.4) has a steeper slope than the β-pinene SOA (S_{VFR} = -16.4). The $T_{VFR0.5}$ for pure pinonic acid and β-pinene SOA was 345.0 K and 364.6 K, respectively. Generally, an increase in $T_{VFR0.5}$ corresponds to less volatile aerosol particles.

Conclusions

The parameters $T_{VFR0.5}$ and S_{VFR} derived from the Hill function have been shown to be valuable for comparing volatility measured using a VTDMA instrument.

The research presented is a contribution to the Swedish strategic research area ModElling the Regional and Global Earth system, MERGE. This work was supported by Formas (214-2010-1756) and the Swedish Research Council (80475101).

Hallquist, M. *et al*., (2009). Atmos Chem Phys, 9, 5155-5236.

Salo, K. *et al*., (2011). *Atmos Chem Phys*, 9, 11055-11067.

Emanuelsson, E. *et al*., Manuskript in preparation

Emissions of particles during hair bleaching

Marini S.[1], Nilsson P. T.[2], Wierzbicka A.[2], Kuklane K.[2], Nielsen J.[3] and Gudmundsson A.[2]

[1]Civil and Mechanical Engineering, University of Cassino and Southern Lazio, Italy
[2]Ergonomics and Aerosol Technology, Lund University, P.O. Box 118, SE-22100, Lund, Sweden
[3]Occupational and Environmental Medicine, Lund University, SE-22100, Lund, Sweden

Keywords: hairdressers, exposure, airborne particles

Introduction

Several studies reported that occupational exposure to chemicals in hairdressing salons is associated with airway disorders (Ma et al. 2010) and dermal diseases (Mendes et al. 2011). In this type of activity, the main routes of chemical exposure are inhalation and dermal contact. The main pollutants contained in chemicals applied in the salons are particles, volatile organic compounds (VOC), ammonia (NH_3) and persulfates.

The aim of this work is to characterize airborne particles that hairdressers are exposed to during bleaching of hair. This work was conducted as a preparation for a human chamber exposure study that will be conducted at Lund University within the Metalund Centre.

Methods

The measurements were performed in a 22 m^3 stainless steel chamber. The air exchange rate in the chamber was 1 h^{-1} and the supplied air was particle free. A thermally heated manikin (Nilsson et al. 2004), fitted with a hair wig, was placed in the center of the chamber. The heated manikin was used in order to consider the effect that the convection, due to the body temperature, may have on the exposure situation.

The measurements consisted of a few phases that resembles real work situation of hairdressers during bleaching. In the beginning, the bleaching product (bleaching powder and hydrogen peroxide) was mixed and prepared outside the chamber. This was done to avoid any emission from the mixing itself and to measure emissions during application of bleaching product. When the applying was done two separate batches of bleaching powder were mixed afterwards inside the chamber (time points 3 and 4 in Figure 1).

In the chamber two different sampling locations were used. A background location was placed in the corner of the chamber. The emissions were sampled above the head of the manikin, above which the ventilation exhaust was placed.

Particle number concentration and size distribution was measured in the range of 0.5 - 20 µm by means of two APS (TSI, Model 3321): one for background measurements and the other to assess the emission near the hairdressing work zone. Particle number concentration and size distribution in the range 10 – 450 nm was performed in the background by means of SMPS (TSI DMA 3071, CPC 3010).

Conclusions

The results in Figure 1 show that no significant particle emissions occurred when the bleaching product was applied to the manikin wig (time point 1 and 2 in Figure 1). This is evident in both the background and in the emission zone where no increase in total particle number was recorded.

Clear emission episodes could be distinguished only during the mixing of the bleaching powder and the hydrogen peroxide (time points 3 and 4 in Figure 1). At these times sharp peaks in the total number concentration were observed in the emission zone. In the background the particle concentrations increased with a slow decay after the mixing was ended. No particles above the background levels were detected with the SMPS, neither during the applying or the mixing of the bleaching product.

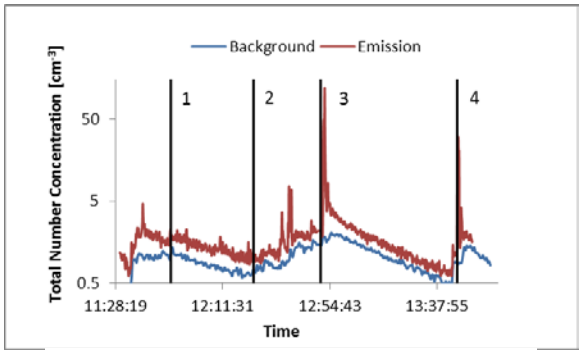

Figure 1. Time series from the two APS at the background and emission sampling location. 1: Start applying, 2: Stop applying, 3: Mixing, 4: Mixing

This project was financed by Swedish Council for Working Life and Research (FAS) and performed within the framework of Metalund, the Centre for Medicine and Technology for Working Life and Society, a competence centre at Lund University, supported by FAS.

Ma C.M. et al. (2010). Volatile Organic Compounds Exposure and Cardiovascular Effects in Hairsalons. *Occup. Med.*, 60, 624-630.

Mendes A. et al. (2011). Chemical exposure and occupation symptoms among Portuguese hairdressers. *J Tox Env Health, Part A* 74(15–16):993–1000.

Nilsson H. O. (2004). Comfort Climate Evaluation with Thermal Manikin, *Doctoral thesis*, University of Gävle, Sweden.

In situ measurements of size resolved sea spray aerosol emissions with the eddy covariance method at Svalbard (78.9°N)

E. Monica Mårtensson[1,2] and E. Douglas Nilsson[1]

[1]Department of Applied Environmental Research, Stockholm University, Sweden
[2]Department of Earth Sciences, Uppsala University, S-752 36 Uppsala, Sweden

Keywords: Primary marine aerosols, sea spray, source emissions, eddy covariance, air-sea exchange

Introduction

The major source of the primary marine aerosol is breaking waves. The aerosol particles are emitted from the water surface into the atmosphere directly as droplets with the composition of seawater enriched with marine organic compounds, bacteria and viruses. With climate change affecting temperature, wind, and ice, the key physical factors driving the sea spray emissions, the production of primary marine aerosols, is expected to change. In situ emission data from Arctic waters are required in order to validate or improve the existing sea spray parameterization for cold waters, *Mårtensson et al. (2003)*. Such improvements or validations are important in order to estimate the over-all sea spray source in a changing climate and represent this large aerosol source in climate models (e.g. *Struthers et al., 2011*). During the Greenhouse Arctic Ocean and Climate Effect of Aerosols (GRACE) field campaign in the summer 2009 direct flux measurements were made from a 10 meter mast on the peninsula Brøggerhalvøya at Svalbard (78.938N, 11.3406E).

Method

The most direct method to quantify the natural emissions is the eddy covariance method. Here the fluctuations in the vertical wind (w') and aerosol/gas concentration (c') are sampled in parallel and processed so that the covariance <c'w'> equals the aerosol/gas fluxes. A Gill HS-50 ultrasonic anemometer measured the vertical and horizontal wind speed. The size resolved aerosol particle concentrations were measured from 0.25 to 2.5 µm diameter with a GRIMM 1.109 Optical Particle Counter and the total aerosol particles concentrations with a TSI 3772 Condensational Particle Counter. CO_2 and H_2O concentration were measured by a Li-7500 Open Path Analyzer.

Results

From the ocean wind sector the upward fluxes totally dominated the aerosol fluxes in the OPC range, to a higher degree than any previous data set we have worked on. This is probably due to the low back ground aerosol concentrations, which minimize the aerosol deposition fluxes. Figure 1 shows the average size distribution of the observed aerosol fluxes for wind speeds larger than 4 ms^{-1}, the minima wind speed when waves are breaking at long fetches. This is in good agreement with the existing Mårtensson *et al.* (2003) sea salt emission parameterisation when average wind speed and sea temperature during the campaign are used in the parameterisation.

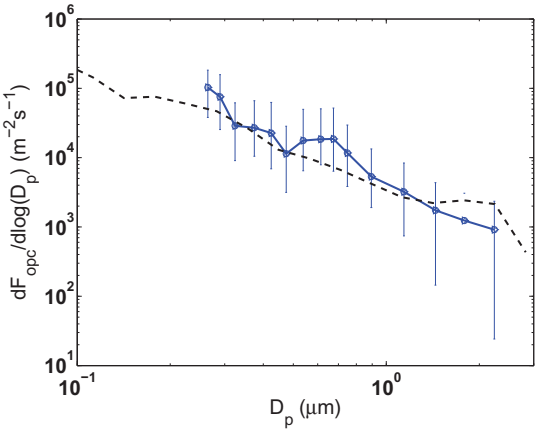

Figure 1. Average aerosol number flux size distributions from the coastal sector. The vertical bars show 25 and 75 percentiles. Dashed line shows the source parameterization according to Mårtensson et al. (2003) for the median wind speed of 5.6 ms^{-1} and 5°C sea surface temperature.

We would like to thank the staff at The Norwegian Polar Institute in Ny Ålesund for support during the campaign and Leif Bäcklin and Kai Rosman at Stockholm University for help with constructions and set up of the equipment. This work was supported by the Swedish research council (VR) through the GRACE project.

Mårtensson, E. M., Nilsson, E. D., de Leeuw, G., Cohen, L. H., & Hansson, H.-C.,2003, *J. Geophys. Res.*, doi:10.1029/2002JD002263.

Struthers, H., Ekman, A.M.L., Glantz, P., Iverssen, T., Kirkeväg, A., Mårtensson, E. M., Seland, Ø, and Nilsson, E. D., 2011, *Atmos. Chem. Phys*, doi:10.5194/acp-11-3459-2011.

Implications for black carbon and sulphate aerosol at a high Arctic site

A. Massling[1], A.G. Grube[1], H. Skov[1], J.H. Christensen[1], B. Jensen[1], Q.T. Nguyen[1, 2], M. Glasius[2], J.K. Nøjgaard[1], L.L. Sørensen[1]

[1]Department of Environmental Science, University of Aarhus, 4000 Roskilde, Denmark
[2]Department of Chemistry, University of Aarhus, 8000 Aarhus, Denmark

Keywords: Arctic, black carbon (BC), sulphate, chemical transport modelling.

Introduction

The temperature increase in the Arctic is observed twice as high as in other parts of the world. Air pollutants that originate from long-range transport to the Arctic may be responsible for these findings. Some of these pollutants are termed short-lived climate pollutants (SLCP) as their lifetime is limited and mitigation strategies on these pollutants give the possibility to act impacting on future climate (Quinn et al., 2008).

Methods

Black Carbon (BC) mass concentrations were measured over a period of two years from January 2009 to January 2011 at a high Arctic site Station Nord in Northern Greenland using a Particle Soot Absorption Photometer. Sulphate mass concentrations were derived for the same period by ion chromatography on filter pack samples that were collected on a weekly base.

In parallel, BC and sulphate mass concentrations were modelled using the Danish Eulerian Hemispheric Model (DEHM). In this study the model was set up with a horizontal resolution of 150 km x 150 km south of 60^0 N and a nested grid of 50 km x 50 km north of 60^0 N, both model domains with the North Pole in the centre.

Results

It was observed that the model could reproduce the seasonal pattern of the observed measured data in the period from January 2009 to January 2011. Little larger discrepancies were found during some periods for the BC comparison. This finding can be explained by the larger uncertainties of BC emission inventories compared to similar emission inventories of sulphur-dioxide both in the total amount but also for the temporal and geographical variations.

For both, measured data and modelled data a high correlation between the concentrations of sulphate and BC was observed throughout the study period from January 2009 to January 2011 (see Figure 1 and 2). This finding indicates that both species undergo common aging process and follow similar transport pattern. In principle it can be suggested that sulphate seems to function as kind of transport container for BC.

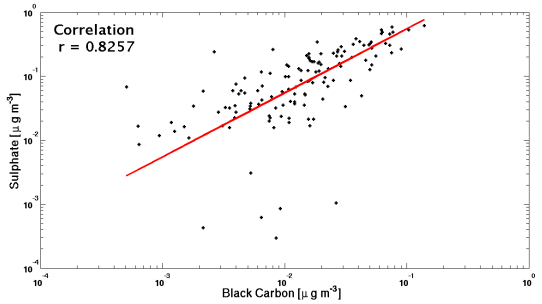

Figure 1. Correlation between BC and sulphate based on measured data.

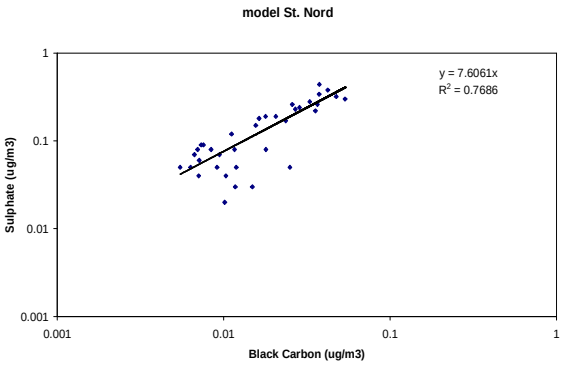

Figure 2. Correlation between BC and sulphate based on modelled data.

Sulphate is formed under atmospheric conditions based on sulphur containing emissions from anthropogenic and/or natural sources. BC particles are primary emitted and exclusively originated from combustion processes.

Acknowledgement

This work was carried out as part of CRAICC (Cryosphere-Atmosphere Interaction in a Changing Arctic Climate). The project was financially supported by The Danish Environmental Agency's program on Arctic air pollution (Monitoring of short lived climate forcers in the Arctic).

References

Quinn, P. K., Bates, T. S., Baum, E., Doubleday, N., Fiore, A. M., Flanner, M., Fridlind, A., Garrett, T. J., Koch, D., Menon, S., Shindell, D., Stohl, A., & Warren, S. G. (2008) Short-lived pollutants in the Arctic: their climate impact and possible mitigation strategies, *Atmos. Chem. and Phys.* 8, 1723-1735.

Chemical and 13-Carbon Isotopic Composition of Secondary Organic Aerosol from Alpha-Pinene Ozonolysis

C. Meusinger[1], U. Dusek[2], S.M. King[1], R. Holzinger[2], M. Bilde[1], T. Röckmann[2] and M.S. Johnson[1]

[1] Copenhagen Center for Atmospheric Research (CCAR), Department of Chemistry, University of Copenhagen, 2100 Copenhagen, Denmark

[2] Institute for Marine and Atmospheric research Utrecht (IMAU), Utrecht University, 3584 CC, Utrecht, The Netherlands

Keywords: SOA, isotopes, carbon, smog chamber.

Presenting author email: came@kiku.dk

Secondary organic aerosol (SOA) formed by the oxidation of volatile organic compounds (VOC) is a key field of atmospheric research as it has a significant impact on climate, health and visibility that is not well understood. After biogenic or anthropogenic emission, VOC are oxidized by different means in the atmosphere and therefore play an important role in photochemistry and by altering the concentrations of oxidants. Although the vast number of reactions and compounds involved in the oxidation of VOCs make detailed reaction mechanisms unclear, lower volatilities are observed in general for more oxygenated compounds (with a higher oxygen-to-carbon ratio, O:C.) This allows an effective age-characterization of the formed SOA.

In addition, isotope measurements allow for distinction of reaction pathways, since the kinetic isotope effect (KIE) alters the isotopic composition of products and reactants in a process-specific way. This in turn helps to establish chemical reaction schemes and to constrain budgets. Studied systems employing isotopes so far cover a wide range including atmospheric samples (Rudolph *et al*, 2002), gas-phase reactions (Iannone *et al*, 2010) and SOA generation (Irei *et al*, 2011).

This study investigates reaction products from alpha-pinene ozonolysis by means of their volatility-resolved isotopic and chemical compositions in order to explore the possible link between ^{13}C fractionation and oxidation state in organic aerosols.

Starting from alpha-pinene with natural isotopic abundance, aerosols were created in chamber experiments by the nucleation of oxidation products from reaction with ozone. Two sets of experiments were performed using 1-butanol and cyclohexane as OH scavengers. The resulting SOA is collected on pre-treated quartz filters and subsequently analyzed for its' chemical and carbon isotopic composition (^{13}C & ^{12}C.)

The experiments were performed under dark, dry and low-NO_x conditions, without seed particles in the new continuous flow smog chamber at the Copenhagen Center for Atmospheric Research to generate the large amounts needed for the isotope analysis. Particle-size distributions and CCN activity were monitored continuously, along with temperature, RH, ozone and NO_x concentrations.

Measurements on the filters were carried out at the Institute for Marine and Atmospheric Research Utrecht using Isotope Ratio Mass Spectrometry (IRMS) and proton-transfer-reaction mass-spectrometry (PTR-MS.) The filters were heated stepwise (100-400 °C) in helium to evaporate organic compounds and convert them to CO_2 for the isotope analysis (Figure 1). In addition, the chemical composition of the evaporated material was determined by PTR-MS at each heating step. After assigning the corresponding chemical formula to the significant masses, the O:C ratio can be calculated and compared to the 13-C data.

The results are furthermore compared to filters loaded with organic aerosol generated by atomising carboxylic acid solutions to distinguish the fractionation in filter handling from the KIE of the initial VOC + ozone reaction.

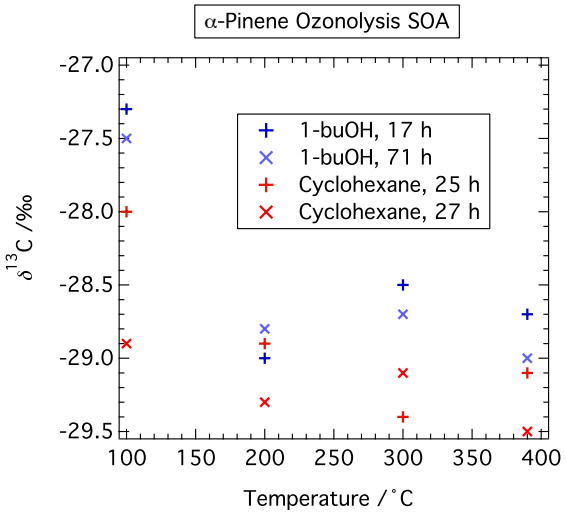

Figure 1. Preliminary isotope data for different OH scavengers and sampling times.

We thank IntraMIF and the Universities of Copenhagen and Utrecht for supporting this research. The research has received funding from the European Community's Seventh Framework Program (FP7/2007-2013) under grant agreement number 237890.

Rudolph, J., Czuba, E., Norman, A.L., Huang, L. and Ernst, D. (2002) *Atmos. Environ.* **36**(7), 1173–1181.

Iannone, R., Koppmann, R. and Rudolph, J. (2010) *Atmos. Environ.* **44**, 4135–4141.

Irei, S., Rudolph, J., Huang, L., Auld, J. and Hastie, D. (2011) *Atmos. Environ.* **45**, 856–862.

An essential formation mechanism to produce sulphuric acid in VOC rich environments

D. Mogensen[1,2], M. Boy[1], S. Smolander[1], L. Zhou[1], P. Paasonen[1], T. Nieminen[1], C. Plass-Dülmer[3], M. Sipilä[1], T. Petäjä[1], L. Mauldin III[4,5], H. Berresheim[6] and M. Kulmala[1]

[1]Department of Physics, P.O. BOX 48, University of Helsinki, FIN-00014
[2]Helsinki University Centre for Environment, P.O. Box 27, University of Helsinki, FIN-00014
[3]Hohenpeissenberg Meteorological Observatory, German Weather Service, Hohenpeissenberg, Germany

[4]Department of Atmospheric and Oceanic Sciences, P.O. Box 311, University of Colorado, CO 80309-0311

[5]Institute for Arctic and Alpine Research, P.O. Box 450, University of Colorado, CO 80309-0450

[6]Center for Climate and Air Pollution Studies, School of Physics, National University of Ireland Galway, Ireland

Keywords: Criegee Intermediates, Sulphuric acid, HUMPPA-COPEC-10, Modelling

Introduction

It is crucial to fully understand the atmospheric sulphuric acid (H_2SO_4) budget in order to predict aerosol formation and growth and hence predict climate change. Traditionally it is thought that H_2SO_4 is produced by OH oxidation of sulphur dioxide (SO_2), and that the sinks of H_2SO_4 in the troposphere are mainly by condensation to the particle phase. We have tested a new oxidation mechanism of SO_2 to form H_2SO_4 that will enhance H_2SO_4 production and hence aerosol formation in VOC (volatile organic compound) rich areas.

Methods

The suggested mechanism is that stabilized Criegee intermediate (sCI) or its derivative can oxidise SO_2 and form H_2SO_4. For our model simulations, we use sCI from ozone (O_3) oxidation of isoprene and three tree emitted monoterpenes; alpha-pinene, beta-pinene and limonene with the rate constants 3.9×10^{-11} cm^3 s^{-1}, 6×10^{-13} cm^3 s^{-1}, 6×10^{-13} cm^3 s^{-1} and 8×10^{-13} cm^3 s^{-1}, respectively based on new laboratory experiments (Welt *et al.*, 2012; Mauldin III *et al.*, 2012). We use the 0D model MALTE-BOX (Boy *et al.*, 2006) with near-explicit chemistry from MCM; http://mcm.leeds.ac.uk/MCM/ and the 1D column model SOSA for vertical investigation of the effect of this new oxidation mechanism on the H_2SO_4 concentration (Boy *et al.*, 2011). The simulations are done for high and low VOC concentrations at two measurement stations: SMEAR II, Hyytiälä (data from HUMPPA-COPEC-10) and Hohenpeissenberg (measurement from spring 2000).

Conclusions

At both stations the differences between measured and modelled H_2SO_4 concentrations, based on the traditional production mechanism, reaches values of more than 50 % when the monoterpene concentrations are above 200 ppt. On days when the monoterpene concentrations are low, the measure/modelled H_2SO_4 concentration difference is around 10 - 20 %. However, if we include the sCI oxidation of SO_2, the measured/modelled ratio of H_2SO_4 approaches unity independently of the magnitude of the measured VOC concentrations. Especially in night time when OH concentrations are low, the contribution of the new oxidation mechanism is crucial in the simulation of H_2SO_4 concentrations.

Boundary layer investigations shows that the contribution from the sCI to H_2SO_4 production is, as expected, most important in the canopy where the concentration of organic compounds are highest. However, our overall results show that the effect of sCI's up to 100 m is very important to consider when calculating the sulphuric acid concentration.

We conclude that the traditional mechanism to form H_2SO_4 can only explain ~ 50 % of the observed H_2SO_4 concentration in VOC rich environments, but 80 – 90 % in VOC poor environments. This new mechanism should be included in global and regional models in order to simulate aerosol formation and growth more accurate and hence improve the prediction of climate change.

We thank the HUPPA-COPEC-10 team for data. This work was supported by the Cryosphere-Atmosphere Interactions in a Changing Arctic Climate (CRAICC), the Helsinki University Centre for Environment (HENVI), the Academy of Finland (251427, 139656) with computational resources from CSC– IT Center for Science Ltd.

Boy, M., Hellmuth, O., Korhonen, H., Nillson, D., ReVelle, D., Turnipseed, A., Arnold, F. & Kulmala, M. (2006) *Atmos. Chem. Phys.*, 6, 4499-4517.

Boy, M., Sogachev, A., Lauros, J., Zhou, L., Guenther, A. & Smolander, S. (2011). *Atmos. Chem. Phys.*, 11, 43-51.

Mauldin III, R. L., Berndt, T., Sipilä, M., Paasonen, P., Petäjä, T., Kim, S., Kurtén, T., Stratmann, F., Kerminen, V.-M., & Kulmala, M. (2012). *Nature*, 488, 193-196.

Welz, O., Savee, J. D., Osborn, D. L., Vasu, S. S., Percival, C. J., Shallcross, D. E., & Taatjes, C. A. (2012). *Science*, 335, 204-207.

Air cleaner device performance tests

B. Mølgaard[1], A.J. Koivisto[2], T. Hussein[1] and K. Hämeri[1,2]

[1]Department of Physics, University of Helsinki, FI-00014, University of Helsinki, Finland
[2]Finnish Institute of Occupational Health, FI-00250, Helsinki, Finland

Keywords: Indoor aerosol, Air cleaning

Introduction

Clean indoor air is important for human health and well-being. Clean air is usually be obtained by reduction of indoor air pollutant sources and by ensuring sufficient ventilation. However, the outdoor air is not always clean, so often the incoming air is cleaned by filtration. Air cleaning devices may also be placed in the indoor environment.

We have tested seven commercially available air cleaning devices which are all designed to remove aerosol particles from the indoor air. Cleaning of coarse particles is good for removing pollen, mould, and dust particles, cleaning of fine particles for removing long-range transported particles, and cleaning of ultra-fine particles for removing particles from local combustion and many indoor sources.

Methods

We performed eight similar experiments in a room, one for each air cleaner and one without any air cleaner. The ventilation rate of the room was about 0.6 air changes/hour. The incoming air was first filtered and then an aerosol generator injected particles into it. The incoming aerosol and the aerosol in the room were monitored with a Scanning Mobility Particle Sizer (SMPS) and an Optical Particle sizer (OPS). Two fans in the room ensured that the air was well mixed. Each experiment lasted about 24 h. In the beginning the aerosol generator was on while the air cleaner was off. Then after 160 min the air cleaner was turned on and the particle concentration decreased. A few hours before the end of the experiment the aerosol generator was turned off. Then the particle concentration decreased rapidly.

The number size distribution in the chamber is described by the balance equation (assuming no indoor sources and neglecting coagulation)

$$\frac{dN_i}{dt} = N_{vent,i}\lambda - N_i(\lambda + \beta_i + \gamma_i)$$

where N_i is the number concentration of particles in size class i in the chamber, $N_{vent,i}$ is the corresponding concentration for the incoming aerosol, λ is the ventilation rate, and β_i and γ_i are respectively the deposition and cleaning rates for particles of size class i.

We used the measured number size distribution data to estimate λ, β_i, and γ_i. This is possible because we measured periods with and without the air cleaners, and with and without incoming particles. By comparing the cleaning rates for the different devices, we can compare their performances.

Results

Two of the air cleaners changed power and thus cleaning rates during the experiments. For these the estimations are difficult and results will not be presented here. For the other five air cleaners the results are given in Figure 1. For four of these we obtained negative cleaning rates for the smallest sizes. This must be caused by a particle source in the room, which was most likely the air cleaners themselves. The calculated cleaning rates may be affected by this source for all sizes below 100 nm. The Lightair device did not cause this problem. This air cleaner functions in a different way than the others. The other air cleaners use fans and filters, but the Lightair removes particles by ionising the air and collecting the ionised particles. This device was, however, clearly less effective for particles larger than 100 nm (Figure 1).

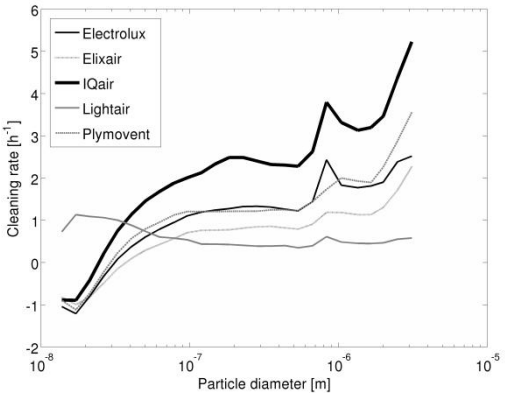

Figure 1. Cleaning rates λ obtained for five air cleaners in a room of volume 81 m^3.

Conclusions

The air cleaning devices all reduced the concentration of particles larger than 100 nm. Some were more effective than others. Most of them, however, seemed to increase the concentration of particles smaller than 25 nm. It is unknown how these extra particles were produced.

Organosulfates at urban curbside and semi-rural background of Denmark: Understanding anthropogenic influence on biogenic SOA

Q.T. Nguyen[1,2], M.K. Christensen[1], F. Cozzi[1], A.M.K. Hansen[1] ,T.E. Tulinius[1], K. Kristensen[1], A. Massling[2], J.K. Nøjgaard[2] and M. Glasius[1]

[1]Department of Chemistry, Aarhus University, Langelandsgade 140, 8000 Aarhus, Denmark
[2]Department of Environmental Science, Aarhus University, Frederiksborgvej 399, 4000 Roskilde, Denmark

Keywords: biogenic secondary organic aerosol, organosulfates, nitrooxy organosulfates, monoterpene oxidation products

Introduction

This work aims to investigate the influence of anthropogenic pollution on the formation and growth of Biogenic Secondary Organic Aerosols (BSOA). Organosulfates which originated from biogenic oxidation products are formed via heterogeneous reactions involving sulphur compounds primarily of anthropogenic origin (Surratt el al., 2008). This class of compounds thus contributes to the formation and growth of Anthropogenically-enhanced BSOA (ABSOA) and as a consequence provides a key coupling between the anthropogenic impacts and biogenic sources (Hoyle et al., 2011). In addition, organosulfates and nitrooxy organosulfates are highly polar which could enhance aerosols to act as cloud condensation nuclei and thus have great climate implications (Hallquist et al., 2009). In this study, organosulfate and nitrooxy organosulfate derivatives of isoprene and monoterpenes and their selected oxidation products were identified and quantified for the campaign period.

Methods

Particles (PM_1) were collected using high volume samplers during a sampling campaign from 19/05 to 23/06/2011 at a Danish urban curbside (Hans Christian Andersen Boulevard, Copenhagen) and at a semi-rural background site (Risø, Roskilde). Filters were extracted and analysed using an HPLC system coupled via an electrospray inlet to a quadrupole time-of-flight mass spectrometer (qTOF-MS) following a method reported by Kristensen and Glasius (2011). Organosulfates and nitrooxy organosulfates were identified using their characteristic MS fragments including HSO_4^-, SO_3^- and HNO_3. The samples were quantified using an in-house synthesized β-pinene-derived organosulfate and camphoric acid as an internal standard.

Conclusions

This study presents a unique data set where ambient organosulfates and nitrooxy organosulfates are identified and quantified concurrently at urban curbside and semi-rural background site. A number of dominant organosulfate and nitrooxy organosulfate species have been identified at both sites, including such as organosulfate Molecular Weight (MW) 154, 200, 216 and in particular, nitrooxy organosulfate MW 295. Results on nitrooxy organosulfate MW 295 are shown in Figure 1. Additional work will include the analysis of air mass back-trajectories using Hybrid Single Particle Lagrangian Integrated Trajectory (HYSPLIT) to investigate the degree of long-range transported SOA in addition to meteorological data and the occurrence of particle formation events at the local site.

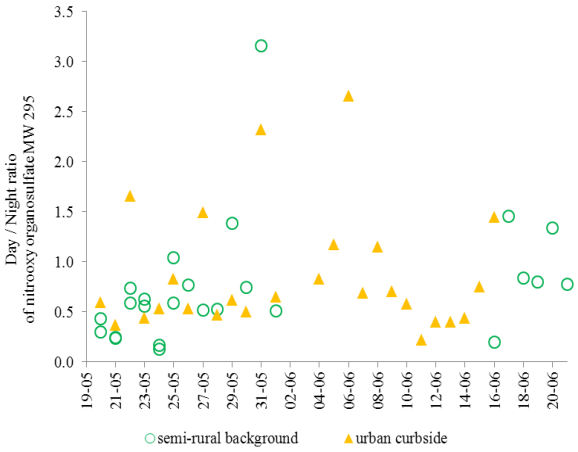

Figure 1. Demonstration of the Day/Night abundance ratio of nitrooxy organosulfate MW 295 during the campaign period. Favored night-time formation of the species as evidenced by the majority of the ratio points below 1 indicates the importance of night-time NO_3 initiated oxidation for its formation. Elevated dominance of day-time formation was also observed at certain points (e.g. 31st May 2011), which can be partly attributed to the high NOx level observed during that day. The comparable ratio between the two sites possibly indicates a regional mechanism for the formation of this species.

This work was supported by the VILLUM Foundation.

Hallquist, M. et al. (2009) *Atmos Chem Phys* 9, 5155.
Hoyle, C.R. et al. (2011) *Atmos Chem Phys* 11, 321.
Kristensen, K. and M. Glasius (2011) *Atmos Environ* 45, 4546.
Surratt, J. D. et al. (2008). *J. Phys Chem A*, 112, 8345.

Atmospheric Fate of an Oxidanyl Radical Formed in The Degradation of Isoprene

Lasse Bo Nielsen, Hasse C. Knap, Kristian B. Ørnsø, Solvejg Jørgensen, Henrik G. Kjaergaard

Department of Chemistry, University of Copenhagen, Universitetsparken 5, DK-2100 Copenhagen Ø, Denmark.

Keywords: Isoprene, Epoxide, Transtion State Theory.

Introduction

Knowledge about the degradation pathways of isoprene is important since it is a major player in the formation of secondary organic aerosols, through the formation of epoxides. Approximately 600 Tg/yr of isoprene is emitted to the atmosphere by terrestrial plants [1]. The degradation of isoprene under high-NO_x conditions leads to the formation of methacrolein (MACR) [2] [3], which then reacts with the hydroxyl radical and oxygen to form the (2-methylprop-2-enoyl)oxidanyl radical (MPOR). Here we have investigated the atmospheric fate of MPOR. We show that it is possible for this radical to form an epoxide (structure B in fig. 1).

Methods

We have used the MP2/6-31+G(d,p) level of theory to optimize the structures along the reaction pathways. Transition states (TS) have been verified with intrinsic reaction coordinate (IRC) calculations. The reaction rate coefficients are estimated by transition state theory. Eckart coefficients have been used to correct the reaction rate coefficients for tunnelling.

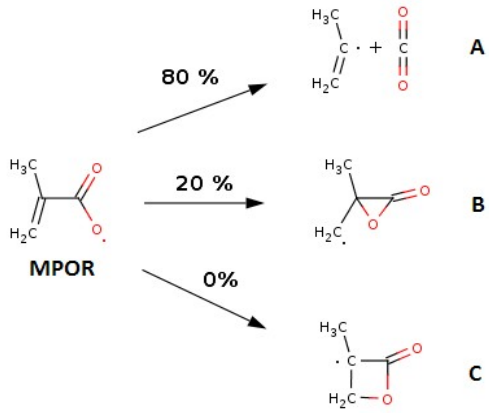

Figure 1. The branching ratio of the unimolecular reaction of MPOR. The major product is isopropenyl radical and CO_2 (reaction pathway A) whereas the minor product is an epoxide (reaction pathway B).

Conclusions

The first step in the degradation of MPOR is probably an unimolecular reaction, where we have found three possible reaction pathways shown in fig. 1. The calculated forward rate coefficients and the total rate coefficient are used to estimate the branching ratio in each reaction pathway. We predict, that at least 80 % of the MPOR ends up as the products, isopropenyl radical and CO_2, and that most 20 % as the epoxide (pathway B).

We are currently investigating the fate of the epoxide. We have found that ring opening via the TS in figure 2. is unfavorable and would lead to back reaction to MPOR. At the moment we are investigating other routes that would not lead to 100 % A.

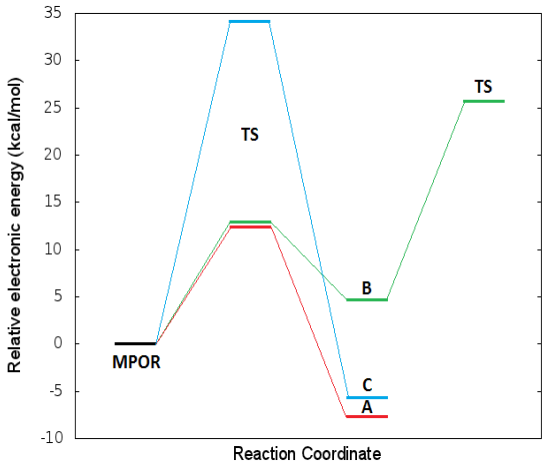

Figure 2. The energy profile of the unimolecular reaction pathways of MPOR.

[1] Guenther, A.; Karl, T.; Harley, P.; Wiedinmyer, C.; Palmer, P. I.; Geron, C.; Atmospheric Chemistry and Physics 2006, 6, p. 3181.

[2] Pierotti, D.; Wofsy, S.C.; Jacob, D.; Rasmussen, R.A.; J. Geophys. 1990, 95, p. 1871

[3] Martin, R.S.; Westberg, H.; Allwine, E.; Ashman, L.; Carl Farmer, J.; Lamb B.; J. Atmos. Chem., 1991, 13, p. 1

[4] Kjaergaard, H.G.; Knap, H.C.; Ørnsø, K.B.; Jørgensen, S.; Crounse, J.D.; Paulot, F.; Wennberg, P.O. ; J. Phys. Chem. A, 2012, 116, p. 5763–5768

One year seasonal cycle of airborne bacteria and fungus in southern Sweden: implications on sinks, sources and turn-over time

E. D. Nilsson[1*], C. Fahlgren[2], U. L. Zweifel[3]

[1]Department of Applied Environmental Science, Stockholm University, SE-10691 Stockholm, Sweden
[2] School of Natural Sciences, Linnaeus University, SE-391 82 Kalmar, Sweden
[3] Department of Cell and Molecular Biology, University of Gothenburg, SE-405 30 Göteborg, Sweden

Keywords: bioaerosols, fungal spores, marine aerosol, bacteria, sea-spray, deposition, source identity, ice nuclei

Introduction and Methods

Colony-Forming Bacteria (CFB) and Fungi (CFF) were determined from samples collected on the east coast of Sweden, Kalmar (56°39.576'N, 16°21.687'E) from April 2007 and September 2008. The aerosol number concentrations of bacteria and fungi (NCFB and NCFF) were interpreted using three dimensional trajectories and a semi-lagrangian approach (Nilsson and Leck, 2003). Fahlgren et al. (2010) showed that NCFB follows the total number of live bacteria, able to grow on solid media and form colonies, and their identity have a high overlap with culture-independent sequencing.

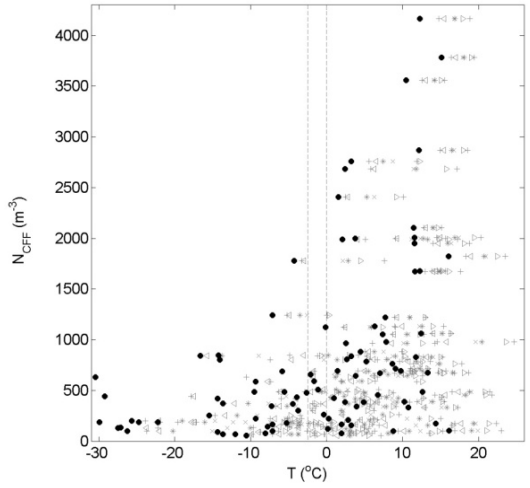

Figure 1. N_{CFF} and air temperature (5 days backward along the trajectories). Grey crosses (x) mark means and pluses (+) mark standard deviation. Grey stars (*) are the median with triangles marking the 25-75% interval. Black filled circles mark minima temperature along the trajectory. Vertical grey lines mark literature values for mortality (0°C) and IN activation (-2.5°C) of fungi.

Results and Conclusions

We found clear seasonal cycles in NCFF and NCFB peaking in summer and winter, respectively, at about 1600 m^{-3} in monthly averages. Fungus and bacteria concentrations were uncorrelated, suggesting different sources. Fungi increased over land, corresponding to a continental fungi source of about 1.4 spores $m^{-3}s^{-1}$. We present parameterizations of NCFF concentration and High NCFB were often associated with transport from both nearby coastal waters and the more distant Atlantic Ocean, as well as higher wind velocities over the seas than for periods with lower NCFB. High NCFB was best correlated to the 10-m wind speed (U_{10}^m) over the upwind ocean, which is consistent with sea spray aerosols. The concentration N_{CFB} increased exponentially with increasing wind speed according to $N_{CFB} = 10^{1.99+0.10U_{10}^m}$, see Fig. 2, in agreement with previous studies for non-biological sea spray. The bacteria emissions are estimated to be about 0.5% of the total sea spray emissions by number. Bacteria concentration did not increase over land. On average 3.4 bacteria $m^{-3}h^{-1}$ were lost over land, corresponding to a sink rate of k_{CFB} =1.49±0.67x10^{-6} s^{-1}, a turnover time of 186h, and an average deposition velocity of 0.6mms^{-1}.

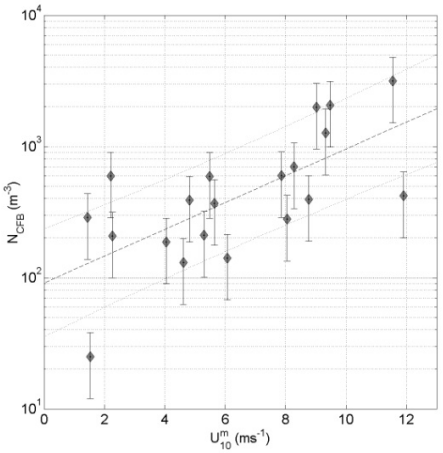

U

Figure 1. NCFB in the air vs. the ten meter wind speed while the air was over oceans, averaged over 168h backward trajectories (grey diamonds) with sample variation error bars (black). Dashed curve is the log-linear fit, while the dotted curves are the errors containing at least 50% of the data.

This work was financed by the Swedish Research Council, the Swedish Research Council for Environment, Agricultural Science and Spatial Planning, and by EU grant SEC6-PR-214400 (AEROBACTICS).

Fahlgren, C., Hagström, Å., Nilsson, D., and Zweifel, U. L., Appl Environ Microb, 76, 3015-3025, 2010.

Nilsson, E. D., and Leck, C., Tellus B, 54, 213-230, 2002.

Sources to Benzo[a]pyrene in Wintertime Urban Aerosols

J.K. Nøjgaard, R. Bossi, A. Massling and T. Ellermann

[1]Department of Environmental Science, Aarhus University, Roskilde, DK-4000, Denmark
Keywords: PAH, benzo[a]pyrene, $PM_{2.5}$, PM_{10}

Introduction

Polycyclic Aromatic Hydrocarbons (PAH) are ubiquitous in ambient air, and partition prevails between the gas and condensed phase according to their vapour pressure. Several PAHs are carcinogenic or suspected carcinogenic, e.g. benzo[a]pyrene (BaP) which is a regulated pollutant within the European Union with a target value of 1 ng/m^3 ambient air. Sources of PAHs include combustion processes, e.g vehicular traffic, coal/oil burning, natural and anthropogenic wood combustion, and other biomass burning (Larsen & Baker, 2003). In a number of studies, vehicular traffic has been identified as a significant contributor to the urban environment, in addition to other fossil carbon sources, whereas the role of biomass burning remains to be addressed. As part of a larger source apportionment study of urban aerosols, $PM_{2.5}$ and PM_{10} associated PAHs and volatile organic compounds (VOC) were sampled in a field campaign from November 7th - December 16th, 2011.

Methods

A busy street in central Copenhagen, Denmark (BS, 60,000 vehicles/day) and an urban background site (UB) located 3 km Northwest of BS was selected for the campaigns. VOCs were sampled on Carbopack X adsorbent (14.4 l/day) and analysed by Thermal Desorption Gas chromatography Mass Spectrometry (Ellermann et al., 2011). $PM_{2.5}$ and PM_{10} particulate matter was sampled on quartz filters using high volume samplers (720 m^3/day). A total of 17 particle-bound PAH were analysed by Gas Chromatography Mass Spectrometry (Glasius et al., 2008).

Conclusions

The wintertime traffic contribution to BaP at a busy street in Copenhagen averaged 34% during the campaign calculated as (BS-UB)/BS. However, large variation was observed (Table 1). Wind from south dominated during the weeks 46-47, where the highest levels of BaP were observed at UB resulting in low relative traffic contributions. Conversely, the vehicular sources contributed by 41-59% of BaP in the remainder of the period (Table 1).

Table 1. Percentage BaP ($PM_{2.5}/PM_{10}$) at BS, and BS percentage contribution to BaP in $PM_{2.5}$

Week	$PM_{2.5}/PM_{10}$ (BS)	$PM_{2.5}$ BaP_{BS}/BaP_{tot}
45	72	54
46	65	21
47	50	-7
48	84	41
49	79	59
mean	**66**	**34**

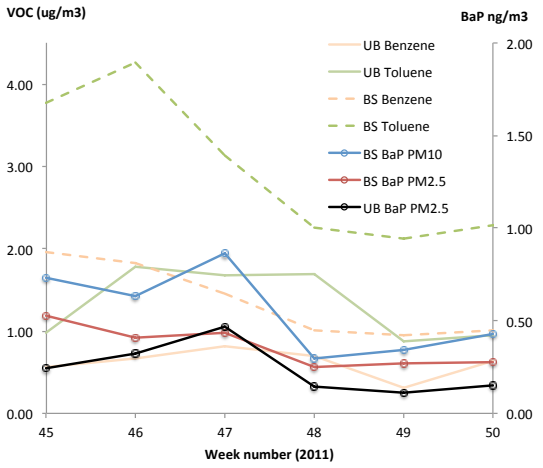

Figure 1. Weekly averages of benzene, toluene and BaP in $PM_{2.5}$ and PM_{10} at UB and BS.

The trends of $PM_{2.5}$ BaP in UB correlated well with benzene in UB during the campaign (Figure 1), suggesting similar sources. At the BS, $PM_{2.5}$ BaP and benzene correlated even better. Conversely, the trend of PM_{10} BaP at the BS resembled that of $PM_{2.5}$ at UB (Figure 1). On average 66% of BaP was confined to the $PM_{2.5}$ fraction where traffic exhaust emissions are expected to be emitted. Hence, about 1/3 of the total BaP is on average in the (PM_{10}-$PM_{2.5}$) fraction, and appears to originate from other sources than traffic exhaust emissions, i.e. other urban sources or long-range transportation. The results will be evaluated in a source apportionment analysis involving PM, trace elements, inorganic species, ^{14}C and organic markers for wood burning, Secondary Organic Aerosols and Primary Biogenic Aerosols Particles.

This work is part of the Particle Project 2011-2013 granted by the Danish EPA, Miljøstyrelsen.

Ellermann, et al., 2011: The Danish Air Quality Monitoring Programme. Annual Summary for 2010. National Environmental Research Institute, Aarhus University. 55 pp. -NERI Technical Report No. 836.

Glasius, M., Ketzel, M., Wåhlin, P., Bossi, R., Stubkjær, J., Hertel, O., Palmgren, F. 2008. Atmospheric Environment 42, 8686-8687.

Larsen, R.K. and Baker, J.E. 2003. Environmental Science & Technology 37, 1873-1881

Physical and Chemical Characterization of Biomass Burning Aerosol

E. Z. Nordin[1], A. C. Eriksson[2], R. Nyström[3], E. Pettersson[3,4], J. Rissler[1], E. Swietlicki[2], M. Bohgard[1], C. Boman[3] and J. Pagels[1]

[1]Ergonomics and Aerosol Technology, Lund University, P.O. Box 118, SE-22100, Lund, Sweden
[2]Nuclear Physics, Lund University, P.O. Box 118, SE-22100, Lund, Sweden
[3]Energy Technology and Thermal Process Chemistry, Umeå University, SE-901 87, Umeå, Sweden
[4]Energy Engineering, Luleå University of Technology, SE-971 86 Luleå, Sweden

Keywords: APM, AMS, morphology, biomass

Introduction

Combustion of biomass fuels for residential heating is considered to be a climate friendly option and is increasing globally. However, this implies potentially increased emissions of aerosol particles. $PM_{2.5}$, which is to a large extent comprised by combustion generated particle matter, co-varies with cardiovascular diseases (Bølling *et al.*, 2009). The composition of biomass burning aerosol can be divided into three main components, soot, alkali salts/ash and organic aerosol and is determined by combustion conditions like oxygen supply and temperature as well as the fuel. Soot and organic aerosol are a result of poor combustion conditions and are considered to be more harmful to human health than ash particles produced under optimal combustion conditions (Bølling *et al.*, 2009). A combustion cycle for example in a wood stove can emit episodes of poor combustion even when the overall combustion is relatively complete. The start-up phase is very sensitive to flash-over which results in air-starved conditions with emissions of soot and polycyclic hydrocarbons (PAHs). The aim of this paper is to study the change in aerosol properties due to different combustion conditions and phases using on-line aerosol measurement techniques.

Methods

The following combustion cases were studied; *i*) a conventional wood stove operated with high burn rate *ii*) a conventional wood stove operated with nominal burn rate, *iii*) a novel pellet reactor operating under air starved conditions, *iv*) a novel pellet reactor operating on optimal conditions, *v*) a modern pellet burner operated under optimal conditions. Mean flue gas and particle characteristics from the combustion cases are shown in table 1. The aerosol from the combustion appliances was diluted 1000-3000 times to concentrations relevant for ambient air before sampling.

Table 1: Particle characteristics and gas concentrations.

Case	CO (mg/MJ)	Total conc. (#*10^{13}/MJ)	Org (mg/MJ)
i	3020±2680	1.4±0.6	9.4
ii	2590±1030	1.3±0.6	8.6
iii	700±1390	1.1±0.3	6.5
iv	120±67	3.3±0.1	0.45
v	110±38	3.8±0.2	0.32

A high resolution aerosol mass spectrometer (HR-TOF-AMS, Aerodyne research Inc.) was used for size resolved composition of compounds vaporised at 600°C. A scanning mobility particle sizer (SMPS) was used for mobility size distributions (10-600 nm) and an aerosol particle mass analyser (APM) operated downstream a differential mobility analyser DMA) and an optional thermodenuder (300 °C) was used to determine the mass mobility relationship (effective density) and assess the size dependent organic mass fraction. Particles for TEM analysis were collected using an electrostatic precipitator. The AMS measures the size resolved chemical composition with very high time resolution and by using specific signatures in the mass spectra, compounds of particular interest like PAHs can be detected. For highly transient conditions like the start-up phase the time-resolution of the APM is not sufficient. Combining AMS and APM measurements will give novel and detailed information about the chemical composition, shape and morphology in all phases of the combustion cycle.

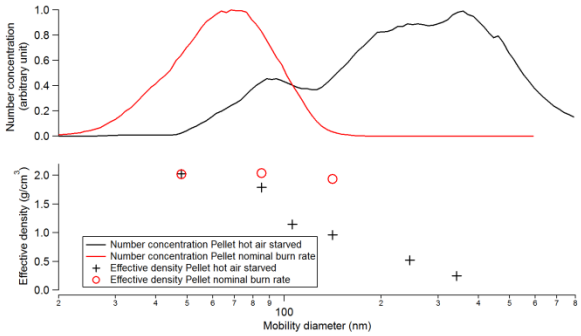

Figure 1: Average number concentration (upper panel) and effective density (lower panel) as a function of mobility diameter.

Conclusions

The effective density from DMA-APM measurements in case *iii* and *iv* (figure 1) gives an indication of the particle shape and composition. Salt aerosols have a relatively high effective density, which does not change with increasing mobility diameter, due to their spherical shape. Soot particles on the other hand have a lower effective density which is decreasing with increased size, due to their agglomerated shape.

This work was supported by the Swedish Energy Agency, the ERA-NET project Biohealth, FORMAS and METALUND.

Bølling A. K. *et al.*, (2009) Particle & Fibre Toxicology, 6:29

Clustering pathways of sulfuric acid, ammonia and dimethylamine molecules

T. Olenius[1], O. Kupiainen[1], I.K. Ortega[1], and H. Vehkamäki[1]

[1] Department of Physics, University of Helsinki, Gustaf Hällströmin katu 2 A, P.O. Box 64, FI-00014 Finland

Keywords: molecular clusters, sulfuric acid, modeling, nucleation

Introduction

Formation of secondary atmospheric aerosol particles begins with individual molecules forming small molecular clusters, which can then grow by colliding with each other. As experimental detection of these clusters still remains challenging, we have used a theoretical model to study the kinetics of a set of clusters.

Methods

We have simulated a set of small molecular clusters containing sulfuric acid (H_2SO_4), ammonia (NH_3) and dimethylamine (DMA, $(CH_3)_2NH$) molecules with the kinetic code ACDC (Atmospheric Cluster Dynamics Code) (McGrath *et al*., 2011) that solves the birth-death equations of the clusters. We have included both neutral and charged clusters that contain up to four sulfuric acid and four base molecules. As an input for the code we have used evaporation rates of the clusters calculated with quantum chemical methods (Ortega *et al*., 2012). We have run the code in atmospherically relevant conditions at 19°C, at sulfuric acid concentration of 10^6 cm^{-3} and with ion production rate of 3 ion pairs s^{-1} cm^{-3} and examined the most significant growth pathways of the clusters in different base concentrations.

Table 1. Main pathways out of the simulated system for all studied ammonia and DMA concentrations.

$[NH_3]$ (ppt)	[DMA] (ppt)	Main pathway out of the simulated system
10	10^{-4}	$1N \rightarrow 1N_{pos} \rightarrow 2N_{pos} \rightarrow 1A2N_{pos} \rightarrow 2A2N_{pos} \rightarrow 2A3N_{pos} \rightarrow 3A3N_{pos} \rightarrow 3A4N_{pos} \rightarrow$ out (5A4N)
10	10^{-2}	$1A \rightarrow 1A_{neg} \rightarrow 2A_{neg} \rightarrow 3A_{neg} \rightarrow$ out ($5A1D_{neg}$)
10	1	$1A \rightarrow 1A1D \rightarrow 2A1D \rightarrow 2A2D \rightarrow 3A3D \rightarrow$ out (5A5D)
100	10^{-4}	$1N \rightarrow 1N_{pos} \rightarrow 2N_{pos} \rightarrow 1A2N_{pos} \rightarrow 2A2N_{pos} \rightarrow 2A3N_{pos} \rightarrow 3A3N_{pos} \rightarrow 3A4N_{pos} \rightarrow 4A4N_{pos} \rightarrow$ out ($4A5N_{pos}$)
100	10^{-2}	$1N \rightarrow 1N_{pos} \rightarrow 2N_{pos} \rightarrow 1A2N_{pos} \rightarrow 2A2N_{pos} \rightarrow 2A3N_{pos} \rightarrow 4A3N1D_{pos} \rightarrow$ out ($4A4N1D_{pos}$)
100	1	$1A \rightarrow 1A1D \rightarrow 2A1D \rightarrow 2A2D \rightarrow 3A3D \rightarrow$ out (5A5D)

Results

Table 1 shows the main pathways out of the system for all studied base concentrations. Figure 1 shows a simplified presentation of collision pathways leading out of the simulated system for the cases where one of the bases has relatively high and the other relatively low concentration. A, N and D denote acid, ammonia and DMA molecules, and subscripts "neg" and "pos" negatively and positively charged clusters, respectively.

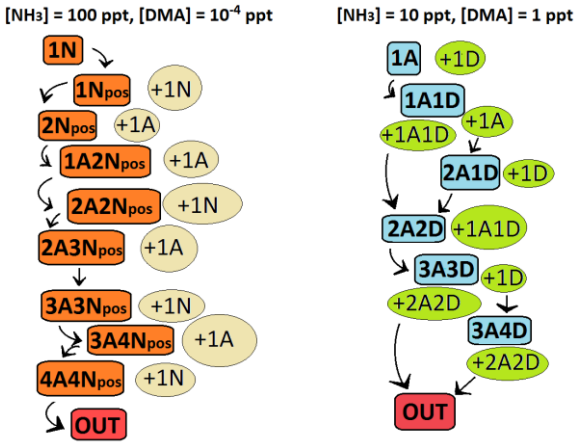

Figure 1. Simplified presentation of the main clustering pathways leading out of the simulated system for two different base conditions.

Conclusions

Our results show that in the case where ammonia is the dominant base, clustering occurs mainly via monomer addition to charged clusters, whereas in relatively higher DMA concentration also cluster-cluster collisions become significant and clusters growing out of the system are mainly electrically neutral. Furthermore, growing clusters contain DMA molecules also in cases where ammonia concentration is few orders of magnitude higher than DMA concentration, indicating that DMA has a significant role in stabilizing the clusters.

This work was supported by FP7-MOCAPAF project No 257360, FP7-ATMNUCLE project No 227463 and Academy of Finland. The authors thank CSC- IT Center for Science in Espoo, Finland for the computing time.

McGrath, M.J. *et al.* (2012). Atmospheric Cluster Dynamics Code: a flexible method for solution of the birth-death equations, *Atmos. Chem. Phys.* 12, 2345–2355.

Ortega, I.K. *et al.* (2012). From quantum chemical formation free energies to evaporation rates, *Atmos. Chem. Phys.* 12, 225-235.

The complexity of aerosols as short-lived climate forcers:

Interactions between soot and secondary organic aerosol (SOA) in a changing climate

R.K. Pathak[1], M. Hallquist[1], A. Watne[1], N. M. Donahue[2], S. N. Pandis[2], T. F. Mentel[3], B. Svenningsson[4], E. Swietlicki[4], W. Brune[5],

[1]Department of Chemistry and Molecular Biology, University of Gothenburg, Sweden

[2]Department of Chemical Engineering, Carnegie Mellon University (CMU), USA

[3] Institute of Energy and Climate Research, Forschungszentrum, Jülich GmbH (FZJ), Germany

[4]Department of Nuclear Physics, University of Lund, Sweden

[5]Department of Mechanical Engineering, Penn State University, USA

Keywords: Soot, SOA, PASS, AMS, CCN

Introduction

The aim of this project is to understand soot-SOA interactions and how this influences properties of the resulting aerosol with emphasis on health and climate by providing high quality data to improve modeling tools for mitigation strategies under a changing climate. In current air quality and climate models, influence of short-lived climate forcers such as O_3, CH_4, and aerosols are not yet well described. For aerosols, uncertainties exist because formation and transformation in the atmosphere are complex with implications for its properties, e.g. soot potentially warms while SOA may cool the planet (*Hallquist et al. 2009*). Regarding the indirect climate effect (influencing cloud properties) the uncertainties are even higher. In the current models, SOA is under-predicted by a factor of 2 to 100 compared to measurements (*Volkamer et al. 2006*). We propose a comprehensive study addressing two key features i.e. influence of SOA on the optical properties of soot and effects of soot by surface acidic catalyzed SOA formation. The experiments will be conducted at our G-FROST (Gothenburg – Flow-tube Reactor for Oxidation Studies at low Temperatures) facility (*Jonsson et al. 2008*) and in collaboration with our international partners e.g. CMU, Penn state, FZJ & U Lund.

Methods

A Schematic flowchart of experimental set-up is shown in the Fig.1. The soot generated will be coated by sulfuric acid and subsequently acidity will be regulated by their NH_3 gas treatment in the modulation chamber. The modified soot aerosol will interact with SOA generated by VOC oxidation in the G-FROST. Along with gas-aerosol composition, size, volatility, hygroscopic, optical and cloud forming properties of the resulting aerosol will be measured downstream using state-of-the-art instruments shown in Fig.1. An alternate stream of aerosol will be fed to potential aerosol mass (PAM) chamber, prior to measurements to study properties of aged aerosol. Work plan is as following:

Task 1: To set up soot generation and modulation unit to produce nuclei for SOA condensation.

Task 2: Experiments at G-FROST, effect of temperature and RH on:

A) Aerosol mass fraction of SOA from oxidation of selected VOCs: i) without seeds; soot as seeds and $(NH_4)_2SO_4$ as seed; ii) with soot seeds and influence of acidity (adding H_2SO_4 and/or NH_3)

B) Aerosol optical properties and CCN ability: i) Soot alone; ii) SOA alone with and without extensive oxidation (PAM chamber); iii) Soot+H_2SO_4/NH_3; iv) Soot+H_2SO_4/NH_3+SOA (w/wo PAM chamber)

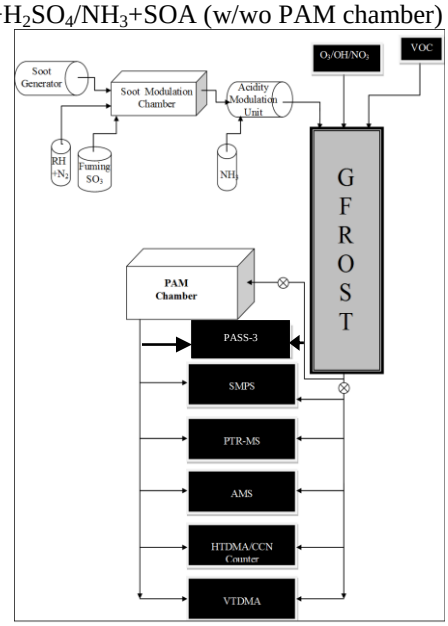

Figure 1: Schematic of experimental set-up

Task 3: Some selected experiments from Task 2 will be investigated in the smog chambers for aging of aerosol (up to 48-hr)

Task 4: Parameterization of experimental data obtained from Task 2 and 3 to develop modeling tools for climate and air-quality predictions.

Conclusion

This project will establish a new research activity on soot-SOA interactions at the Gothenburg University with extensive high profile international network. It will strengthen the knowledge transfer from laboratory to modeling tools for policy making. It will also induce changes in treatment of short lived climate forcers (SLFC) within Swedish and international abetment strategies.

Hallquist et al. (2009). *Atmospheric Chemistry and Physics*, 9: - 5155–5236.

Volkamer, et. al. (2006) *Geophysical Research Letter*, 33, L17811.

Jonsson et al. (2008). Atmospheric Chemistry and Physics, 8: 6541–6549.

Pollen forecast – from pollen counts to model-assisted allergen information service

A.-M. Pessi, S. Saaranen, and A. Rantio-Lehtimäki

Aerobiology unit, Centre for Environmental Research of the University of Turku, Turku, FI-20014 Turku, Finland

Keywords: pollen information, allergen forecasts

Introduction

During the last 30 years, the prevalence of allergy and asthma in Europe has increased four-fold reaching 15%-40% of population; in Finland over 20% of population is sensitized to birch pollen.

Pollen information service is a useful tool to reduce disease burden of allergy and hence, health care costs. Pollen reports help allergic people to understand the symptoms, and avoid exposure to aeroallergens by planning travelling and time of staying outdoors, and even reduce drug consumption by correct timing. Moreover, pollen information is a practical tool for clinicians in pollen allergy diagnostics.

Pollen information, based on pollen counts has been disseminated in Finland since 1976. The public information is an established practice among Finnish population and it is effectively distributed in the media (TV, radio, newspapers, Internet).

Since 2002 Aerobiology unit at the University of Turku has co-operated with the Finnish Meteorological Institute, in order to achieve SILAM-based pollen dispersion models (silam.fmi.fi). At present, 2012, this European-scale system (Siljamo *et al.*, 2012; Sofiev *et al.*, 2012) performs assessment and short-term (up to 120 hours) forecasting of development of birch and grass pollen seasons and pollen dispersion in Europe.

Methods

Pollen is monitored in Europe using a Hirst-type pollen and spore trap (Hirst, 1952), and pollen counts are based on visual identification of pollen grains (see e.g. Smith *et al.*, 2009). Concentrations are expressed as a daily mean of pollen grains per cubic meter of air (grains/m^3). Similar data is collected to a database maintained by the European Aeroallergen Network (EAN; www.polleninfo.org); at present the database holds information from more than 600 pollen-monitoring stations ~~from~~ all over Europe, including 9 stations in Finland.

The project HIALINE (www.hialine.com; 2009-2011) monitored ambient aeroallergens of birch (Bet v 1), grasses (Phl p 5), and olive (Ole e 1) at 11 sites in Europe (Buters *et al.*, 2012).

The pollen counts at sampling sites and EAN-database, as well as emission and dispersion data from the continuously improving SILAM model have been used in our pollen information and forecasts since 2006.

Conclusions

The SILAM dispersion model has been found to be a useful tool in daily information service to predict long (LDT) and medium distance transport of pollen. Especially in case of birch in Finland there have been significant LDTs almost every year. The dispersion model is shown to a user by a dynamic map, animated to display hourly changes. Besides the forecasts it has improved daily information remarkably: formerly the information was based on data at 9 sites, analysed twice a week.

It has been shown that the amount of allergenic protein per pollen grain is not stable. Buters *et al.* (2010) found that the same amount of pollen in different years, different trees and even different days released up to 10-fold different amounts of allergen. Referring to the results of the HIALINE project, birch pollen and Bet v 1 allergen concentrations in ambient air are not always correlated. There are episodes when allergen content per pollen decreases from the average several-fold. According to Buters et al. (2012), especially based on footprint analyses these decreases can be correlated with the geographical location of actual pollen sources.

In future, pollen information targeted to allergic people cannot rely only on pollen quantities but needs also information about the quality of pollen. The source, as an important factor for pollen allergen content, is detectable only by using dispersion models.

Buters, T. M. & al. (2012). *Atmos. Environ.*, 55, 496-505.

Buters, T. M. & al. (2010). *Allergy*, 65, 850-858.

Hirst, J.M. (1952). *Ann. Appl. Biol.*, 36: *257-265*.

Siljamo, P. & al. (2012), *Int, J. Biometeorol.* DOI: 10.1007/s00484-012-0539-5.

Smith, M. & al. (2009). *Aerobiologia*, 25, 321–332.

Sofiev, M. & al. (2012), *Int. J. Biometeorol.* DOI: 10.1007/s00484-012-0532-z.

MODELING AEROSOL WATER UPTAKE IN THE ARCTIC AND ITS DIRECT EFFECT ON CLIMATE

N. RASTAK[1], S. SILVERGREN[4], P. ZIEGER[3], U. WIDEQVIST[1],
J. STRÖM[1], B. SVENNINGSSON[4], A. EKMAN[2], P. TUNVED[1] and I. RIIPINEN[1]

[1]Department of Applied Environmental Science and Bert Bolin Centre for Climate research, Stockholm University, Sweden
[2]Department of Meteorology (MISU), Stockholm University, Sweden
[3]Paul Scherrer Institute, Switzerland
[4]Division of Nuclear Physics, Lund University

Introduction

Hygroscopicity is one of the most fundamental properties of atmospheric aerosols. Aerosol particles containing soluble materials can grow in size by absorbing water in ambient atmosphere. Hygroscopicity controls the size of an aerosol particle and therefore its optical properties in the atmosphere. Hygroscopic growth depends on the dry size of the particle, its chemical composition and the relative humidity in the ambient air (Fitzgerald, 1975; Pilinis et al., 1995). One of the typical problems in aerosol studies is the lack of measurements of aerosol size distributions and optical properties in ambient conditions. The gap between dry measurements and the real humid atmosphere is filled in this study by utilizing a hygroscopic model which calculates the hygroscopic growth of aerosol particles at Mt Zeppelin station, Ny Ålesund, Svalbard during 2008.

Methods

A hygroscopic growth model was built on the κ-Köhler theory (Petters and Kreidenweis, 2007). The monthly chemical composition of the aerosol particles is represented by observations of inorganic ions obtained from the Norwegian Institute for Air Research (NILU) and filter sample analysis for the organic and elemental carbon (OC/EC) concentration (Silvergren et al., unpublished manuscript). The final assumed components are thus: soluble and insoluble organics, sulfate, sea salt and soot. Internally mixed aerosol particles with homogenous chemical composition are assumed. After using the hygroscopic model, the radiative properties and radiative influence of the aerosols on the Arctic environment are studied using a Mie scattering model (Wiscombe, 1979) and a radiative transfer model (Richiazzi et al., 1998).

Conclusions

The evaluation of the hygroscopic model calculations with HTDMA measurements (Silvergren et al., unpublished manuscript) and the Mie scattering model calculations with humid nephelometer measurements during a 90 days campaign at Zeppelin station (Zieger et al., 2010) shows a good agreement.

Sensitivity tests show that increasing the relative humidity and dry size of particles by 10% increases the annual mean scattering coefficient by 50% and 36% respectively, while replacing the monthly chemical composition by pure ammonium sulphate decreases the annual mean scattering coefficient by only 13%. Considering the hygroscopic growth of aerosol particles in ambient atmosphere increases the annual mean scattering coefficient by a factor of 4.8±0.9. The monthly differences between the dry calculation and the ambient humid calculations are shown in fig 1. In the same figure a clear seasonal trend in scattering coefficients at Zeppelin station can be seen, with the lowest values during summer followed by a moderate increase towards fall and winter with highest values in spring. December should be removed due to lack of number size distribution measurements.

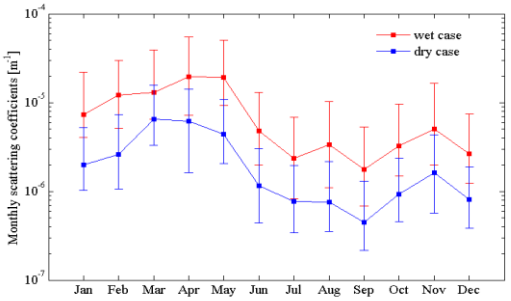

Figure 1. Median scattering coefficients calculated for dry case and ambient humid (wet) case with 25th-75th percentile ranges indicated

Petters, M. D., Kreidenweis, S. M.(2007), *Atmos. Chem. Phys.*, 7, 1961–1971.

Wiscombe, W., (1979), Available from National Technical Information Service as NTIS PB 301388.

Richiazzi, P., et al. (1998) *B. Am. Meteorol. Soc.*, 79, 2101–2114.

Zieger, P., et al. (2010), *Atmos. Chem. Phys.*, 10, 3875–3890.

ADCHAM - A multilayer aerosol dynamics, gas and particle chemistry chamber model

P. Roldin[1], E.Z. Nordin[2], A.C. Eriksson[1], D. Mogensen[3], A. Rusanen[3], E. Swietlicki[1], M. Boy[3] and J. Pagels[2]
[1]Division of Nuclear Physics, Lund University, P.O. Box 118 SE-221 00 Lund, Sweden
[2] Ergonomics and Aerosol Technology, Lund University, Lund, Sweden
[3]Atmospheric Sciences Division, Department of Physics, University of Helsinki, Finland

Keywords: Secondary organic aerosol, multilayer, aerosol dynamics, gas phase chemistry

Laboratory experiments show that SOA particles can form a solid or semi-solid amorphous phase (e.g. Virtanen *et al*., 2010). If an amorphous solid phase is formed gas to particle partitioning will not be well represented by a thermodynamic equilibrium process (Pöschl, 2011).

ADCHAM combines an updated version of the aerosol dynamics and particle phase chemistry module from ADCHEM (Roldin *et al*., 2011) and the gas phase Master Chemical Mechanism (MCMv3.2). ADCHAM explicitly treats the bulk diffusion of all compounds (including O_3) between different particle layers and bulk reactions analogous to Shiraiwa *et al*. (2010). For all compounds except O_3 the gas-surface exchange is modeled with a condensation/evaporation equation which considers the gas-surface diffusion limitations and non-unity dissolution probability in the surface bulk layer (mass accommodation). In each particle layer the model considers oligomerization, equilibrium reactions between crystalline inorganic salts and their dissolved ions, and oxidation of SOA with O_3. The oligomerization and solid salt formation increases the viscosity of the particle bulk which limits the diffusion of the liquid compounds. We estimate the pure liquid saturation vapor pressures, p_0, using either the group contribution method SIMPOL (Pankow & Asher, 2008) or the method by Nannoolal *et al*. (2008). The corresponding equilibrium vapor pressures over each particle size are derived with Raoult's law, using the activity coefficients calculated with AIOMFAC (Zuend *et al*., 2011) and the Kelvin effect.

ADCHAM is currently used to model smog chamber experiments for both anthropogenic and biogenic SOA. Figure 1 shows the model layer structure when modeling SOA and NH_4NO_3 formation on dry $(NH_4)_2SO_4$ particles. Figure 2a illustrates modeled evaporation time scales for α-pinene SOA particles in vacuum, 1) when SOA is liquid-like, 2) when SOA is amorphous (solid), 3) when SOA particles are amorphous and partly oxidized with O_3 forming 50 % non-volatile and 50 % more volatile ($p_0 = 1\ Pa$) oxidation products, and 4) when SOA is amorphous and partly oligomerized. The slow evaporation of amorphous particles is due to the accumulation of low or non-volatile (NV) compounds in the particle surface layer (Fig 2b).

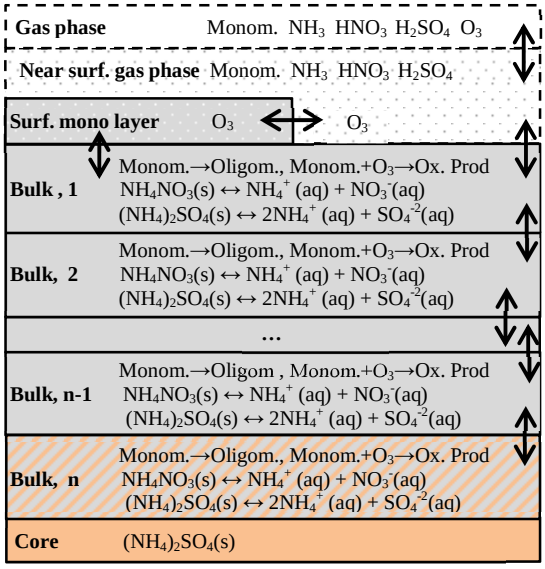

Figure 1. Model layer structure.

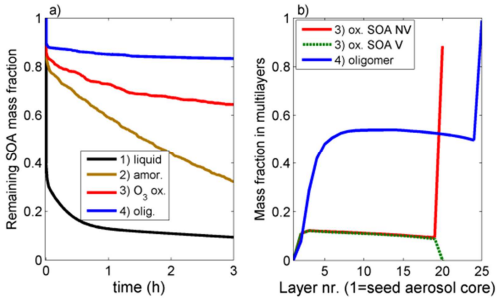

Figure 2. a) modeled SOA evaporation, b) fraction of SOA+O_3(p) oxidation products from simulation 3 and oligomer mass fraction from simulation 4, in each particle layer after 3 hours of evaporation.

Nannoolal, J., Rarey, J., Ramjugernath, D., (2010), *Fuild Phase Equilibria*, 269, 117-133
Pankow, J. F. & Asher, W. E. (2008), *Atmos. Chem. Phys*., 8, 2773–2796
Pöschl, U., (2011), *Atmos. Res.* 101, 562–573.
Roldin et al., (2011), *Atmos. Chem. Phys*., 11, 5867-5896
Virtanen et al., (2010), *Nature*, 467, 824-827.
Zuend et al., (2011), *Atmos. Chem. Phys*., 11, 9155–9206
Shiraiwa, M., Pfrang, C., Pöschl, U., (2010), *Atmos. Chem. Phys*., 10, 3673–3691

X-ray absorption photofragmentation of ammonium bisulphate cluster-ions

Mauritz J. Ryding[1], Minna Patanen[2], Grazieli Simões[2], Alexandre Guiliani[2], Olle Björneholm[3], Glenn B. S. Miller[1], Tuija Jokinen[4], Catalin Miron[2], and Einar Uggerud[1]

[1] Centre for Theoretical and Computational Chemistry, Department of Chemistry, University of Oslo, PO box 1033, Blindern NO-0315 Oslo, Norway
[2] SOLEIL, St Aubin, BP48, 91192 Gif sur Yvette Cedex, France
[3] Department of physics, Uppsala University, PO Box 516, SE-751 20 Uppsala, Sweden
[4] Laboratory of Analytical Chemistry, Department of Chemistry, University of Helsinki, P.O. BOX 55, FI-00014, Finland

Keywords: Ammonia, Sulphuric acid, ions, XAS

Introduction

Sulphuric acid and ammonia have for many years been considered two of the main compounds involved in formation of new atmospheric nanometre-sized particles (Kulmala 2003). During more recent years, the involvement of amines other than ammonia has been gaining interest and experimental results indicate that cluster ions of ammonia– sulphuric-acid salts would exchange ammonia for amines very quickly in the atmosphere (Bzdek et al. 2010). Nevertheless, it is necessary to improve our fundamental understanding of the interactions between ammonia and sulphuric acid in salt clusters; this work present results of core level X-ray absorption photofragmentation of cationic ammonium bisulphate clusters.

Methods

The experiments were performed at the PLEIADES beamline at the SOLEIL synchrotron radiation facility (France), using a linear ion-trap mass spectrometer (LTQ XL, Thermo Electron, San Jose, CA, USA). Clusters ions $(NH_4)_{n+1}(HSO_4)_n^+$ were produced by electrospray ionization of 17 mM ammonium sulphate solution in water/methanol 1:1. The ions were transferred to the linear ion-trap, and a single size $n \leq 6$ was selected before the ions were exposed to X-rays for 600 ms and the resulting fragmentation products detected. Three ranges of photon energies were covered: 167–180 eV, 397–415 eV and 525–549 eV, corresponding to the absorption edges of sulphur (SE), nitrogen (NE) and oxygen (OE), respectively. Abundances were normalized to the reactant ion intensity and corrected for variations in photon flux with photon energy.

Conclusions

For the SE, measurements were performed on clusters with size 3–6. The first fragmentation peak corresponded to loss of ammonium bisulphate or, equivalently, ammonia and sulphuric acid (AS). The first AS loss is a smooth function of X-ray energy, and increases monotonously with the latter. The increased fragmentation associated with the SE can be detected in the subsequent fragmentation peaks (see Fig. 1).

Product size-dependence can vary in non-trivial ways. For instance, while the loss of a single AS from $(NH_4)_7(HSO_4)_6^+$ is the most abundant product by an order of magnitude, the next largest product is loss of 4 AS, followed by −3 AS and −2 AS (see Fig. 1).

For the NE and OE, only the $(NH_4)_7(HSO_4)_6^+$ cluster was measured; overall, results are similar to those of the SE.

With this study, we aim to improve our understanding of these clusters with regards to energetics and structure.

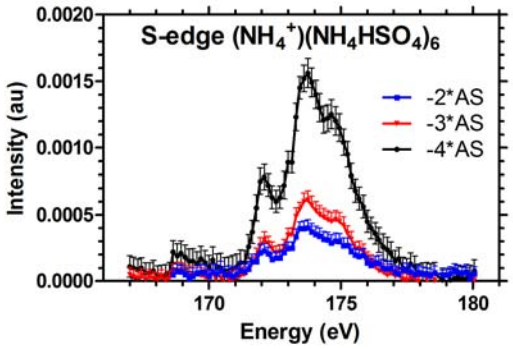

Figure 1. Loss of ammonium bisulphate (AS) from $(NH_4)_7(HSO_4)_6^+$ as a function of photon energy in the region of the sulphur absorption edge.

The team is grateful to the SOLEIL Synchrotron facility for beamtime and for excellent experimental infrastructure.

Bzdek, B. R., D. P. Ridge, et al. (2010). *Amine exchange into ammonium bisulfate and ammonium nitrate nuclei*. Atmospheric Chemistry and Physics 10(8): 3495-3503.

Kulmala, M. (2003). *How particles nucleate and grow*. Science 302(5647): 1000-1001.

Determination of Nanoparticles Surface Tension in the Case of Ibuprofen and Elemental Sulfur

A.V. Samodurov[1,2], S.V. Valiulin[2], V.V. Karasev[2] and S.V. Vosel[1,2]

[1]Novosibirsk State University, Pirogova st., 2, 630090, Novosibirsk, Russia
[2]Laboratory of Nanoparticles, Institute of Chemical Kinetics and Combustion SB RAS, Institutskaya st., 3, 630090, Novosibirsk, Russia

Keywords: nanoparticles, homogenous nucleation, ibuprofen, sulfur

Introduction

Past years of investigations have shown that properties of nanoscaled matter can dramatically differ from that of a bulk matter. The thermodynamic properties of interphase boundary can be fully characterised by the state function called surface tension, σ. In Gibbs rigorous theory surface tension is the function of curvature radius. So the information of surface tension dependence on nanoparticle radius R is very important when investigating colloid systems (i.e. processes of formation, aging, stability). It is not easy to measure nanoparticle surface tension in direct experiments. It is possible to numerically calculate surface tension of nanoparticles by the means of i.e. MD simulations, but only for simple systems (LJ fluids). On the other hand the homogeneous nucleation rate is a function of surface tension. Therefore experimentally determined homogeneous nucleation parameters (nucleation rate, temperature, supersaturation ratio) can be used for $\sigma(R)$ dependence evaluation. Recently a new rigorous formula for homogeneous nucleation rate has appeared (*Vosel et al.,* 2009). This formula takes into account not only the dependence σ on nanoparticle radius but also translation-rotation of a critical nucleus. The goal of this work was to determine homogeneous nucleation parameters of two systems: ibuprofen and sulfur and to determine critical nuclei surface tension.

Methods

In our experiments we utilized laminar flow horizontal nucleation chamber. It was a glass or quartz tube with an external heater. An inert gas (argon, 99.999% purity) entered the chamber and passed through heated zone of the tube. A crucible with a substance was located in the maximum inner temperature zone of the heated area. The substance evaporated from the crucible. A gas flow containing substance vapors entered a cool zone after the heater. While gas was cooling vapors became saturated first, then supersaturation ratio increased and homogeneous nucleation occurred in some area of the chamber. New formed critical nuclei grew fast due to vapor condensation on them.

The number concentration and average diameter of aerosol particles at the exit of the chamber were measured by automatic diffusion battery (ADB). In order to obtain the approximate location of nucleation zone a new “supersaturation cut-off” technique was used. Also heat and mass transfer equations were solved in the case of sulfur. 3D supersaturation and temperature profiles were obtained. Experimental data was used to calculate homogeneous nucleation rate. Then using the rigorous formula (*Vosel et al.,* 2009) surface of tension of critical nuclei was obtained.

Results

It was found that the surface tension of 1.6 nm ibuprofen critical nuclei is about 1.06 times bigger than surface tension of bulk ibuprofen. In the case of elemental sulfur the surface tension of 1 nm nuclei is about 1.05 times bigger than that of bulk sulfur. One can see that substances with similar molecular weights (243 g/mol for ibuprofen vs. 240 g/mol for sulfur vapor) have a similar trend of surface tension being larger than that of bulk substance.

Financial support for this work was provided by Russian Federation for Basic Research (RFBR) Project No. 11-08-01204-a, and joint research project between SB RAS and NSC Taiwan 2011–2013.

1. S.V. Vosel, A.A. Onischuk, P.A. Purtov // J. Chem. Phys. 2009. V. 131. P. 204508-1.

Are agricultural areas the main source of *Alternaria* fungal spores in the atmosphere?

Carsten A. Skjøth[1], Janne Sommer[2] and Ulrich Gosewinkel Karlson[1]

[1]Department of Environmental Science, Aarhus University, Frederiksborgvej 399, 4000 Roskilde, Denmark
[2] Astma-Allergy Denmark, Universitetsparken 4, 4000, Roskilde, Denmark

Keywords: Long Distance Transport (LDT), Danish Pollen and Spore program, Copenhagen

Introduction

The fungal genus *Alternaria* includes numerous plant pathogens, some of which are not only an agricultural problem, but can also threaten human health. How *Alternaria* is distributed in time or space has rarely been investigated, and the main source to airborne *Alternaria* spores remains to be identified. In this study we hypothesize that agricultural areas with certain types of crops and production systems such as rotation with mechanical harvest are the main source of *Alternaria* spores in the air.

Methods

Measurements from the long term Danish Pollen and Spore program have been analysed at Copenhagen during 2005-2010 with respect to *Alternaria* spores. Back trajectories and land cover with respect to agricultural areas from the CLC2000 data set are combined and analysed using similar protocols as previous trajectory studies on data from the Danish or English monitoring programmes. Local emission studies from Danish agricultural fields are used to identify if they could be a potential source of *Alternaria* spores. Counting of spores from the potential source was done using a similar methodology as in the Danish pollen monitoring programme.

Results

The analysis of bi-hourly *Alternaria* spore concentrations shows a typical daily pattern with peak concentrations in the late afternoon (Fig. 1).

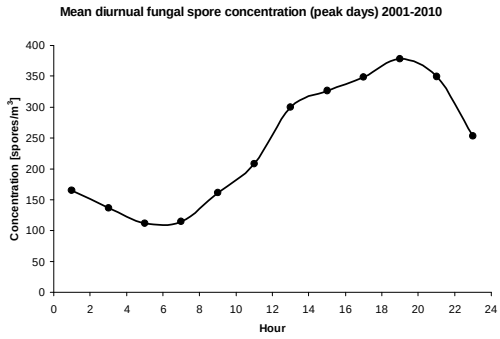

Fig. 1. Mean diurnal *Alternaria* spore concentration for days above 100 spores/m^3, n=232

The emission studies verify that local fields can be a source to Alternaria spores. The source strength between individual fields and between individual sampling days can vary with a factor of 2.

A typical episode with possible Long Distance Transport (LDT) was identified. Back trajectories during the selected period show that during the period with elevated concentrations, air masses arrived from Central Poland. Data CLC2000 show that large parts of Denmark, central and northern Germany and central Poland are dominated by agricultural production under rotation.

Conclusions

The measured airborne concentrations of *Alternaria* spores in Copenhagen suggest that the daily load of *Alternaria* spores is dominated by local or near local sources. The emissions studies verify, that this hypothesis is true, but also that the source strength in between fields is large. The measurements from the monitoring programme also indicate episodes of LDT of *Alternaria* spores that originate from central Poland with areas that are dominated by agricultural areas under rotation systems such as barley, wheat and potatoes. Previous studies in Poland have highlighted central Poland around Poznan and Warszawa as areas with a very high load of *Alternaria* spores compared to e.g. southern Poland such as Krakow. It is well known that the species *Alternaria alternata* (Fr.) Keissl. (common name: early blight) is a problematic fungal pathogen in certain agricultural crops, especially potatoes. This study supports the hypothesis that agricultural areas can be the major source of elevated *Alternaria* spores in the air and that measured concentrations are mainly due to local sources with intermittent LDT from major agricultural areas in rotation.

This work received funding from a post doc grant (to Carsten Ambelas Skjøth) provided by the Villum Kann Rasmussen foundation.

C. Ambelas Skjøth, J. Sommer, L. Frederiksen and Ulrich Gosewinkel Karlson. Crop harvest in Central Europe causes episodes of high airborne *Alternaria* spore concentrations in Copenhagen. Atmospheric Chemistry and Physics Discussions, i 12, 14329-14361, 2012, http://www.atmos-chem-phys-discuss.net/12/14329/2012/acpd-12-14329-2012.html

The fate of aerosol AuNP upon deposition into physiological fluids – Protein corona and aggregation in solution

C.R. Svensson[1], M. E. Messing[2], M. Lundqvist[3], A. Schollin[3], K. Deppert[2], S. Snogerup Linse[3], J. Pagels[1], J. Rissler[1] and T. Cedervall[3].

[1]Ergonomics and Aerosol Technology, Lunds University, Sölveg. 26, 22100, Lund, Sweden.
[2]Solid State Physics, Lunds University, Box 118, 22100, Lund, Sweden.
[3]Department of Biochemistry and Structural Biology,Lund University, Sölveg. 39, 22100, Lund, Sweden

Keywords: Aerosol, Protein corona, Air Liquid Interface, Biomolecules

Introduction

During the last decade traditional forms of toxicological methodology has been discussed with regards to nanoparticle toxicology. As a result toxicological experimentation in the so called Air Liquid Interface is becoming more common, where conditions in the Lung is mimicked using various cell types (Savi et al 2008).. In addition to dose administered to the cells or organisms the particles aggregation and protein coating is believed to be crucial for the understanding of toxicological effects (Lynch et al 2008). This work addresses these issues in the Air Liquid Interface by depositing gold nanoparticles (AuNP) from an aerosol phase into solution. After deposition agglomeration, size and protein corona are determined. The work represents a novel combination of techniques to address multidisciplinary questions.

Methods

An AuNP aerosol is generated by the high temperature evaporation condensation method. The aerosol is characterized using an aerosol particle mass analyser in combination with a differential mobility analyser and an electrometer. A sintering furnace is placed before the characterization system. Agglomerate and spherical, AuNPs with a mobility diameter of 60 nm are deposited into 35 mg/ml albumin in buffer and into diluted (10%) and undiluted porcine blood serum and lung fluid. After deposition the particle solutions is characterized using a combination of particle tracking analysis, UV spectroscopy, dynamic light scattering, and SDS-PAGE.

Conclusions

Spherical AuNP deposited into BSA and serum solutions results in distinct particle sizes measurable by both particle tracking analysis and dynamic light scattering. UV spectroscopy show that the AuNP is stabilized by proteins/biomolecules and form AuNP:Protein complexes rather than AuNP:AuNP complexes. In undiluted serum larger AuNP:protein complexes form compared to BSA and diluted serum, supported by both size measurements and UV spectroscopy. The AuNP:Protein complex sizes in BSA, undiluted serum, diluted and lung fluid is 75, 114, 73 and 105 nm hydrodynamic peak mode diameter respectively, figure 1, as measured by particle tracking analysis. The AuNP hydrodynamic size of 75 nm, measured by particle tracking analysis for AuNP in BSA, is consistent of a monolayer of albumin on a spherical 60 nm particle. The same size trend is seen when measured by dynamic light scattering.

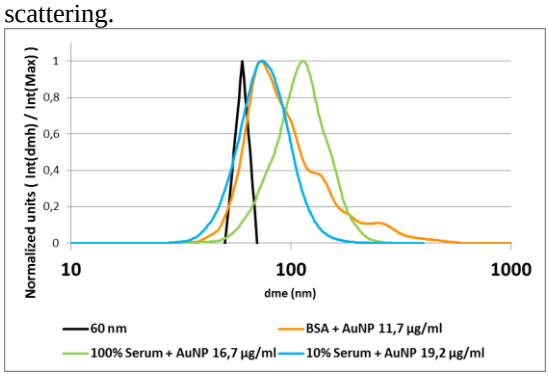

Figure 1. Particle tracking analysis of deposited spherical AuNP into physiological solutions. The black line represents the deposited particle size.

After deposition and characterization of the AuNP the protein corona is identified. The agglomerate AuNP cannot be characterized by dynamic light scattering or UV spectroscopy. This is most likely due to the fact that the primary particles stand for the interaction with electromagnetic radiation. In conclusion the method is successful and depending on the physiological environment various AuNP: Protein complex sizes form with different aggregation states. The next step is to employ this methodology in studying nanoparticle toxicology on various cell types. In addition to the administered amount of particles, the aggregation, size and protein corona is also determined. The interaction of nanowires with physiological fluids will also be studied.

This work was supported by the Nanometer Structure Consortium at Lunds University, nmC@LU. http://www.nano.lth.se, and the Swedish research council FAS, http://www.fas.se/.

Savi, M. (2008). *Environ. Sci. Technol*, 42, 5667-5674.
Lynch, I. (2008). *Nanotoday*, 3, 41-47.

Can the diverse bacterial community grow on dissolved organic matter in a storm cloud?

T.Š. Temkiv[1,2,3], K. Finster[2], T. Dittmar[4], B.M. Hansen[1], R. Thyrhaug[5], N.W. Nielsen[6] and U.G. Karlson[1]

[1] Department of Environmental Science, Aarhus University, 8000 Aarhus, Denmark
[2] Department of Bioscience, Aarhus University, 8000 Aarhus, Denmark
[3] Stellar Astrophysics Centre, Department of Physics and Astronomy, Aarhus University, 8000 Aarhus, Denmark
[4] Max Planck Research Group for Marine Geochemistry, University of Oldenburg, 26129 Oldenburg, Germany
[5] Department of Biology, University of Bergen, 5020 Bergen, Norway, opus posthum
[6] Danish Meteorological Institute, 1000 Copenhagen, Denmark

Keywords: atmospheric microorganisms, bioaerosols, storm clouds, cloud chemistry

Introduction

Due to their inaccessibility and extremely short lifetimes, storm clouds are among the least studied habitats of the atmosphere. We have carried out the first comparative study, analysing 50 individual large hailstones as replicate samples, in order to study the dissolved organic matter (DOM) as well as the microbiome of a storm cloud.

Methods

Catalytic high temperature combustion was used to determine the concentrations of dissolved organic carbon (DOC) and total dissolved nitrogen (TDN). Ultrahigh-resolution mass spectrometry was used to characterize DOM.

Bacterial density was analysed by flow cytometry, while bacterial community composition and diversity was assessed by both cultivation-dependent and independent techniques. Phenotype Microarrey plates were used to investigate the metabolic potential of bacteria.

Conclusions

The identification of ~3000 organic compounds showed that less than 3% of the compounds were suitable for microbial degradation. However, the high concentrations of TDN (30 µM, Q1–Q3 = 27–35 µM) and DOC (Me=179 µM, Q1–Q3 = 132–220 µM) and the low bacterial densities (Me=1973 cells/ml, Q1-Q3=1485-2960) indicated that cloud water was a sparsely populated and nutrient-rich microbial environment, where bacteria could be metabolically active and multiply even if only 3 % of DOM can be used by bacteria. As the residence time of bacteria in cloud droplets is short, only bacteria with opportunistic metabolic strategy, i.e. having fast growth responses and fast growth rates are likely to grow in clouds.

We found a diverse bacterial community with representatives from 11 phyla that was dominated by bacterial groups, coming from plant surfaces, a pattern that was repeated in the cultivable fraction of the community. Of the 424 culture strains the majority was related to plant-associated genera (*Methylobacterium* and *Bradyrhizobium*). The study of DOM, on the contrary, showed that the majority (60%) of detected compounds, and thus aerosols, were derived from soils. The enrichment of plant-associated bacterial strains points at a positive selection of microbes in the course of cloud formation, which is likely a consequence of intrinsic growth and survival properties of plant-associated bacteria over microbes that are derived from other habitats such as soils. In fact, analyzing the metabolic potential of isolates, we found that they grew on a diverse menu of organic compounds, and thus had an opportunistic metabolic strategy (Temkiv *et al.*, 2012). In addition, they may be preadapted for survival in the atmosphere, as they meet similar stress factors, e.g. UV radiation and desiccation on plant surfaces and in the atmosphere. Based on the spectrum of biodegradable organics as well as bacterial numbers and types, we conclude that storm clouds likely contain metabolically active bacteria, which affect the chemical makeup of the atmosphere.

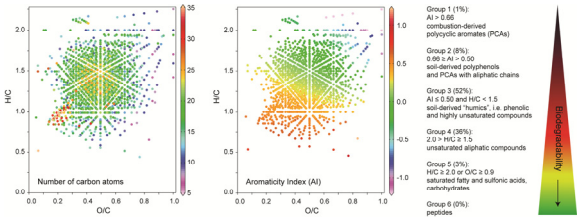

Figure 1. The molecular composition of dissolved organic matter in hail.

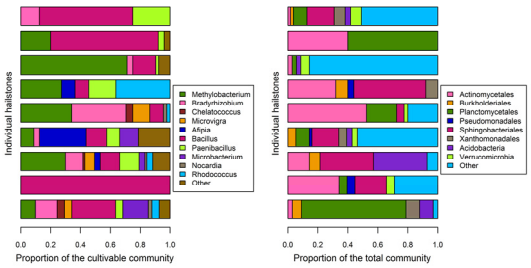

Figure 2. Community composition in the storm cloud.

Temkiv, T. S., Finster, K., Hansen, B. M., Nielsen, N. W., & Karlson, U. G. (2012). *FEMS Microbiol Ecol*, 81(3), 684-95.

Gase-phase oxidation of SO_2 by $O_2^-(H_2O)_n$ molecular clusters – a density functional theory study

N. Tsona[1], N. Bork[1,2] and H. Vehkamäki[1]

[1]Department of Physics, University of Helsinki, Helsinki, 00014, Helsinki, Finland
[2]Department of Chemistry, University of Copenhagen, Copenhagen, 2100, Copenhagen, Denmark

Keywords: Ion-induced nucleation, aerosol catalysis, charged particles, molecular clusters.

One of the most active areas of atmospheric chemistry is related to understanding cloud formation. The first step in this mechanism is known as nucleation, and despite much research dedicated exclusively to this process, it is still not properly understood. Although clouds are mainly composed of water, it is well known that at least one other particle or chemical is needed to initiate the nucleation. In numerous studies sulphuric acid has been identified as the primary candidate for this (Kulmala *et al.*, 2004). The most important mechanism of H_2SO_4 formation is the well-known UV induced oxidation of SO_2, following a neutral pathway.

Currently, the properties of atmospheric ions are receiving increased attention from both theoretical, field based, and chamber studies. It has thus firmly been established that ions increase nucleation rates and hence aid cloud formation. However, the underlying mechanism is currently unknown. Several possible mechanisms may be responsible but since ionic chemistry also opens a mechanism for formation of sulphuric acid this might explain the observations. It is well known that the majority of atmospheric ions originate from cosmic ray impacts, producing free electrons and a variety of cations. A free electron may easily attach to O_2 with an energy gain of ca. 40 kJ/mol. The resulting ion has been found to form stable clusters with at least 5 water molecules (Bork *et al.*, 2011).

Few chemical properties of $O_2^-(H_2O)_n$ clusters have been investigated but experiments have shown that

$$O_2^-(H_2O)_n + SO_2 \rightarrow SO_4^-(H_2O)_n \qquad \text{(R1)}$$

for n = 1 and 2. Further, it has been shown that the reaction is fast at ambient temperatures (Möhler *et al.*, 1992). Also in recent field measurements SO_4^- has been observed (Ehn *et al.*, 2010). SO_4^- is hence known to be stable and it seems plausible that SO_4^- may react further to H_2SO_4 or a related species and thereby contribute to nucleation and cloud formation. This confirms the need to understand the origin of SO_4^-. However, neither the structures, the reaction mechanism, nor the possible catalytic effects of water molecules are properly understood.

The main goal of this research is to provide a plausible mechanism and reaction rates for the formation of SO_4^-. We have used density functional theory calculations and basis sets successfully used in previous studies. Since it is known that the reactants are containing at least 5 water molecules, we have included that amount in our studies. We model the entire reaction from the initial collision and clustering, over intermediate structures (see Figure 1) to products.

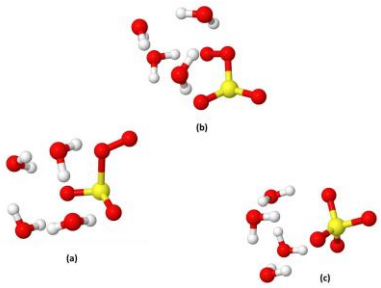

Figure 1. Structures of reactant (a), transition state (b) and product (c), including 4 water molecules. Colour coding: yellow = sulphur, red = oxygen, and white = hydrogen.

The following results will be reported and analysed:
- the structures of hydrated clusters
- the thermodynamics of the reactions
- comparison to experimental results and field studies
- the atmospheric relevance of the reaction

This work is supported by Academy of Finland LASTU program project number 135054, and CSC- IT Center for Science in Espoo, Finland for computing time.

Bork, N., Kurten, T., Enghoff, M. B., Pedersen, J. O. P., Mikkelsen, K. V. & Svensmark, H. (2011). *Atmos. Chem. Phys.*, 11, 7133–7142.

Ehn, M., Junninen, H., Petäjä, T., Kurten, T., Kerminen, V.-M., Schobesberger, S., Manninen, H. E., Ortega, I. K., Vehkamäki, H., Kulmala, M. & Worsnop, D. R. (2010). *Atmos. Chem. Phys.*, 10, 8513–8530.

Kulmala, M., Vehkamäki, H., Petäjä, T., Dal Maso, M., Lauri, A., Kerminen, V.-M., Birmili, W. & McMurry, P.H. (2004). *J. Aerosol Science*, 35, 143-176.

Möhler, O. Reiner, T. and Arnold, F. (1992). *J. Chem. Phys.*, 97(11), 8233-8239.

New particle formation events at the Lille Valby semi-rural background site in Denmark

F. Wang[1], M. Ketzel[2], A. Massling[2] and A. Kristensson[3]

[1]National Climate Center, Beijing, 100081, China
[2]Department of Environment Science, Aarhus University, 4000 Roskilde, Denmark
[3]Department of Physics, Lund University, 22100 Lund, Sweden

Keywords: nucleation events, growth rate, air mass origin

Introduction

Anthropogenic and natural aerosol particles are recognized as important atmospheric substances as they have significant influence on the global radiation balance and thereby on climate. One of the important sources of both natural and anthropogenic origin for atmospheric particles is the so called new particle formation process (NPF), which is dependent on the existence of gaseous precursors.

In this work we characterize the particle formation and growth events observed at a semi-rural site in Denmark (Wang et al. 2012). The dataset is based on regularly measured submicrometer particle number size distributions from February 2005 to December 2010. Results are statistically evaluated and linked to air mass origins using backward trajectory analysis and an evaluation of the oxidation capacity of the atmosphere.

Methods

Particle number size distributions in the size range from 6 to 700 nm have been measured at a semi-rural site in Denmark, Lille Valby (LVBY, 12.1185°E, 55.6944°N) located in an agricultural area about 30 km west of Copenhagen.

We choose to follow the methodology for the classification of formation events thoroughly described by Dal Maso et al. (2005). The classification is based on a visual inspection of these daily contour plots. It is made by three persons to avoid subjective bias. For the clearest events (Type I) several relevant nucleation parameters (formation rate dN_6/dt, growth rate GR, condensational sink CS and condensable vapor source rate Q) have been calculated and analysed as described in Kristensson at al. (2008).

Conclusions

Around 17% of the in total 1383 days (total data coverage 63%) were classified as event days, which is lower compared to the results reported from Finnish and southern Swedish measurement stations. Similar seasonal variations were found in Denmark in comparison to the other two studies showing that particle formation occurred from March to September, and most frequently in June (Figure 1). Sunny days with below-average NO_x concentrations and above-average oxidation capacity ($O_x=O_3+NO_2$) were observed to be favorable conditions for particle formation and growth.

The parameters used to characterize the formation events were calculated for all type I events. The mean value of the growth rate during type I events was about 2.6 nm h^{-1} (median 2.31 nm h^{-1}), the mean apparent 6 nm formation rate was 0.36 cm^{-3} s^{-1} (median 0.23 cm^{-3} s^{-1}), the mean value of the condensation sink 4.27×10^{-3} s^{-1}, and the mean condensable vapor source rate was 1.96×10^{5} molecules cm^{-3} s^{-1}. All these parameters depict a monthly variation. The event days were mostly associated with northwesterly winds, and the backward trajectories were indicating air mass transport from the North Sea.

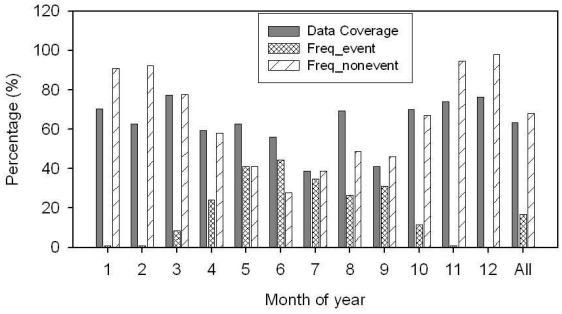

Figure 1. Monthly variation of measured DMPS data coverage and frequency of event days and non-event days.

We acknowledge the Danish Environmental Protection Agency for the financial support of the study. Furthermore, we would like to thank also Ilona Riipinen and Mikka Dal Maso for assisting in the NPF classification analysis.

Dal Maso M, Kulmala M, Riipinen I, Wagner R, Hussein T, Aalto PP, Lehtinen KEJ (2005) Formation and growth of fresh atmospheric aerosols: eight years of aerosol size distribution data from SMEAR II, Hyytiälä, Finland. *Boreal Environ Res* 10: 323-336.

Kristensson A, Dal Maso M, Swietlicki E, Hussein T, Zhou J, Kerminen V-M, Kulmala M. (2008) Characterization of new particle formation events at a background site in southern Sweden: relation to air mass history. *Tellus* 60B: 330-344.

Wang F, Zhang Z, Massling A, Ketzel M, Kristensson A (2012) Particle formation events measured at a semirural background site in Denmark. *Environ Sci Pollut Res*: DOI 10.1007/s11356-012-1184-6.

Characterization of secondary organic aerosol from ozonolysis of β-pinene

Ågot K. Watne, Eva U. Emanuelsson, Anna Lutz and Mattias Hallquist

Department of Chemistry and Molecular Biology, University of Gothenburg, Gothenburg, Sweden

Keywords: Secondary Organic Aerosol, Volatility, Aerosol Chemistry, Ozonolysis

Introduction

A large fraction of the atmospheric aerosol contains organics. Particulate organics can be formed in the atmosphere through oxidation of organic precursors to secondary organic aerosol (SOA). The processes of formation of SOA are currently not well understood. In order to predict and represent the SOA for instance on cloud formation and climate, an accurate description of formation and properties of SOA is needed (Hallquist *et al*., 2009).

The effects of humidity, temperature and OH radical chemistry on the SOA formed from the ozonolysis of β-pinene were studied in Gothenburg Flow Reactor for Oxidation Studies at low Temperatures (G-FROST).

Methods

G-FROST is a laminar flow reactor where SOA can be formed under well-controlled conditions (Figure 1). Through the flow reactor there is a continuous laminar flow. As new particles are formed, old are pumped out. This creates a stable aerosol output and imposed changes to the chemistry can be monitored and analyzed.

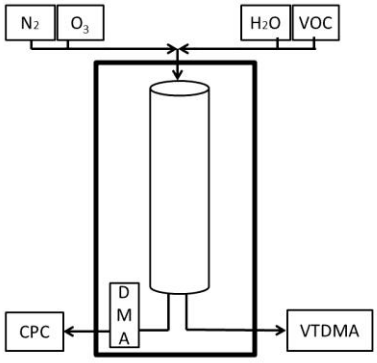

Figure 1: Schematic of G-FROST.

Three sets of relative humidity (RH) variation experiments were conducted at 288 K and at 298 K using three different β-pinene concentrations: low, intermediate and high. In addition, the effect of using 2-butanol or cyclohexane as OH-scavenger was studied. In all experiments, the RH was changed in four steps aiming at 12, 15, 30 and 50 %. Figure 2 shows an example of an experiment.

In addition to the number and mass of SOA produced the volatility of the aerosol was characterized using a Volatility Tandem Differential Mobility Analyser (VTDMA). The VTDMA provides several aspects of volatility where e.g. the volume fraction remaining at 383K (VFR_{383K}) is shown in Figure 2.

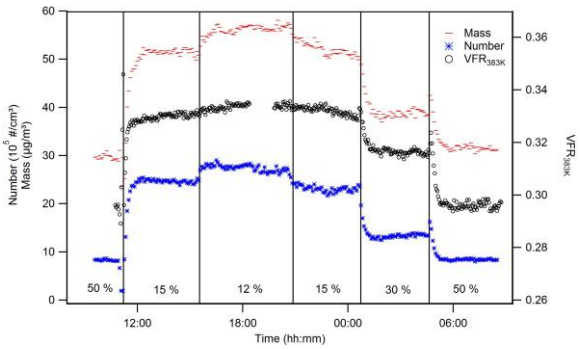

Figure 2: Change in particle number, mass concentration and VFR_{383K} in an experiment with stepwise change in RH.

Conclusions

As can be seen in Figure 2, SOA formed from ozonolysis of β-pinene shows a negative RH dependence. This was valid for all experiments and it shows the opposite trend of what has been observed from the ozonolysis of α-pinene (e.g. Jonsson *et al*, 2008).

Regarding the volatility, several aspects were revealed. It was demonstrated that volatility of SOA did change for the different conditions (e.g. temperature, RH and use of scavenger). These features links back to the changes in chemical mechanism affecting SOA number and mass.

The results from this study suggest inclusion of new chemistry in atmospheric chemical models in order to cover relevant atmospheric changes in humidity, temperature and oxidant levels.

The research presented is a contribution to the Swedish strategic research area ModElling the Regional and Global Earth system, MERGE. This work was supported by Formas (214-2010-1756) and the Swedish Research Council (80475101).

Hallquist et al, (2009) *Atmospheric Chemistry and Physics*, 9, 5155-523.
Jonsson et al, (2008) *Atmospheric Chemistry and Physics*, 8, 6541-6549.

Direct probing of liquid and aerosol surfaces by XPS

J. Werner[1,2], N. Ottosson[1,6], G. Öhrwall[3], J. Söderström[1], N. L. Prisle[2], M. Dal Maso[2], J. Julin[5], I. Riipinen[5], O. Björneholm[1] and I. Persson[2],

[1]Dept. of Physics and Astronomy, Uppsala University, P.O. Box 516, 751 20 Uppsala, Sweden
[2]Dept. of Chemistry, Swedish University of Agricultural Sciences, P.O. Box 7015, 75 007 Uppsala, Sweden
[3]MAX-lab, University of Lund, P.O. Box 118, 22100 Lund, Sweden
[4]Dept. of Physics, University of Helsinki, P.O. Box 48, 00014 University of Helsinki, Finland
[5]Dept. of Applied Environmental Science, Stockholm University, Svante Arrhenius väg, 11418 Stockholm, Sweden
[6]Present address: FOM Institute AMOLF, Science Park 104, 1098 XG Amsterdam, Netherlands
Keywords: Aerosol characterization, Photoelectron spectra, Surface activity, Instrumentation/chemical char.
Presenting author email: Josephina.Werner@physics.uu.se

Many of the compounds, both inorganic and organic, identified in atmospheric aerosol particles are from studies of macroscopic aqueous systems known to have either positive or negative surface propensity. This means that the composition of the surface will be different than in the bulk. Since the surface fraction increases with decreasing aerosol size, such surface effects are especially important for microscopic systems, such as molecular clusters and aerosol particles in the atmosphere. There is an urgent need to qualitatively explore these surface phenomena, as well as to quantify the effects for specific environmentally important systems.

Our main tool to probe the model systems is core-level X-ray Photoelectron Spectroscopy (XPS) using synchrotron radiation, which is a well-established and very successful technique to characterize solids, surfaces, molecules, clusters and liquids[b]. The key advantages of core-level spectroscopy are that both the chemical state and the microscopic spatial distribution of the component species are probed. Utilizing its chemical and surface sensitivity, we are using XPS together with our liquid micro-jet setup to provide information on how the surface composition of atmospherically relevant aqueous systems, such as inorganic ions and carboxylic acids varies with factors such as pH, concentration and co-solvation[c,d]. Recent results from the liquid micro-jet experiments will be presented.

In addition we are developing a novel laboratory setup for direct probing of the surface propensity and speciation of aerosols. As schematically shown in the figure below, we produce aerosols in an atomizer, dry them in a diffusion dryer and use an aerodynamic lens system to focus them into a beam. Further downstream in a vacuum chamber, the aerosols are exposed to X-rays and the kinetic energies of the emitted electrons are determined by an electron spectrometer. The setup will be taken into operation during the upcoming months, and we will present the setup in detail and possibly first results.

References:

[a]Fourth Assessment Report on Climate Change, IPCC http://www.ipcc.ch/.
[b]Hüfner, Photoelectron spectroscopy; Springer Verlag, 1995
[c]Ottosson, N. *et al* 2009, 2010, 2011, 2011
[d]Prisle, N.L. *et al* 2012

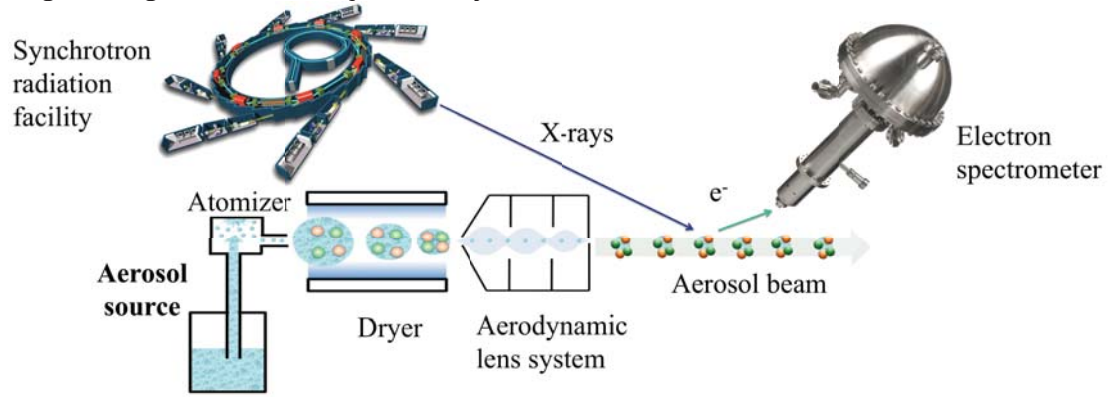

Changes in Hygroscopicity and Cloud-Activation of Diesel Soot upon Ageing

C.Wittbom[1], B. Svenningsson[1], J.Rissler[2], A. Eriksson[1], E. Swietlicki[1], E. Z. Nordin[2], P. T. Nilsson[2] and J. Pagels[2]

[1]Department of Physics, Lund University, P.O. Box 118 SE 221 00, Lund, Sweden
[2] Ergonomics and Aerosol Technology, Lund University, P.O. Box 118 SE-221 00 Lund, Sweden

Keywords: H-TDMA, CCN, AMS, Organic compounds.

Introduction

The contribution from fresh diesel exhaust particles to the cloud condensation nuclei (CCN) population is negligible (e.g. Tritscher *et al.*, 2011). However, complex gas-to-particle conversion processes in the atmosphere form secondary organic aerosol (SOA) from emitted exhaust gases and particles, which significantly may influence the cloud drop formation process. Results from two Lund University smog chamber campaigns (#I & #II), are presented. The CCN and hygroscopic properties of diesel soot particles and the accompanying organic coating were investigated during ageing.

Methods

Exhaust from a light-duty diesel vehicle at warm idling were transferred to a smog chamber and photochemically aged (Nordin *et al.*, 2012). VOCs and IVOCs (Intermediate Volatile Organic Compounds) in the diesel exhaust were used as SOA precursors. Selected amounts of toluene and m-xylene were added to allow investigations of the full particle transformation from agglomerates to spheres.

Hygroscopic properties were analysed using a Hygroscopic Tandem Differential Mobility Analyzer (H-TDMA; Nilsson *et al.*, 2009), and the cloud-activation properties were measured using a Cloud Condensation Nucleus Counter (CCNC; DMT 100). A soot particle aerosol mass spectrometer (SP-AMS, Aerodyne Research) determined the composition of the soot cores and the particle coatings. The particle mass-mobility relationship was characterized using a Differential Mobility Analyzer-Aerosol Particle Mass Analyzer (DMA-APM; Kanomax Japan 3600). During Campaign II, the CCNC measurement procedure was changed from the traditional Stepping-ΔT to Scanning Flow CCN Analysis (SFCA) (Moore & Nenes, 2009), enabling rapid measurements of the supersaturation spectra with high time resolution, revealing more detailed, accurate and continuous results.

Conclusions

During the ageing process, the transformation of the hygroscopic behaviour and its link to the effect on cloud droplet activation were related to the organic fraction in the particle as well as particle size and morphology. The properties of the organic material strongly influence the activation of the coated soot particles, both regarding the change of chemical composition, and also the change of critical supersaturation (SS_c, Fig.1) upon UV exposure.

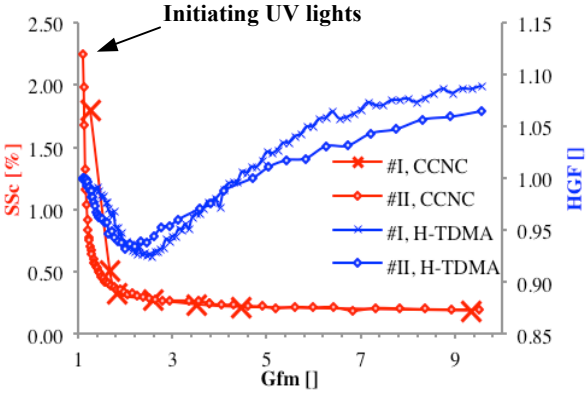

Figure 1.Ageing results in an increase in the mass growth factor (Gfm, x-axis), which is the ratio of total particle mass divided by the soot core mass. During ageing, the critical supersaturation (SS_c) decreases (red, left y-axis) and the corresponding hygroscopic growth factor (HGF, at 90% RH) increases (blue, right y-axis). Results are for diesel soot particles ($d_{m,dry}$=150 nm) from two experiments, Campaign #1 and #2.

Fresh diesel soot particles show no hygroscopic growth (HGF, Fig.1). Due to the morphology, the mobility diameter is not a relevant size measure for predicting cloud activation of fresh soot particles and is thereby not an accurate input parameter when calculating neither HGF (Fig.1) nor when modelling the SS_c. The cloud droplet activation starts long before the particles show any hygroscopic growth at all at 90% relative humidity (RH) (Fig.1). The soot particles gradually collapse to spheres up to a coating of 50-60% condensed organic material (HGF≈0.93; Gfm≈2-2.5, Fig.1). These results indicate that diesel soot particles, when aged, do affect the cloud forming process in the atmosphere.

The Swedish Research Council (VR), FORMAS and CRAICC supported this work.

Moore, R. & Nenes, A. (2009) *Aerosol Sci. & Tech.* 43:1192-1207.

Nilsson, E. et al. (2009) *Atmos. Meas. Tech.*, 2, 313-318.

Nordin, E.Z., et al. (2012) Smog chamber studies of SOA formation from Gasoline Vehicles & Aromatic precursors. *To be submitted to ACP* .

Tritscher, T., et al. (2011) *Environ. Res. Lett.* 6:3:034026.

Nordic Society for Aerosol Research NOSA

The local organizing team and the NOSA board members thank you for your contribution!

DANALYTIC Oleico AB ZenZor DEKATI TSI DIGITEL enviro-sense AARHUS UNIVERSITY

NOSA

www.dmu.dk/nosa2012